UNIVERSIDADE DE LISBOA
FACULDADE DE CIÊNCIAS
DEPARTAMENTO DE BIOLOGIA VEGETAL

Deletion of *sdaB* reduces the susceptibility to vancomycin in *Clostridioides difficile*

Inês Dias Morais

Mestrado em Microbiologia Aplicada

Dissertação orientada por:
Professor Dr. Adriano O. Henriques
Professor Dr. Francisco Dionísio

2021

This Dissertation was fully performed at *Instituto de Tecnologia Química e Biológica António Xavier/UNL* under the direct co-supervision of Professor Drª. Mónica Serrano.

Professor Francisco Dionísio was the internal supervisor designated in the scope of the Master's in Applied Microbiology of the Faculty of Sciences of the University of Lisbon.

Acknowledgements

First of all, I would like to thank the Scientific Committee of the MSc in Microbiologia Aplicada of Faculdade de Ciências of Universidade de Lisboa for the planning and organization of this master. I also want to thank to the Instituto de Tecnologia Química e Biológica António Xavier of Universidade Nova de Lisboa for allowing and receiving me as a master student throughout this year.

I want to express my gratitude to Prof. Dr. Adriano Henriques, my advisor at ITQB, for the privilege of working under his guidance in this dissertation, for the tireless support and motivation, and for improving my scientific and critical reasoning with the immense knowledge transmitted. To Dr. Mónica Serrano, who I also consider as an (informal) advisor at ITQB, I want to thank the constant support and availability, the never-ending patience to teach me and clarify all of my doubts and the theoretical and practical knowledge she passed onto me and without which I couldn't have possibly done this work.

To my advisor in FCUL, Prof. Dr. Francisco Dionísio, I thank the constant availability to answer all of my questions and the suggestions and dissertation review.

I am extremely thankful to Diogo Martins for being the first person to receive and supervise me in ITQB, teaching me and helping me with various techniques that made much of my work possible, and for the constant support, encouragement, for believing in me even in those moments that I didn't. To all my MDL colleagues, Aristides Mendes, Carmen Olivença, Isabel Roseiro, Khira Amara, Lourenço Bonnevile, Mariana Ferreira, Mariana Valente, Mónica Louro, Sara Ramalhete and Zoé Vaz da Silva, who have always provided a good work environment, for all the cakes and the moments of fun. I am grateful to Professor Ricardo Louro and Inês Trindade for welcoming me in their laboratory, for helping me with the anaerobic purification, for the availability to teach me and clarify all of my doubts and the theoretical and practical knowledge they passed onto me. To Professor Lígia Martins and André Taborda, who helped me with the UV-Vis spectrum. Also, to Teresa Silva, for all the help in several tasks crucial for me to continue my work.

To my parents, to whom I owe much of who I am, I want to thank the unconditional support and love and for allowing me to dream unrestrictedly and get to where I am today. I thank to my mom, in particular, for always being there in the difficult moments, for believing in me, for the infinite optimism and, most of all, for the irreplaceable friendship and love. To my brother, my always and forever friend for the talks and laughs, for the patience, kindness, and love.

Finally, to all my family and best friends, thank you for constantly helping me remember the most important things in life and for always aiding me to see the best in me. Hope you can forgive my absence and distance in the darkest times.

Abstract

The intense and often inappropriate use and disposal of antibiotics have led to a world-wide rise in the pervasiveness of antibiotic-resistant bacteria, thereby strongly impairing our ability to treat bacterial infections in both humans and animals. *Clostridioides difficile* is a major nosocomial pathogen and the leading cause of a range of intestinal conditions linked to antibiotic therapy. Antibiotic treatment causes dysbiosis and allows ingested spores of *C. difficile* to germinate and the resulting cells to grow into a population that produces the two main virulence factors of this organism, the TcdA and TcdB toxins. *C. difficile* strains that are resistant to multiple antibiotics are at an advantage and have been responsible for a rise in the number of out-breaks associated with higher morbidity and mortality caused by this organism. An important antibiotic used to treat infections by *C. difficile* is the glycopeptide vancomycin. The lethal target of vancomycin (VAN) is the D-Ala-D-Ala motifs in lipid II. Resistance often depends on the expression of van clusters which allow remodelling of the dipeptide termini of peptidoglycan (PG) precursors from D-Ala-D-Ala to D-Ala-D-Lac or D-Ala-D-Ser, with reduced affinity for VAN. Other mechanisms of resistance are less understood. Susceptibility to VAN in *C. difficile* is intriguing because most strains carry a functional van^{G} type cluster. However, disruption of the $vanG^{Cd}$ cluster in *C. difficile*, lowers only slightly the MIC^{VAN}. One strain with reduced susceptibility to VAN bears three mutations, including the *sdaB* gene, coding for a putative L-Serine deaminase that converts L-Ser into pyruvate. In this study, we focused on the role of the *sdaB*. We found that *sdaB* is not under sporulation control and does not respond to the branched chain amino acids that are sensed by the global regulatory protein CodY. Deletion of *sdaB* decreases the susceptibility of *C. difficile* to VAN, suggesting that the mutation favours the channelling of L-Ser into the PG biosynthetic pathway. In line with this prediction, the mutant shows reduced labelling of living cells with a fluorescent derivative of VAN, which binds to D-Ala-D-Ala motifs. Deletion of *sdaB* also increases biofilm formation, possibly because the mutation reduces the intracellular level of pyruvate and stimulates its uptake from the extracellular medium. We purified SdaB under anaerobic conditions and we have shown that its UV/VIS absorption spectrum is consistent with that of an [4Fe-4S] cluster protein. In conclusion, the availability of L-Ser may be a bottleneck in the expression of VAN resistance even when VAN induces the $vanG^{Cd}$ operon. Thus, the *sdaB* mutation may synergize with other mutations to confer VAN resistance.

Keywords: Antibiotic resistance; *Clostridioides difficile* infection (CDI); Vancomycin; Biofilms; Sporulation

Resumo

O uso intenso e por vezes inapropriado de antibióticos, levou a um aumento à escala mundial de bactérias resistentes, comprometendo seriamente a nossa capacidade de tratar infeções causadas por microrganismos em animais e em humanos. *Clostridioides difficile* é uma bactéria Gram-positiva, anaeróbica obrigatória e produtora de esporos. Pode ser encontrada assintomaticamente em 1 a 3% dos adultos saudáveis, podendo causar infeção associada à terapia com antibióticos, essencialmente em ambiente hospitalar, assim como, cada vez mais, na comunidade. É atualmente a principal causa de colite pseudomembranosa e de diarreia infeciosa em países desenvolvidos. Em 2017, um estudo epidemiológico reportou que aproximadamente 45% das infeções gastrointestinais eram causadas por *C. difficile*. A infeção do cólon por *C. difficile* é potencialmente fatal, especialmente em idosos e em pacientes que, por terem sido expostos a antibióticos, apresentam disbiose intestinal. A disbiose permite que os esporos ingeridos de *C. difficile* germinem e que as células resultantes desde que resistentes ao antibiótico em uso, expandam numa população capaz de produzir os dois principais fatores de virulência deste organismo, as toxinas TcdA e TcdB. Estirpes multirresistentes de *C. difficile* têm sido responsáveis por um aumento de surtos associados a maior morbidade e mortalidade. Certos antibióticos como as fluoroquinolonas, as cefalosporinas e clindamicinas são conhecidos por aumentar o risco da infeção por *C. difficile*. Para sobreviver no hospedeiro, esta bactéria deve induzir uma estratégia de sobrevivência adequada, que pode ser uma ativação da resposta ao stress, a produção de fatores de virulência (produção de toxinas, camada S, flagelo, fímbrias, etc.), a esporulação ou a formação de biofilmes. Os fatores de virulência TcdA e TcdB, que levam à disrupção do citoesqueleto de actina das células do epitélio intestinal, e à morte celular, causam os sintomas de infeção por *C. difficile*. A esporulação é um processo de diferenciação de células bacterianas que permite a conversão de células vegetativas em esporos através de uma série de etapas morfológicas. Em *C. difficile*, a transmissão entre hospedeiros é feita através de esporos, resistentes ao oxigénio. Os biofilmes são comunidades de microrganismos estruturadas associados a superfícies e embebidos numa matriz extracelular, que contém proteínas, DNA e exopolissacáridos. A formação dos biofilmes é importante pois este modo de crescimento resulta numa resistência inerente ao tratamento com antibióticos sendo associado à natureza crónica das infeções. Os fatores de risco associados a infeções por *C. difficile* podem ser classificados em várias categorias, como farmacológicos (ex.: uso de antibióticos), relacionados com o hospedeiro (ex.: idade ≥ 65 anos e/ou pacientes imunocomprometidos) ou associados com intervenções clínicas (ex.: duração de uma hospitalização). Os tratamentos para pessoas sintomáticas infetadas com *C. difficile* incluem o transplante de microbiota fecal, as vacinas, os fagos, o tratamento com probióticos e o tratamento com antibióticos.

O tratamento com antibióticos causa disbiose permitindo a colonização do trato intestinal por *C. difficile*. Os principais antibióticos usados para tratar a infeção com *C. difficile* são o metronidazol e a vancomicina. Contudo, a resistência ao metronidazol, determinada por um plasmídeo, tem vindo a aumentar. A vancomicina é um antibiótico tradicionalmente usado como último recurso para o tratamento de infeções bacterianas Gram-positivas, incluindo casos graves de infeções com *C. difficile*, mas é cada vez mais usado como medicamento de primeira linha. A disseminação da resistência à vancomicina seria, portanto, um problema sério. O alvo letal da vancomicina é o motivo D-Alanil-D-Ala no lípido II, um intermediário ligado à membrana na via de biossíntese de peptidoglicano (PG). Esta ligação impede as atividades de transpeptidação das sintetases de PG (PBPs, ou proteínas que ligam penicilina), comprometendo a integridade do envelope celular e levando à morte celular. Em vários organismos, a expressão de um cluster designado *van* é suficiente para conferir resistência à vancomicina. Estes clusters codificam para enzimas que permitem a alteração do motivo D-Alanil-D-Ala para D-Alanil-D-Lac ou D-Alanil-D-Ser, apresentando ambos uma afinidade reduzida para a vancomicina. Os clusters *van* incluem um regulador transcricional (VanR) que consiste num domínio recetor N-terminal e um domínio de ligação de DNA, e uma cinase sensora (VanS) que contém um domínio N-terminal membranar e um

domínio C-terminal citoplasmático de cinase. VanR é ativado através de fosforilação por VanS. Após a exposição à vancomicina, VanS autofosforila e transfere o grupo fosforil para VanR. VanR fosforilado ativa a transcrição da parte "enzimática" do cluster que codifica para as enzimas responsáveis pela introdução de D-Ala-D-Glu ou D-Ala-D-Ser no PG.

A suscetibilidade de *C. difficile* à vancomicina é inesperada porque a maioria das estirpes epidémicas têm um cluster do tipo *vanG* no qual o gene *vanG* codifica para uma ligase de D-Alanil-D-Ser, *vanXY* codifica para uma enzima com atividade hidrolítica contra D-Alanil-D-Ala e UDP-NAG-pentapéptido[D-Ala] e *vanT* codifica para uma racemase de D-Ser. O cluster de *C. difficile* é funcional, pois a indução de *vanG* resulta numa acumulação de NAG-NAM-pentapéptido[D-Ser] na parede celular e o transplante de *vanG* para *E. coli* permite a sobrevivência deste organismo na presença de vancomicina. Posto isto, deve haver um ou mais estrangulamentos que impeçam a expressão de resistência à vancomicina em *C. difficile*. Em 2014, Leeds e coautores reportaram o isolamento de uma estirpe com um valor de MIC de 16 mg L^{-1}, oito vezes superior ao valor normal encontrado para *C. difficile*. A suscetibilidade reduzida à vancomicina foi atribuída a mutações nos genes *murG, CD3659* e *sdaB*. *murG* codifica para uma transferase que catalisa a formação de uma ligação glicosídica entre o undecaprenil-pirophosphoril-N-acetilmuramoil (NAM)-pentapeptide (lípido I) e a N-acetil glucosamina (NAG) para formar undecaprenil-pirophosphoril-N-acetilmuramoil (NAM)-pentapeptide-NAG (ou lípido II). Este é o substrato que é translocado para o lado trans da membrana e utilizado para a extensão (transglicosilação) das cadeias de PG. MurG é uma enzima essencial e é conservada em quase todas as espécies bacterianas. O alelo $murG^{P108L}$, presente na estirpe resistente, causa uma substituição no local de ligação do lípido I, perto da membrana. Isto sugere que MurG pode ter menor afinidade para substratos terminados em D-Ala-D-Ser e que $MurG^{P108}$ pode utilizar com maior eficiência estes substratos ultrapassando um dos estrangulamentos postulados acima. A mutação em *CD3659* introduz um codão STOP após o aminoácido 326 numa exonuclease de RNA/DNA de cadeia simples. A mutação em *rpoC* causa uma substituição em D244Y, na subunidade β' da RNA polimerase. Finalmente, *sdaB*, codifica para uma deaminase que converte L-Ser em piruvato. A mutação causa a eliminação em fase de um de quatro resíduos de alanina consecutivos perto do centro ativo e possivelmente interfere com a atividade da enzima. Em *E. coli*, existem três genes que codificam para deaminases da L-Serina, e a eliminação de todos resulta num forte defeito na forma e na divisão celular. Isto sugere que um aumento na concentração intracelular de L-Ser afeta de algum modo a via de síntese do PG, um dos determinantes mais importantes da forma celular. Embora os mutantes nunca tenham sido estudados em pormenor, o isolamento destas estirpes sugere que a resistência à vancomicina possa surgir através de diferentes mecanismos. No entanto, a contribuição das diferentes mutações para o fenótipo de resistência nunca foi estudada.

O principal objetivo deste trabalho foi o de determinar a contribuição de *sdaB* para a resistência à vancomicina. No processo, estudámos a expressão do gene *sdaB* durante o crescimento e a esporulação. Concluímos que a expressão de *sdaB* não responde aos aminoácidos de cadeia ramificada, leucina, isoleucina e valina que controlam a atividade do regulador global CodY. Descobrimos ainda que a expressão do gene *sdaB* não é afetada num mutante *spo0A,* incapaz de produzir a proteína, Spo0A, que governa a entrada em esporulação. Em fases tardias do processo, contudo, a expressão do gene parece ocorrer especificamente no pré-esporo, por um mecanismo desconhecido. Construímos um mutante de eliminação em fase do gene *sdaB* e estudámos os fenótipos associados. A eliminação do *sdaB* aumenta a resistência de *C. difficile* à vancomicina. Esta observação sugere um modelo no qual a impossibilidade de produzir piruvato permite canalizar mais L-Ser para a via de síntese de PG, resultando num aumento da representação de D-Ala-Ser e num aumento de resistência à vancomicina. Em apoio deste modelo, a marcação de células vivas com um derivado fluorescente da vancomicina, que marca os motivos D-Alanil-D-Ala no peptidoglicano, é reduzida. A eliminação do gene *sdaB* aumenta ainda a capacidade de a bactéria formar biofilmes. Em linha com a literatura existente, propomos que reduções nos níveis

intracelulares de piruvato induzam a produção dos componentes de um transportador que importa piruvato do meio extracelular, e induz a formação de biofilme. Estes resultados revelam assim uma ligação funcional entre resistência à vancomicina e a formação de biofilmes já que se verifica um aumento da resistência à vancomicina em condições que também promovem a formação de biofilme. Finalmente, produzimos e purificámos SdaB em condições de anaerobiose e iniciámos a sua caracterização bioquímica; SdaB é uma deaminase da L-Serina que exibe um espectro de UV/VIS característico de proteínas com um centro de [4Fe-4S].

Em resumo, os resultados apresentados nesta dissertação sugerem que a disponibilidade de L-Ser pode ser um fator limitante para a resistência à vancomicina, mesmo em condições que induzem o operão $vanG^{Cd}$. Além disso, como parece ocorrer uma maior incorporação de D-Alanil-D-Ser no PG, é possível que a eliminação de *sdaB* possa interagir com outras mutações, tais como $murG^{P108L}$, conferindo resistência à vancomicina. Embora não saibamos ainda se esta interação é sinergística ou aditiva, a resistência à vancomicina pode emergir mediante diversos mecanismos e envolver interações entre diferentes mutações. Um entendimento aprofundado dos mecanismos que levam à resistência à vancomicina pode levar à identificação de alvos para novas terapias com o objetivo de aliviar a ameaça representada pelo surgimento e disseminação de estirpes resistentes a este antibiótico.

Palavras-Chave: Resistência a antibióticos; Infeção por *Clostridioides difficile*; Vancomicina; Biofilmes; Esporulação

Index

List of figures

Symbols and abbreviations

%	Percentage
::	Insertion
µg	Microgram
µL	Microliter
µm	Micrometre
µM	Micromolar
Abs	Absorbance
ACE	Allele-Coupled Exchange
Amp^R	Ampicillin resistance
aTc	Anhydrotetracycline
BHI	Brain Heart Infusion
BHISG	BHI medium supplemented with L-cysteine hydrochloride and D-glucose
bp	Base pair or pairs
CCR	Carbon Catabolite Repression
CDI	*Clostridioides difficile* Infection
CDMOB	*C. difficile* medium optimized for biofilm formation
Cm^R	Chloramphenicol resistance
CstA	Pyruvate-import system
DDTs	D,D-transpeptidases
DOC	Sodium deoxycholate
DTT	Dithiothreitol
erm	Erythromycin resistance determinant
FMT	Faecal Microbiota Transplantation
g	Acceleration of gravity
g	Gramme
GDH	Glutamate Dehydrogenase
GI	Gastrointestinal
GTP	Guanosine triphosphate
h	Hour
IPTG	Isopropyl β-D-1-thiogalactopyranoside
kDa	Kilodalton
L	Litre
LB	Luria-Bertani Medium
lb/in^2	Pound per Square Inch
LDTs	L,D-transpeptidases
L-SD	L-Serine deaminase
M	Molar
MC	Mother cell
mg	Milligram
min	Minutes
MIC	Minimal inhibitory concentration
mL	Millilitre
mM	Millimolar

MTZ	Metronidazole
NAG	N-acetylglucosamine
NAM	N-acetylmuramic acid
ng	Nanogram
nM	Nanomolar
ºC	Degree centigrade
PAGE	Polyacrylamide gel electrophoresis
PaLoc	Pathogenicity Locus
PBS	Phosphate Buffered Saline
PCR	Polymerase chain reaction
PG	Peptidoglycan
PS	Forespore
PVDF	Polyvinylidene difluoride
RBS	Ribosome Binding Site
rpm	Revolutions per minute
s	Seconds
TCS	Two-component system
Tm^R	Thiamphenicol resistance
Tris	Tris(hydroxymethyl)aminomethane
V	Volt
v	Volume
VAN	Vancomycin
WT	Wild type
Δ	Deletion
σ	Sigma

1. Introduction

1.1. General aspects of *Clostridioides difficile*

Clostridioides difficile (formally *Clostridium difficile*) is a Gram-positive, anaerobic, spore-forming bacterium with a low genome GC content (Lawson et al., 2016). It can be found asymptomatically in 1 to 3% of healthy human adults. It also colonizes the mammalian intestinal tract as well as that of reptiles and birds (Saujet et al., 2011; Boudry et al., 2015; Taggart et al., 2021).

C. difficile was first identified in 1935 as part of the normal gut microbiota of neonates and hence thought to be non-pathogenic (O'Toole, 1935). Its association with disease was not described until the 1970s following several studies (Bartlett, 1994). At the time, Hall and O'Toole (1935) named the bacterium *Bacillus difficilis* due to its difficult isolation and slow growth in culture. On the basis of 16S rDNA analysis the *Clostridium* genus was divided into several clusters. *C. difficile* belonged to cluster XI, along with other closely related *Clostridium spp*. such as *Clostridium sordellii* and *Clostridium bifermentans*, as well as other species such as *Peptostreptococcus anaerobius* and *Eubacterium tenue*. In 2013, it was proposed that *C. difficile* should be reclassified as *Peptoclostridium difficile* (Smits *et al.*, 2016). The genus name, however, was rejected since it did not follow the rules of the Bacteriological Code as defined by the International Committee on Systematics of Prokaryotes (ICSP) and the International Code of Nomenclature of Bacteria (Lawson *et al.*, 2016). In 2016, Lawson et al. proposed the name *Clostridioides difficile*, and placed the organism in the Peptostreptococcaceae family (Lawson *et al.*, 2016; Elliott *et al.*, 2017).

C. difficile is the most common cause of nosocomial infections associated with antibiotic therapy worldwide (Saujet *et al.*, 2011; Boudry *et al.*, 2015). It has been classified as an urgent threat by the Centers for Disease Control and Prevention (CDC) as it is one of the most common causes of healthcare-associated infection (HAI) in the United States (US) as well as the leading cause of a range of antibiotic-associated gastrointestinal (GI) conditions. Moreover, in younger and healthier patients *C. difficile* infection (CDI) has become increasingly prevalent as a community associated infection (Frieden, 2019; Knippel *et al.*, 2020; Taggart *et al.*, 2021). In 2017, an epidemiological study on HAIs reported that almost 45% of healthcare-associated GI infections in Europe were caused by *C. difficile* (Taggart *et al.*, 2021). During antimicrobial therapy and four weeks thereafter, the risk for development of CDI is 8- to 10-fold higher, and, in the next two months, it becomes 3-fold higher (Czepiel *et al.*, 2019). Furthermore, this organism caused around 225 000 infections and 13 000 deaths in US, with about 30% of CDI leading to recurrence, with an estimated annual cost of CDI to healthcare systems of $5 billion in the US and 3€ billion in Europe (Donnelly *et al.*, 2020; Mondal *et al.*, 2021).

1.1.1. Infection biology

Infection of the colon with *C. difficile* is potentially life threatening, especially in elderly people and in patients who, because they have been exposed to antibiotics, show gut dysbiosis. The main sources of CDI are healthcare facilities, food, animal and the environment (Shen, 2020). The *C. difficile* life cycle is influenced by antimicrobial agents, the host immune system, and the host microbiota and its associated metabolites (Smits *et al.*, 2016). During its infection cycle, *C. difficile* survives within bacteriophage rich gut communities and is therefore expected to possess efficient systems to control genetic exchanges favoured in such environments. The highly mobile and mosaic genome of *C. difficile* could reflect the continuous balance between the acquisition of adaptive traits for GI lifestyle and the efficient defence against abundant invaders, such as phages and plasmids (Boudry *et al.*, 2015). Spores are the infectious units of *C. difficile*, and patients with CDI excrete around 1×10^7 spores per gram of faeces. These highly infectious spores can remain in a dormant state in the hospital environment for longer than six months and, following ingestion, can cause CDI in a susceptible host (Ghose *et al.*, 2016).

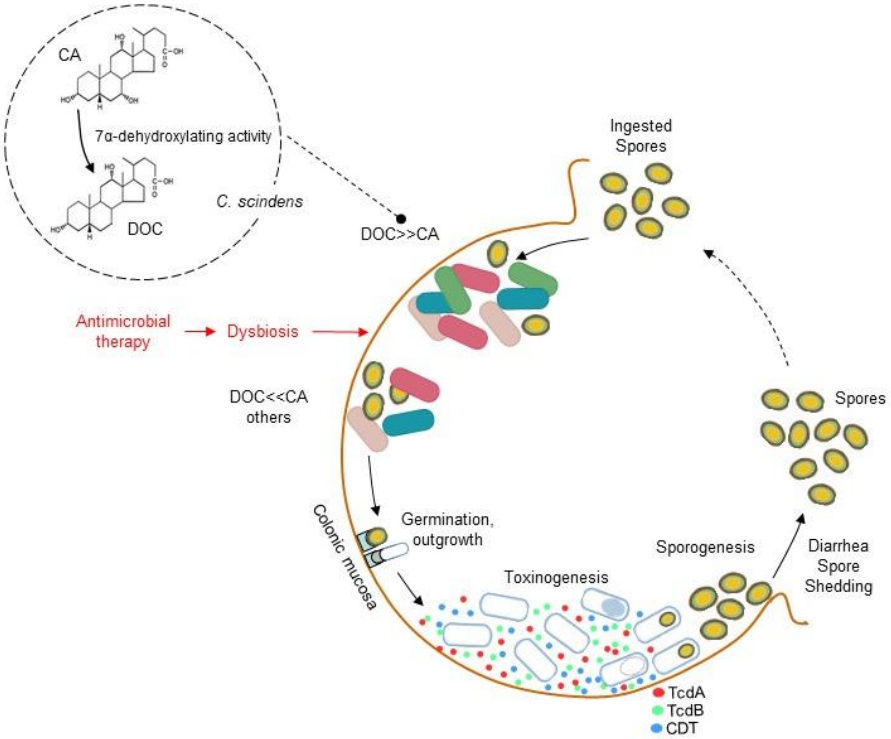

Figure 1.1: Schematic representation of the *C. difficile* infectious cycle. Ingested spores are the infectious units of *C. difficile* that can pass the gastric barrier. After antibiotic treatment the commensal gut microbiota is disturbed and the representation of species, such as *C. sciendens* that produce a 7α-dehydroxylating enzyme which converts CA into DOC, is reduced. Thus, germination is enhanced in the small intestine, and the level of secondary bile salts in the large intestine is reduced, leading to host colonization. *C. difficile* colonization leads to secretion of large toxins (TcdA and TcdB) that can induce massive inflammation of the gut epithelium, causing disease symptoms ranging from mild diarrhoea to pseudomembranous colitis and toxic megacolon and that may cause death. Other virulence factors (*e.g.,* the flagellum, the S-layer, and others) are not represented for simplicity. Shedding of the spores to the environment will allow the infection of new hosts, while spores that remain in the host can be the cause of disease recurrence. Adapted from (Isidro et al., 2017), with permission.

Once ingested, spores germinate in the ileum and then vegetative cells colonize the colon and the caecum (**Figure 1.1**) (Ribis *et al.*, 2018; Tremblay *et al.*, 2021). Spore germination is dependent on sensing primary bile acids produced in the liver (*i.e.,* taurocholate) by the germinant receptor protein CspC, and is inhibited by some secondary bile acids. The spore can also germinate in the presence of amino acids, like glycine and histidine that act as co-germinants (Lawler *et al.*, 2020). In a healthy gut microbiota state bile salts derivatives of deoxycholate (DOC) are more abundant than the bile salts derived from cholate (CA), which act as germinants. After antibiotic treatment the commensal gut microbiota is disturbed and the representation of species, such as *C. sciendens* that produce a 7α-dehydroxylating enzyme which converts CA into DOC, is reduced. Thus, germination is enhanced in the small intestine, and the level of secondary bile salts in the large intestine is reduced, leading to host colonization (Dubois, Yannick D.N. Tremblay, *et al.*, 2019; Mondal *et al.*, 2021). People with an adequate immune response will either eliminate the infection or become asymptomatic carriers. Spore germination allows the bacteria to propagate and produce the two main virulence factors of *C. difficile*, the TcdA and TcdB cytotoxins (see below), and more spores. Both TcdA and TcdB glycosylate thereby inactivating a family of small Rho GTPases, causing the destruction of the epithelium (Sorg, 2014; Wu *et al.*, 2014; Tremblay *et al.*, 2021). Finally, the shedding of the highly resistant spores will allow their accumulation into the environment and the infection of new hosts.

Certain antibiotics like the fluoroquinolones, the cephalosporins, and clindamycin are known to increase the risk of CDI. In addition to antibiotics, vegetative cells also encounter secondary bile salts, host-secreted antimicrobial peptides, and reactive oxygen and nitrogen species produced during inflammation (Cuenot *et al.*, 2019). To survive in the host, *C. difficile* must detect the host environment and

induce an appropriate survival strategy, which may include activating the general stress response, production of virulence factors (toxin production, S-layer, flagella, fimbriae, *etc*.), sporulation, and biofilm formation (Awad *et al.*, 2015; Smits *et al.*, 2016; Isidro, Menezes, *et al.*, 2018; Tremblay *et al.*, 2021).

1.1.2. Toxin production

The main virulence factors of *C. difficile* are two large toxins, TcdA (308 kDa) and TcdB (270 kDa), that lead to the disruption of the actin cytoskeleton of intestinal epithelium cells, therefore causing the CDI symptoms (diarrhoea, epithelial apoptosis, and ulceration) (Awad *et al.*, 2015; Álvarez *et al.*, 2020). The toxin-encoding genes, *tcdA* (2711 codons) and *tcdB* (2367 codons), are found, with three other genes, *tcdR*, *tcdC* and *tcdE*, on a 19.6 kb chromosomal element called the pathogenicity locus or PaLoc (Dineen *et al.*, 2007; Tsutsumi *et al.*, 2014; Kodori *et al.*, 2020). *tcdR* is an alternative sigma factor that directs transcription from the *tcdA* and *tcdB* promoters (Dineen *et al.*, 2010; Geiger and Wolz, 2014). Toxin production by *C. difficile* is positively controlled by up-regulation of *tcdR* expression by sigma factor *sigD*. *sigD* in turn, is negatively controlled by cyclic di-guanosyl-5′ monophosphate (c-di-GMP) levels (McKee *et al.*, 2013). *tcdC* is thought to be an anti-sigma factor, which modulates the expression of *tcdA* and *tcdB* by blocking the association of *tcdR* with the core of RNA polymerase. However, since there are multiple contradictory studies, its function and relevance remain unclear (Awad *et al.*, 2015). Finally, the *tcdE* gene encodes a holin-like protein that is required for the release of the toxins from the cell (Dineen *et al.*, 2007; Dubois *et al.*, 2016). CDT, or binary toxin, is a third toxin produced by about 35% of *C. difficile* strains, including those of ribotype 027 (Antunes *et al.*, 2012; Smits *et al.*, 2016). CDT has received more attention in recent years because of its increasing prevalence in isolates of both human and animal origin. CDT is encoded by two genes, *cdtA* and *cdtB*, that are in an operon on the binary toxin locus (CdtLoc; 6.2 kb). CDT belongs to the binary ADP-ribosylating toxin family and consists of two components: an enzymatic component (CDTa) and a binding/translocation component (CDTb). CDTa has ADP-ribosyl transferase activity, whereas CDTb facilitates the passage of the enzymatic component to the cell cytosol. CDTa leads to the complete destruction of the actin cytoskeleton and, ultimately, cell death (Smits *et al.*, 2016).

Toxin synthesis increases as cells enter in stationary phase, and many environmental factors influence their production. In the presence of phosphotransferase system (PTS) sugars, such as glucose, biotin and some amino acids, like cysteine or proline, toxin production is inhibited (Dubois *et al.*, 2016). Three important regulators of toxin synthesis are CcpA, CodY and Spo0A (Gu *et al.*, 2018). CcpA represses toxin expression in response to PTS sugar availability by binding to the regulatory regions of the *tcdA* and *tcdB* genes, as well as to the regulatory regions of *tcdR* and *tcdC*, mediating glucose-dependent repression. CodY, the global regulator involved in the adaptive response to nutrient limitation, represses toxin gene expression via direct binding to the *tcdR* promoter region (Antunes *et al.*, 2012; Dubois *et al.*, 2016). Binding of CodY to the *tcdR* promoter region is enhanced in the presence of GTP and branched-chain amino acids (Dineen *et al.*, 2007; Geiger and Wolz, 2014). CodY is a repressor of sporulation in *C. difficile* and is involved in regulating genes associated with sporulation, including the *sinR* and *opp* operons (Nawrocki *et al.*, 2016). *sinR* encodes a regulatory protein that enhances *spo0A* transcription (Shen, 2020). Spo0A is the master regulatory protein, activated by phosphorylation, which governs entry into sporulation (Pereira *et al.*, 2013; Alabdali *et al.*, 2019) in response to environmental and nutritional signals (Shen, 2020). How Spo0A is phosphorylated is not yet fully understood. Three orphan histidine kinases with significant similarity to the *B. subtilis* family of sporulation-associated phosphotransfer histidine kinases, CD1579, CD1492 and CD2492, have been studied. *In vitro*, Spo0A is phosphorylated by the CD1579 kinase and inactivation of CD2492 reduces the sporulation capacity of *C. difficile*; CD1492, however, functions as a phosphatase rather than a kinase (Saujet *et al.*, 2011; Shen *et al.*, 2019).

1.1.3. Sporulation

Sporulation is an ancient bacterial cell differentiation process that allows the conversion of a vegetative cell into a mature spore through a series of morphological steps (Ribis *et al.*, 2018). Many bacilli, clostridia and related organisms form bacterial spores (Serrano, Kint, *et al.*, 2016). In *C. difficile*, the transmission is mediated by spores (Saujet *et al.*, 2011). Spores are highly resistant, oxygen-tolerant, multi-layered structures composed of a tightly packed, dehydrated inner core surrounded by the inner membrane, a germ cell wall, a thick modified peptidoglycan (PG) layer known as cortex, an outer membrane, and layers of coat protein. In some spore formers, like *C. difficile*, an exosporium layer surrounds the coat (**Figure 1.2**) (Ribis *et al.*, 2018; Zhu *et al.*, 2018). Spores released from infected patients or animal hosts remain in the environment due to their resistance to oxygen, common disinfectants, high temperatures, radiation, and contribute to different species survival during antibiotic therapy (Fimlaid *et al.*, 2013; Dembek *et al.*, 2018). In case of *C. difficile*, the disruption of the colonic microflora by antibiotic therapy causes CDI and colonization of the intestinal tract. Due to the resistance properties of spores to a variety of chemical and physical conditions, in particular their resistance to oxygen, spores are essential for transmission and disease recurrence (Saujet *et al.*, 2011).

1.1.3.1. Sporulation in *C. difficile*

Sporulation involves a series of morphological stages. In *C. difficile*, as in most spore-formers that have been studied, these changes start with the rod-shaped cell undergoing an asymmetric division originating two cells of unequal sizes, a larger mother cell (MC) and a smaller forespore (PS), the future spore (Pereira *et al.*, 2013; Dembek *et al.*, 2018). The MC engulfs the PS and eventually releases it as a free protoplast within its cytoplasm. At this stage, the PS is surrounded by the MC cytoplasm, and isolated from the external medium. In subsequent steps, the spore cortex and coat layers are assembled and finally MC lyses to release the mature spore into the environment. The central compartment of the mature spore contains the genome (Pereira *et al.*, 2013; Saujet *et al.*, 2015).

At the transcriptional level, sporulation is triggered by the phosphorylation and activation of Spo0A. When Spo0A-P level reaches a critical threshold, Spo0A-P controls division site placement at one pole of the cell entering sporulation. It also drives transcription of *spoIIE* as well as both the *spoIIAA-spoIIAB-sigF* and the *spoIIGA-sigE* operons encoding σ^F and σ^E, respectively, and proteins involved in their activation (Saujet *et al.*, 2013). Spo0A and the σ^A-containing form of RNA polymerase drives transcription of the *spoIIG* operon and the *spoIIE* gene, whereas RNA polymerase containing σ^H, is required for the transcription of *spo0A* and *sigF*. Once the MC and the PS are formed, gene expression in either cell is mainly governed by a cascade of cell type-specific RNA polymerase sigma (σ) factors: σ^F in the PS and σ^E in the MC control early stages of development, prior to engulfment completion, and are replaced by σ^G and σ^K following engulfment completion (**Figure 1.2**) (Pereira *et al.*, 2013; Saujet *et al.*, 2013). There are several differences in the activation and windows of activity of the various cell type-specific sigma factors with respect to the *B. subtilis* model. For example, unlike in *B. subtilis*, σ^E remains active until the late stages of sporulation. Also unlike in *B. subtilis*, σ^G-dependent transcription is detected in the PS before engulfment is completed, and is partially independent of σ^E, although its activity increases following engulfment completion (Fimlaid *et al.*, 2013; Serrano, Kint, *et al.*, 2016). This is interesting because in *B. subtilis*, the activity of σ^G is only detected following engulfment completion and is dependent in the assembly of a MC-to-PS channel through which the MC is thought to supply essential metabolites for continued macromolecular synthesis in the PS (Serrano, Kint, *et al.*, 2016). The channel is assembled from the products of the conserved MC-specific *spoIIIA* operon and *spoIIQ*, expressed in the PS (Serrano, Crawshaw, *et al.*, 2016). In *C. difficile*, assembly of the channel is only required for the post-engulfment period of activity (Serrano, Crawshaw, *et al.*, 2016; Dembek *et al.*, 2018).

In *C. difficile*, the activity of σ^K is detected during engulfment, although it increases following engulfment completion. The σ^E regulon in *C. difficile* is not strictly under σ^F control even though the product of the PS gene *spoIIR* is required for pro-σ^E processing by the SpoIIGA membrane-embedded protease. This appears to result from residual *spoIIR* expression even in a *sigF* mutant (Pereira *et al.*, 2013). σ^K lacks a pro-sequence and its activity is independent of σ^G. A key element in the control of σ^K activity is the excision of the *skin* element, which interrupts the *sigK*-encoding gene. Excision of the *skin* element is required for proper control of σ^K activity and involves a constitutively active recombinase and a recombination directionality factor produced in the MC under control (Serrano, Kint, *et al.*, 2016). Even though the activity of σ^K is largely independent on the PS line of gene expression, a control of the PS on σ^K target genes seems to be maintained through a σ^F-dependent as yet uncharacterized mechanism (Saujet *et al.*, 2013). Together, σ^E and σ^K are the main effectors in the assembly of the spore surface layers, *i.e.*, the cortex PG layer and the coat and exosporium (**Figure 1.2**) (Pereira *et al.*, 2013).

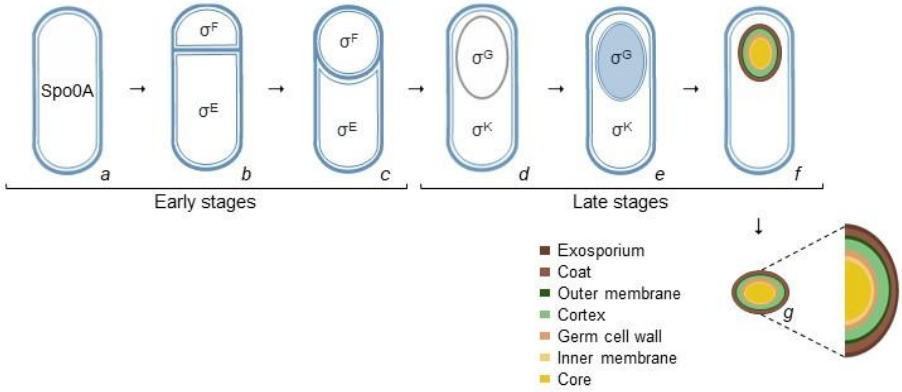

Figure 1.2: Morphological stages and compartmentalized activation of the sporulation specific σ factors of *C. difficile*. Sporulation involves asymmetric cell division (predivisional cell) and during which a copy of the genome is partitioned into each of the sister cells. The smaller cell, or PS, develops into the mature endospore and the larger cell, or MC, contributes to the differentiation process but undergoes autolysis following its completion to release the endospore into the surrounding medium. Soon after division, the MC initiates a membrane migration and fusion process analogous to phagocytosis whereby it engulfs the PS, insulating it within a double membrane system derived from the septum. Following engulfment completion, two types of PGs are layered between the inner and outer membranes surrounding the PS. The surface of the inner spore membrane is the site of assembly of a thin layer of PG called the primordial germ cell wall (orange), similar in composition to the vegetative cell wall that serves as the primordial wall of the newly formed vegetative cell following spore germination. The outer PS membrane is the site of assembly of a second, thicker, and chemically distinct layer of PG called the spore cortex (green) and coat (brown) layer which is synthesized and deposited around the developing spore (Henriques and Moran, 2007). The cell where σ^F, σ^G, σ^E and σ^K are active and their main period of activity is indicated (Pereira *et al.*, 2013).

1.1.4. Biofilms

Biofilms are structured communities of microorganisms associated with surfaces (biotic or abiotic) and encased in a self-produced extracellular matrix, which contain proteins, DNA, and exopolysaccharides (EPS). The composition of the extracellular matrix varies among bacterial species (Dubois, Yannick D.N. Tremblay, *et al.*, 2019; Du *et al.*, 2020). Although biofilms are often attached to solid surfaces, they can also form in other environments, for example, at liquid-air interfaces (Nobile and Johnson, 2015; Greenwich *et al.*, 2019). Biofilm formation is important because this mode of growth is associated with the chronic nature of infections, such as those related to the use of catheters, and with their inherent resistance to antibiotic chemotherapy (Stewart and Costerton, 2001; Høiby *et al.*, 2010). Biofilm formation is a multistage process that can be summarized in three stages: attachment, maturation, and detachment. The first stage can be divided into two other steps: initial reversible attachment and initial irreversible attachment, characterized by the production of a matrix and microcolonies develop into multi-layered cell clusters (Rabin *et al.*, 2015). During the maturation phase, chemical signals help recruit more cells to the biofilm, which starts to assume different roles and are distributed according to their metabolism and aerotolerance. Throughout this phase, bacteria produce more matrix components to fortify and consolidate the structure (**Figure 1.3**). The last stage is detachment of the biofilm, allowing

the cells to take on a planktonic state which allows the formation of a new biofilm in new surfaces (Soto, 2013; Van Acker *et al.*, 2014; Mitrofanova *et al.*, 2017). The National Institutes of Health estimate that biofilms are responsible, in one way or another, for over 80% of all microbial infections in the US (Nobile and Johnson, 2015; Goodwine *et al.*, 2019). Several mechanisms are thought to be involved in biofilm tolerance and resistance, including slow penetration of antimicrobial agents, changes in the chemical microenvironment within the biofilm, adaptive stress responses, and the presence of a small population of extremely antibiotic-tolerant 'persister' cells. In addition, rates of horizontal gene transfer are typically higher in biofilms than in planktonic cultures, and increased transfer of antibiotic resistance determinants on mobile genetic elements was noted for biofilms of various organisms (Stewart and Costerton, 2001; Van Acker *et al.*, 2014).

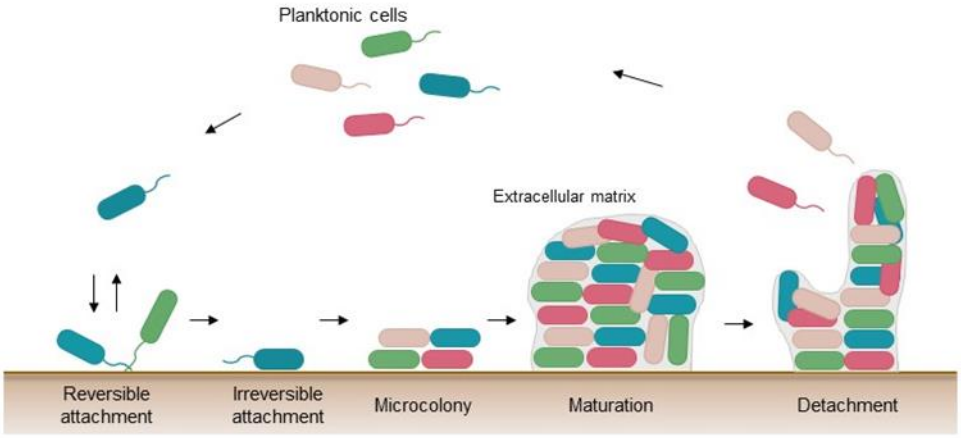

Figure 1.3: Schematic representation of bacterial biofilm formation. Biofilm formation is a multistage process in which free-floating planktonic cells adhere to the surface (initial reversible attachment), whereas the subsequent production of an extracellular matrix (containing exopolysaccharides, proteins, and DNA) results in a firmer attachment. Cells with different functions (represented by the different colours) co-exist within the biofilm, which is hold together by an extracellular matrix. Adapted from (Taggart et al., 2021).

In *C. difficile*, the interest in biofilm formation increased in the last years. In fact, Taggart and co-workers affirmed that biofilm formation and bacterial overgrowth in the gut is a serious threat because of increasing antibiotic resistance, making treatments less effective (Taggart *et al.*, 2021). Furthermore, it has been hypothesized that *C. difficile*'s virulence and recurrence are due, at least in part, to its ability to form biofilms in the gut (Taggart *et al.*, 2021). *C. difficile* can form biofilms as a single species or with other anaerobic intestinal bacteria on different abiotic surfaces. Moreover, *C. difficile* can incorporate a multi-species biofilm formed in a chemostat modelling the human gut or cell communities *in vivo*. There are several factors that influence *C. difficile* biofilm formation, including adherence and motility, cell surface components and regulators (*e.g.*, pili and the S-layer), environmental factors (*e.g.*, DOC and sub-MIC of metronidazole and vancomycin), quorum sensing (*e.g.*, *luxS*), pyruvate and other factors (*e.g.*, c-di-GMP). Furthermore, in *C. difficile*, inactivation of the gene coding for the global regulator of carbon catabolic repression (CCR) system, *ccpA*, reduces biofilm formation in response to DOC (Dubois, Yannick D.N. Tremblay, *et al.*, 2019; Tremblay *et al.*, 2021). Nevertheless, the biology of biofilm formation by *C. difficile* in the GI environment is still poorly characterized (Dubois, Yannick D.N. Tremblay, *et al.*, 2019).

1.1.5. Epidemiology and risk factors of CDI

Epidemiology has been changing in the past years and one of the most notorious changes has been the apparent increased incidence among populations in the community who were historically considered to be at low risk, such as healthy peripartum women, children, antibiotic-naïve patients, and those with minimal or no recent healthcare exposure (Depestel and Aronoff, 2013). As described before, *C. difficile*

was identified as the causative organism of antibiotic-associated colitis, in the 1970s. From 2003 to 2006, CDI was observed to be more frequent, associated with more severe cases and outbreaks, refractory to standard therapy and more likely to relapse. These more severe outbreaks have been attributed to the emergence of a new strain designated BI, NAP1 or ribotype 027 (RT027). This strain is associated with its ability to produce high concentrations of toxins, high transmissibility, high sporulation rate, production of the binary toxins, variation in the *tcdC* repressor gene and resistance to fluoroquinolones due to the presence of mutations in *gyrA* (Janoir *et al.*, 2013; Goudarzi *et al.*, 2014; Harnvoravongchai *et al.*, 2017). The use of fluoroquinolones strongly correlated with the emergence of fluoroquinolone-resistant strains of RT027; on the other hand, development of fluoroquinolone resistance was associated with the increased frequency of CDI outbreaks (Goudarzi *et al.*, 2014; Abdrabou *et al.*, 2021). The molecular epidemiology of *C. difficile* is varied: a different ribotype can predominate in a particular area during certain periods and at the same time is extremely rare elsewhere. From 1998 to 2009, the number of US hospitalizations with a principal diagnosis of CDI increased from 25,200 to 110,600, reaching a plateau from 2008 to 2009. Like ribotype 027 in North America, ribotype 078 has been on the rise in Europe since 2005. Strains of this ribotype are also associated with increased community-acquired disease, younger age, a possible zoonotic origin for some strains, and lack of preceding antibiotic therapy (Burke and Lamont, 2014; Zhang *et al.*, 2019). From 2007 to 2010, a 61% reduction in the incidence of CDI was observed in England, presumably because of the success of expanded prevention and control efforts, changes in the prevalence of epidemic strains (*i.e.*, ribotype 027) or both (Depestel and Aronoff, 2013). Nowadays, in Europe, RT027 strains are still a concern, even though their impact varies considerably from country to country. However, on a local level, larger regional differences may be evident, with RT018 dominating in Italy, RT176 playing an important role in Poland and the Czech Republic (Abdrabou *et al.*, 2021), and RT017 in Portugal, the only European country to report a prevalence higher than 10% (Isidro, Santos, *et al.*, 2018; Zhang *et al.*, 2019).

Risk factors for CDI are classified as pharmacological (*e.g.*, use of antibiotics, non-steroidal anti-inflammatory drugs, and corticosteroids), host-related (*e.g.*, age ≥65 years, or having chronic kidney disease, diabetes mellitus, lymphoma, and congestive heart disease), or associated with clinical interventions (*e.g.*, duration of hospitalisation, nasogastric tube feeding, intensive care unit stay, and surgery) (Wolfe *et al.*, 2018; Al-Tawfiq *et al.*, 2020; Enoch *et al.*, 2020). In fact, exposure to clindamycin and broad-spectrum antibiotics (*e.g.*, 2nd and 3rd generation cephalosporins, broad spectrum penicillins and fluoroquinolones), which disrupt the natural gut microbiota, allows the growth of toxigenic antibiotic-resistant *C. difficile* from spores followed by colonization and infection (Goudarzi *et al.*, 2014; Nagy, 2018; Czepiel *et al.*, 2019).

1.1.6. Diagnosis and treatment of CDI

The diagnosis of CDI is based on detection of *C. difficile* toxins directly in a stool sample, most commonly with an enzyme immunoassay (EIA), which provides rapid turnaround time, as well as high sensitivity and specificity (Elliott *et al.*, 2017; Nagy, 2018; Czepiel *et al.*, 2019). Since it has a low cost, this is the most popular laboratory test. Tests detecting *C. difficile* antigens are based on the detection of glutamate dehydrogenase (GDH) and are characterized by ease of use and rapid turnaround time as well as a specificity of nearly 100%; they do not inform, however, on whether the individual is infected by a toxinogenic strain (Smits *et al.*, 2016; Nagy, 2018; Czepiel *et al.*, 2019). Tests that use amplification of nucleic acid (nucleic acid amplification test, or NAAT) were introduced in 2009 (Czepiel *et al.*, 2019; Webb *et al.*, 2020). They are based on either a conventional PCR method or isothermal amplification. NAAT has higher sensitivity and specificity compared to an EIA test. The specificity is especially important in the presence of a negative result in which case another cause of diarrhoea should be considered. PCR detects the presence of a toxin encoding gene, thus confirms the presence of *C. difficile* toxin-producing strain, but it doesn't necessarily mean that the toxins were being produced. A cytotoxic assay

test (CYTA) is not routinely used in microbial culture due to its slow turnaround time and lack of standardization. According to the European Society of Clinical Microbiology and Infectious Diseases (ESCMID) the best way to optimize diagnosis of CDI is the combination of two tests. Another way to diagnosis is endoscopy which is only indicated if problems occur before, like a typical CDI presentation with negative *C. difficile* test results, no response to standard course of antibiotics or when an alternative diagnosis is suspected, and direct visualization and/or biopsy of the bowel mucosa is needed (Czepiel *et al.*, 2019).

Treatments for symptomatic CDI include Faecal Microbiota Transplant (FMT)/Live Biotherapeutics (LB), vaccines, phage, probiotic therapy and antibiotic therapy (Tsutsumi *et al.*, 2014; Frieden, 2019; Mondal *et al.*, 2021). FMT and LB use helpful bacteria that may assist in repairing a person's microbiome upon dysbiosis (Frieden, 2019). FMT has been known for over 1000 years and has the highest rate of prevention of recurrent CDI among all therapeutic options (Czepiel *et al.*, 2019). This is a treatment of last resort following multiple recurrent disease episodes, even though it is highly effective, cheap, and safe. The main drawbacks to the use of faecal transplantation are concerns of potential transmission of unscreened or undetected transmittable infectious diseases (Tsutsumi *et al.*, 2014).

As mentioned above, symptoms of CDI are mediated by the TcdA and TcdB toxins and the presence of antibodies against TcdA or TcdB is associated with protection against CDI (Antunes *et al.*, 2012; Saujet *et al.*, 2013). This suggests that a toxoid vaccine could prevent or reduce the incidence of infection or mitigate its symptoms. The low number and moderate efficacy of available treatment options for CDI, as well as the high incidence of disease recurrence, makes the development of such a vaccine for the prevention of symptomatic CDI a priority (Hong *et al.*, 2017). In recent years, several vaccines have been under development for CDI. One, from Sanofi Pasteur, is a formalin-inactivated formulation of *C. difficile* Toxin A and Toxin B; however, in 2017 this product was discontinued since the results of trials did not fulfil the primary object. Valneva has developed a recombinant fusion protein consisting of truncated *C. difficile* Toxin A and Toxin B, but phase III trials are not yet completed. A recombinant toxin-based vaccine developed by Pfizer, is currently in phase III (Awad *et al.*, 2015; Smits *et al.*, 2016; Pizarro-Guajardo *et al.*, 2019). A last one, is an oral based on the display at the surface of *B. subtilis* spores of a peptide derived from the receptor-binding region of TcdA; immunization with the recombinant spores afforded protection to mice in subsequent challenge experiments with *C. difficile* (Permpoonpattana *et al.*, 2013; Hong *et al.*, 2017; Shen, 2020).

Phage therapy involves the targeted application of phages, with a narrow spectrum host range infecting and killing specific pathogenic bacteria. Bacteriophage-derived lytic enzymes, or endolysins, are potential antimicrobial candidates. Endolysins or lysins rapidly degrade the cell wall PG at the end of the lytic cycle to allow release of the phage progeny. Bacteriophage endolysins have been investigated as potential antimicrobials via their ability to degrade Gram-positive cell walls when applied externally. Although *C. difficile* lysin research still in the beginning, phage therapy has raised interest as an alternative therapeutic for CDI (Mondal *et al.*, 2021).

Probiotics are preparations of live microorganisms which help to restore the balance of indigenous GI microbiota that may be altered for example during antibiotic therapy. Proposed mechanisms of probiosis in restoring the normal flora or help prevent colonization by *C. difficile* include competing for nutrients (nutrient competition and exclusion), stimulating the host's immune function (immune exclusion), and inhibiting and maintaining integrity of the GI mucosa by preventing adhesion and invasion by other pathogenic microbial flora (Tsutsumi *et al.*, 2014). Probiotic therapy is promising, but further comprehensive research and studies are still essential (Mondal *et al.*, 2021). The use of non-toxinogenic strains of *C. difficile* as probiotics has been proposed (Brouwer *et al.*, 2013; Isidro *et al.*, 2017).

Finally, antibiotic therapy remains the main treatment of choice for CDI. Oral antibiotics such as metronidazole (MTZ) and vancomycin (VAN) are commonly prescribed for the first line treatment of CDI. These antibiotics impact considerably the commensal gut microbiota and increase the possibility

of post-treatment relapse. MTZ was first-line drug in non-severe CDI, while VAN was the drug of choice for severe CDI (Czepiel *et al.*, 2019). Approximately 24% and 27% of patients experience recurrence of CDI following VAN or MTZ treatment, respectively (Louie *et al.*, 2011; Rohani *et al.*, 2018). Relapse could happen because of the incomplete removal of *C. difficile* and resumption of the primary infection, which accounts for most cases, or the acquisition of a new strain. In both cases, patients are particularly at risk following antibiotic-induced dysbiosis of the gut microbiota (Liu and Breukink, 2016). Fidaxomicin is another option, available since 2011, it is less toxic to obligate anaerobic commensal bacteria and more effective against recurrent CDI, although it has a high cost associated which limits its clinical use. Fidaxomicin acts through the inhibition of RNA polymerase (Harnvoravongchai *et al.*, 2017; Banawas, 2018), and shows better performance than VAN at preventing disease recurrence (Wolfe *et al.*, 2018; Polivkova *et al.*, 2021). Since disease relapse is linked to the formation and persistence of spores in the organisms and the immediate environment, the superior performance of fidaxomicin at preventing recurrence may arise from its ability to prevent entry into sporulation (Babakhani *et al.*, 2012; O'Grady *et al.*, 2021).

The use of additional antibiotics (other than those treating CDI) is associated with an increased risk of prolonged diarrhoea and CDI recurrence, which is why they should be discontinued. Therefore, the development of new drugs is vital. An ideal candidate would be a bactericidal agent with targeted activity against *C. difficile* without causing collateral damage to the indigenous gut microbiota (Czepiel *et al.*, 2019; Mondal *et al.*, 2021).

1.2. Antibiotic resistance

1.2.1. General mechanisms of resistance

Antibiotic resistance is a global health crisis exacerbated by a deficiently unhealthy antibiotic drug pipeline (Wolfe *et al.*, 2018; Frieden, 2019). The supply of new medicines is insufficient to keep up with the increase in drug resistance as older medicines are used more widely and microbes develop resistance. At the same time, the demand for these medicines is very badly managed; large quantities of antimicrobials, in particular antibiotics, are wasted globally on patients and animals who don't need them, while others who need them don't have access (Derouaux *et al.*, 2011; Jim O'Neill, 2016). A dramatic change in the epidemiology of CDI has been noted in the last decades. The emergence and spread of hypervirulent *C. difficile* strains are probably responsible for the increased morbidity and mortality of CDI (Kouhsari *et al.*, 2019).

In *C. difficile*, antibiotic resistance is multifactorial and complex (Harnvoravongchai *et al.*, 2017). Genetic analysis has shown that *C. difficile* has a versatile genome, and several mechanisms responsible for antibiotic resistance have been identified, including horizontal gene transfer, chromosomal resistance genes, mobile genetic elements (MGEs), alterations in the antibiotic targets and/or in metabolic pathways, and biofilm formation (Peng *et al.*, 2017; Isidro, Menezes, *et al.*, 2018; Spigaglia *et al.*, 2018). Treatment with broad-spectrum antibiotics disrupts the naturally diverse intestinal microbiota, enabling the growth of *C. difficile*, with antibiotic resistant strains at a clear advantage, including toxin-producing pathogenic strains (Yamaguchi *et al.*, 2020).

1.2.2. The peptidoglycan biosynthetic pathway

Some of the most successful and widely-used antibiotics, such as the β-lactams and glycopeptide antibiotics, target the PG synthesis pathway. PG is a rigid molecule that provides cells shape, protection, and scaffolding for extracellular proteins and structures (Fay *et al.*, 2010a). Compromising the PG layer renders the cell susceptible to the osmotic pressure and can lead to cell death (Liu and Breukink, 2016; Isidro *et al.*, 2017). PG is composed of two alternating sugar derivatives, N-acetylglucosamine (NAG) and N-acetylmuramic acid (NAM) linked by β-1,4-glycosidic bonds (Sapkota *et al.*, 2020). The NAM

residue has a stem peptide linked to the carboxyl group and adjacent chains are cross-linked through the formation of peptide bonds between the stem peptides of alternating strands (Sauvage and Terrak, 2016). In Gram-negative bacteria, the stem peptide typically has the sequence L-Ala, D-Glu, meso-diaminopimelate (mDAP), D-Ala and D-Ala. In some Gram-positive bacteria, however, mDAP is replaced by L-Lys (Scheffers and Pinho, 2005; Sobhanifar *et al.*, 2013; Isidro *et al.*, 2017).

The biosynthesis of PG can be divided into three different stages (**Figure 1.4**). The first stage occurs in the cytoplasm and results in the production of the nucleotide precursors UDP-NAG and UDP-NAM-pentapeptide. In the second stage, which takes place at the cytoplasmic membrane, precursor lipid intermediates are synthesized. The final stage takes place at the outer side of the cytoplasmic membrane, and results in the polymerization of the disaccharide-peptide units into the growing PG (Scheffers and Pinho, 2005; Barreteau *et al.*, 2008; Liu and Breukink, 2016). First, synthesis of the nucleotide sugar-linked precursors UDP-NAM-pentapeptide takes place in a series of reactions catalysed by the Mur ligases (Mur A to F) from UDP-NAG. Two sequential reactions catalysed by MurA and MurB converts UDP-NAG to UDP-NAM. Next, the amino acids of the stem peptide are added to the UDP-NAM residue through the sequential action of MurC, D, E and F. MurC is responsible for the addiction of the first amino acid, L-Ala. MurD recognizes the UDP-NAM-L-Ala and adds the second amino acid (D-Glu). Mur E adds the third amino acid, either mDAP or L-Lys. Finally, MurF adds the fourth and fifth as a dipeptide D-Ala-D-Ala (D-Ala-D-Ser or D-Ala-D-Ala in some VAN-resistant organisms; see also below), leading to the formation of UDP-NAM-pentapeptide. D-cycloserine inhibits the Alr2 racemase, involved in the formation of D-Ala from L-Ala, and the Ddl D-Alanyl-D-Ala ligase (**Figure 1.4**) (Barreteau *et al.*, 2008; Liu and Breukink, 2016).

In the following stage, the phospho-NAM-pentapeptide moiety of UDP-NAM-pentapeptide is transferred to the membrane receptor undecaprenyl pyrophosphate (bactoprenol), a reaction catalysed by the integral membrane protein MraY; this reaction produces undecaprenyl-pyrophosphoryl-NAM-pentapeptide (lipid I). At this point MurG catalyses formation of a glycosidic bond between NAM and NAG molecules, generating the PG monomer undecaprenyl-pyrophosphoryl-NAM-pentapeptide-NAG (lipid II), which is the substrate for the polymerization reactions in bacteria that have direct cross-linked PG (Scheffers and Pinho, 2005). The use of a lipophilic molecule such as bactoprenol enables the cell to transport highly hydrophilic precursors from the cytoplasm, through the hydrophobic membrane, and to the external sites of incorporation into the growing PG. Translocation of the lipid-linked precursor from the cytoplasmic side to the trans side of the membrane is catalysed by translocases (or flippases), such as the MurJ and SpoVB (which functions during spore formation) proteins in *B. subtillis* (**Figure 4**) (Scheffers and Pinho, 2005; Liu and Breukink, 2016; Isidro *et al.*, 2017).

The third and final stage of PG biosynthesis involves the polymerization of the newly synthesized disaccharide-peptide units and incorporation into the growing PG. In the transglycosylation reaction, for the formation of glycan strands, the C1 from the NAM residue of the nascent strand is likely transferred onto the C4 from NAG residue of the lipid II-linked precursor. Cross-linking of the glycan strands generally occurs between the D-Ala at position 4 of the stem peptide and the mDAP (or L-Lys) at position 3 of a stem peptide from an adjacent strand to form a 4-3 cross-link. This reaction is catalysed by the transpeptidase domain present in all D,D-transpeptidases [TPases, or penicillin-binding proteins (PBPs)] that can cleave the D-Ala-D-Ala bond of the stem peptide, releasing the last D-Ala residue, which energizes the transpeptidase reaction (Isidro et al., 2017). The undecaprenyl-pyrophosphate is translocated back to the inner side of the membrane and recycled, to receive a new UDP-NAM-pentapeptide molecule (Scheffers and Pinho, 2005).

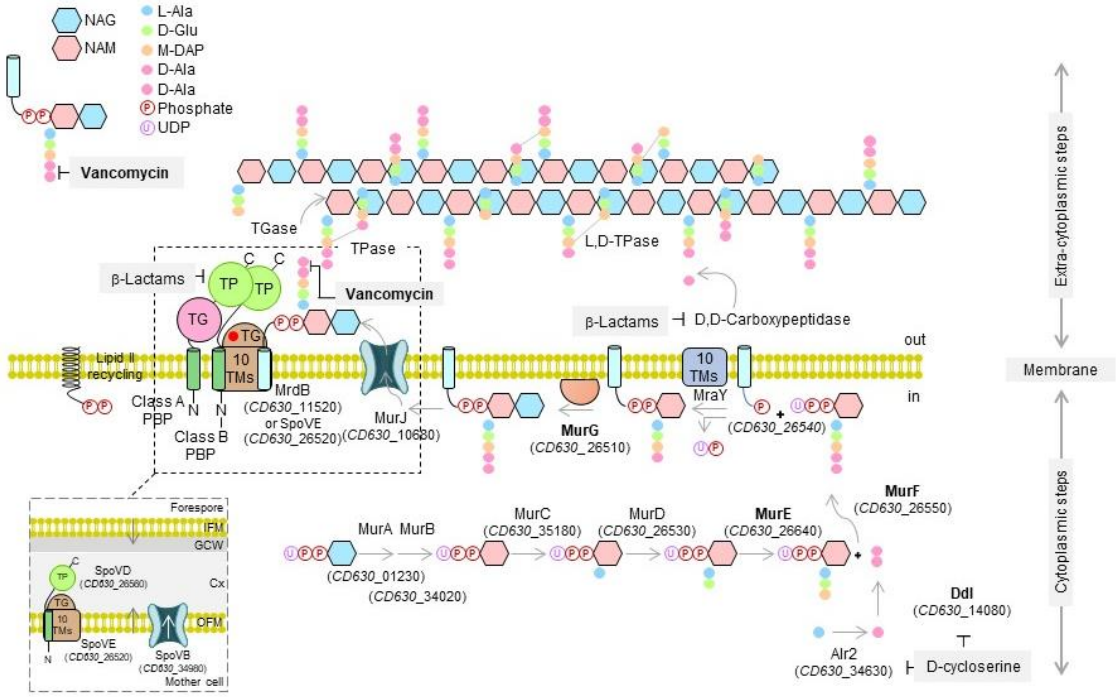

Figure 1.4*:* Representative PG synthesis pathway. The *C. difficile* counterparts of the genes known to intervene at the represented steps in the cytoplasmic, membrane-bound, and extracellular steps of PG biogenesis are highlighted. No cytoskeletal proteins are drawn for simplicity. Synthesis of the spore cortex (Cx) PG (boxed complex) follows a similar pathway but may involve sporulation-specific proteins, including a complex between a SEDS-type transglycosylase, SpoVE, and SpoVD a Class B PBP; SpoVB may be a MC-specific lipid II flippase (IFM, inner PS membrane; OFM, outer PS membrane). The direction of synthesis of the Cx and the primordial germ cell wall is shown by arrows. Steps blocked by β-lactams and VAN are shown. TM, transmembrane domain; TG, transglycosylase domain; TP, transpeptidase domain. Adapted from (Isidro *et al.*, 2017), with permission.

As mentioned before, the spore cortex is composed of a thick layer of PG that is the main responsible for the resistance of spores to heat and desiccation. The cortex is formed between the inner and outer PS membranes (**Figure 1.2**) and requires the activity of several proteins that are synthesized in the MC, including SpoVE, the founding member of the SEDS (Shape, Elongation, Division and Sporulation) protein family (Henriques *et al.*, 1995; Henriques and Moran, 2007; Real *et al.*, 2008; Fay *et al.*, 2010b). *spoVE* mutants fail to form the cortex and accumulate cytoplasmic PG precursors, which indicates a defect at an initial step in PG polymerization and emphasizes the role of SpoVE in cortex PG synthesis (Henriques *et al.*, 1992; Vasudevan *et al.*, 2007). Also, this protein localizes to the outer membrane and interacts both *in vivo* and *in vitro* with SpoVD, a PBP controlled by σ^E that is also required for spore cortex synthesis (**Figure 1.4**) (Real *et al.*, 2008; Fay *et al.*, 2010a; Alabdali *et al.*, 2019). The interaction with SpoVD and the accumulation of PG precursors are consistent with the recent characterization of members of the SEDS family as a new class of membrane embedded transglycosylases which form complexes with dedicated PBPs TPases to drive PG synthesis during elongation (RodA), division (FtsW) and sporulation (SpoVE) (Real *et al.*, 2008; Fay *et al.*, 2010a; Higgins and Dworkin, 2012). SpoVE and the TPase SpoVD are thought to be the core of the PG-synthesizing complex that drives biogenesis of the spore cortex in *B. subtilis*, and it is likely that such a complex also operates in *C. difficile* (Alabdali *et al.*, 2019; Srikhanta *et al.*, 2019). As stated before, another protein needed for spore cortex synthesis is SpoVB, possibly a MC-specific lipid II flippase (**Figure 1.4**) (Isidro *et al.*, 2017).

The structure of the cell wall PG is unusual in *C. difficile*, since most of the cross-links (around 80%) are of the 3-3 type formed by L,D-transpeptidases (LDTs) (Barreteau *et al.*, 2008). In most other bacterial species that have been studied the PG contains mainly or exclusively 4-3 cross-links formed by the D,D-transpeptidase activity of classical PBPs synthases (Barreteau *et al.*, 2008). LDTs and PBPs are structurally unrelated and have different catalytic residues (Cys and Ser, respectively). PBPs are

potentially inhibited by all classes of β-lactams, whereas LDTs are inhibited only by carbapenems (Peltier *et al.*, 2011; Isidro *et al.*, 2017; Sutterlin, 2018). Importantly, LDTs and PBPs use distinct acyl donors for the cross-linking reaction; the PBPs use as substrates muropeptides ending in D-Alanyl-D-Ala while the LDTs use tetrapeptides, which are generated through the activity of carboxypeptidases (Peltier *et al.*, 2011). The genome of *C. difficile* codes for three Ldts designated Ldt_{CD1}, Ldt_{CD2} and Ldt_{CD3}. Inactivation of the $ldt_{CD1}ldt_{CD2}$ genes, decreases the abundance of 3-3 cross-links and the overall PG reticulation, without affecting the growth rate. This suggests that Ldt_{CD1} and Ldt_{CD2} have redundant roles in cross-linking (Sutterlin, 2018). Interestingly, while at least the functional prevalence of the LDTs and thus the reduced presence of D-Alanyl-D-Ala-ending stem peptides could contribute to VAN resistance, *C. difficile* is susceptible to this antibiotic (Ghosh *et al.*, 2008; Mainardi *et al.*, 2008; McBride and Sonenshein, 2011; Peltier *et al.*, 2011; Ammam *et al.*, 2013; Isidro *et al.*, 2017).

1.2.3. Resistance to vancomycin

VAN is a glycopeptide antibiotic traditionally used as a "last resort" for the treatment of Gram-positive bacterial infections, including serious cases of CDI. VAN, however, is increasingly used as a first-line drug in part because resistance to another effective antibiotic used for CDI, MTZ, is rising (Yarlagadda *et al.*, 2014; Kouhsari *et al.*, 2019). Resistance to VAN was reported over 30 years ago when VAN resistant enterococci (VRE) were isolated, and has become a major health problem (Ammam *et al.*, 2013; Stogios and Savchenko, 2020). Therefore, the emergence and wide spreading of VAN resistance would be catastrophic. Reduced susceptibility of *C. difficile* to VAN was already observed in two emergent RTs (RT018 and RT356) in a pan-European survey and also among US isolates of RT027 (Tickler *et al.*, 2014; Freeman *et al.*, 2015). The lethal target of VAN is the D-Ala-D-Ala motif in lipid II, the membrane-bound intermediate in the pathway of PG biosynthesis (Scheffers and Pinho, 2005; Gardete and Tomasz, 2014; Liu and Breukink, 2016; see above; **Figure 1.4**). In several pathogens, the expression of *van* gene clusters is sufficient to afford resistance to VAN (Derouaux *et al.*, 2011).

The susceptibility of *C. difficile* to VAN is intriguing because most epidemic strains carry a *vanG*-type cluster ($vanG^{Cd}$; present in 85% of the clinical isolates) (**Figure 1.5A**). *van* clusters code for enzymes that synthesize PG precursors ending in D-Ser or D-Lac and that eliminate the natural D-Ala-D-Ala precursors. There are three enzymes required for the synthesis of D-Ala-D-Ser ending precursors: *vanT* codes for a racemase that converts L-Ser and L-Ala to D-Ser and D-Ala; *vanG* codes for a ligase that synthesis D-Ala-D-Ser; and *vanXY* codes for a bifunctional dipeptidase/carboxypeptidase that hydrolyses the C-terminal D-Ala residue of the natural PG precursors (Ammam *et al.*, 2013). Precursors ending in D-Ser or D-Lac show reduced affinity for VAN relative to D-Ala-D-Ala (Gardete and Tomasz, 2014; Yarlagadda *et al.*, 2014; Stogios and Savchenko, 2020). The *van* operon *C. difficile* cluster is functional; its induction results in the accumulation of UDP-NAM-pentapeptide ending in D-Ser in the cell wall and the transplantation of the *van* cluster to *E. coli* allowed survival in the presence of VAN (Ammam *et al.*, 2013; Tsutsumi *et al.*, 2014; Stogios and Savchenko, 2020). Moreover, the activities of the VanG, VanT and VanXY enzymes have been verified, although VanT shows a slight preference for L-Ala over L-Ser (Ammam *et al.*, 2013).

van clusters include a transcriptional regulator (*vanR*) and a membrane-associated kinase (*vanS*) (Ammam *et al.*, 2013; Stogios and Savchenko, 2020) (**Figure 1.5A**). VanR consists of a N-terminal response regulator receiver domain and a C-terminal winged helix-turn-helix DNA binding domain and is activated through phosphorylation by *vanS*. *vanS*, in turn, is a histidine kinase which contains a N-terminal membrane-embedded half that includes an extracellular sensor domain thought to bind VAN and a C-terminal cytoplasmic kinase domain (Ammam *et al.*, 2013; Stogios and Savchenko, 2020).

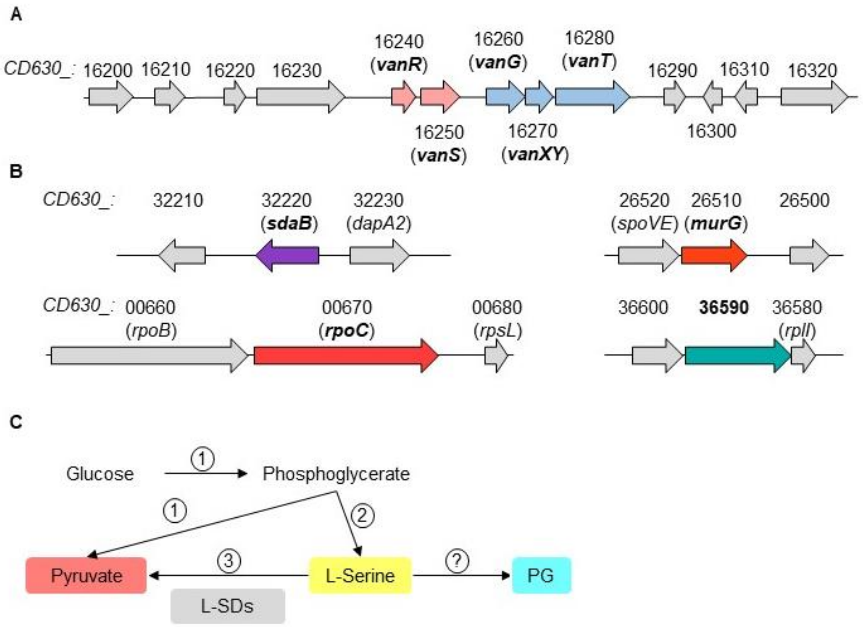

Figure 1.5: A: Schematic representation of the *vanG*^{Cd} gene cluster. Transcription of the *vanG*^{Cd} cluster is inducible by VAN. **B:** Schematic representation of the *sdaB*, *murG*, *rpoC and CD630*_36590 regions of the *C. difficile* 630Δ*erm* chromosome, where mutations possibly associated with VAN resistance have been found. **C:** Conversion of serine into pyruvate catalysed by L-Serine Deaminases (L-SDs) in *E. coli*. Glucose is converted to phosphoglycerate and pyruvate via the Embden Meyerhof pathway (1). Phosphoglycerate is the first precursor of L-Serine (2) which may be converted to pyruvate by any of the three L-SDs (3). In *C. difficile* the conversion of pyruvate can only be made by *sdaB*, which is the only gene coding for a L-SD. Adapted from (Zhang and Newman, 2008).

Two strains of *C. difficile* with reduced susceptibility to VAN have been isolated (Ammam *et al.*, 2013). One strain bears mutations in three genes, *murG*, *CD630*_36590 and *sdaB* (**Figure 1.5B**) (Leeds *et al.*, 2014). *murG* codes for a NAG transferase that attaches NAG from UDP-NAG to lipid I, producing lipid II during the membrane-bound stage of PG biosynthesis (Ammam *et al.*, 2013; Stogios and Savchenko, 2020; Liu and Breukink, 2016). The mutation in *murG* causes the replacement of a conserved proline at position 108 by a leucine, in a region of the protein involved in binding the charged phosphate groups of UDP-NAG (Ha *et al.*, 2000; Leeds *et al.*, 2014). Possibly, the substitution could favour resistance by allowing a better interaction with lipid I ending in D-Ser or D-Lac. The mutation in *CD630*_36590 results in a stop codon after amino acid 326 in an RNA/single stranded DNA exonuclease (Leeds *et al.*, 2014). Finally, a single amino acid deletion in a stretch of alanines (positions 292–295) in L-Serine deaminase (coded for by *sdaB*). A second strain bears a mutation in *rpoC* causing a substitution, D244Y, in the RNA polymerase subunit β'. *rpoC* mutations are associated with resistance not only to RNAP inhibitors such as rifampicin but to other antibiotics (Venugopal and Johnson, 2012; Leeds *et al.*, 2014; Banawas, 2018). Interestingly the D244Y substitution is in a region of β' not previously associated with resistance to RNAP inhibitors. Both the mutations in *rpoC* and in *CD630*_36509 are likely to cause changes in gene expression that promote VAN resistance. Although the mutants were never studied in detail, the isolation of these strains suggests that VAN resistance can emerge by different mechanisms an inference that is supported by studies in *Staphylococcus aureus* (Gardete and Tomasz, 2014). In this work, we focused on the possible individual contribution of *sdaB* to VAN resistance.

1.2.3.1. The *sdaB* gene

The enzymatic nonoxidative deamination of serine to pyruvate and ammonia is performed by many organisms, including bacteria, yeast, plants and vertebrates (Shao *et al.*, 1994; Ogawa *et al.*, 2006). Glycolysis and the deamination of both serine and cysteine are likely the largest sources of pyruvate in *C. difficile* and serine deaminase activity was found to be especially high during growth in Brain Heart

Infusion (BHI) (Gencic and Grahame, 2020). The *C. difficile sdaB* gene (*CD630*_32220) encodes a serine deaminase (also named serine dehydratase) with a high degree of sequence similarity to the 4RQO protein of *Legionella pneumophila* (**Figure 1.6**) (Onainor, 2012; Yan *et al.*, 2015). SdaB appears to be a type 2 L-Serine deaminase (L-SD2), a family that is widely distributed in prokaryotes (Gencic and Grahame, 2020). L-SD2 enzymes are pyridoxal-5'-phosphate (PLP)-independent, iron sulfur cluster-containing [4Fe-4S] and consists of a single polypeptide chain (Gencic and Grahame, 2020). In *C. difficile*, the expression of *sdaB* is induced by glucose and positively controlled by *ccpA* (Antunes *et al.*, 2012).

In *E. coli*, L-Serine is deaminated by three very specific L-Serine deaminases, *sdaA*, *sdaB* and *tdcG*, which use a [4Fe-4S] cluster to catalyse the deamination of serine to pyruvate (**Figure 1.5C**) (Grabowski and Buckel, 1991; Zhang and Newman, 2008). Pyruvate is a central metabolite of bacteria, and its cellular concentration is under tight control (Dubois *et al.*, 2016). Deletion of all three deaminases results in a strong defect in cell shape and cell division (Shao *et al.*, 1994). These phenotypes are rescued by overproduction of MurC, which adds L-Ala to NAM, or by the overproduction of FtsW, a transglycosylase required for cell division (Taguchi *et al.*, 2019). This suggest that the MurC-catalysed reaction may represent a bottleneck in the pathway of precursor biosynthesis (see **Figure 1.4**); it also suggests that FtsW may not efficiently accept D-Ala-D-Ser precursors, which in turn may point to an essential requirement for D-Ala-D-Ala for cell division (Taguchi *et al.*, 2019). The genes coding for the three L-SDs of *E. coli* are expressed under different conditions: in minimal (*sdaA*) and complex media (*sdaB, tdcG*), during aerobic (*sdaA, sdaB*) and during anaerobic (*tdcG*) growth (Shao and Newman, 1993; Leeds *et al.*, 2014). *tdcG* is coded by a gene in an anaerobic threonine utilization operon, although it doesn't deaminate threonine but L-Serine deaminase (Zhang and Newman, 2008). In *E. coli, sdaB* is controlled by cabolite repression via cAMP and the catabolite activator protein, which suggests it is an essentially catabolic enzyme (Shao and Newman, 1993). In glucose-minimal medium with L-leucine, the regulatory protein Lrp affects expression of *sdaB* (Lin *et al.*, 1992). This suggests that L-Serine utilization must be of fundamental importance to the cell (Shao and Newman, 1993; Leeds *et al.*, 2014). SdaB is an iron-sulfur protein devoid of pyridoxal phosphate (Hofmeister *et al.*, 1993). Some serine deaminases are L-Serine-specific enzymes with an absolute requirement for ferrous iron (**Figure 1.6**). The low concentration of iron required to produce maximal activity suggests that the ion may be involved in catalysis. As mentioned above, the enzyme contains a [4Fe-4S] cluster that is bound to the protein via three cysteine residues that are coordinated to three of the irons of the cluster. The fourth iron is not coordinated by a cysteine residue but contains a bound hydroxyl group. In addition, the hydroxyl group of the substrate, as well as one of the substrate carboxylates groups, ligate the fourth iron in a bidentate fashion, resulting in hexa-coordination at this site (Cicchillo *et al.*, 2004). Cysteine is the sulfur donor for the biogenesis of the iron-sulfur clusters found in the catalytic site of several enzymes and assists in protein folding and assembly by forming disulfide bonds. Furthermore, cysteine can be catabolized by cysteine desulfhydrases or cysteine desulfidase, producing pyruvate and hydrogen sulfide (H_2S) (Dubois *et al.*, 2016). It is likely that the SdaB protein of *C. difficile* shares the main structural and enzymatic features of *E. coli* SdaB, but this has not yet been verified.

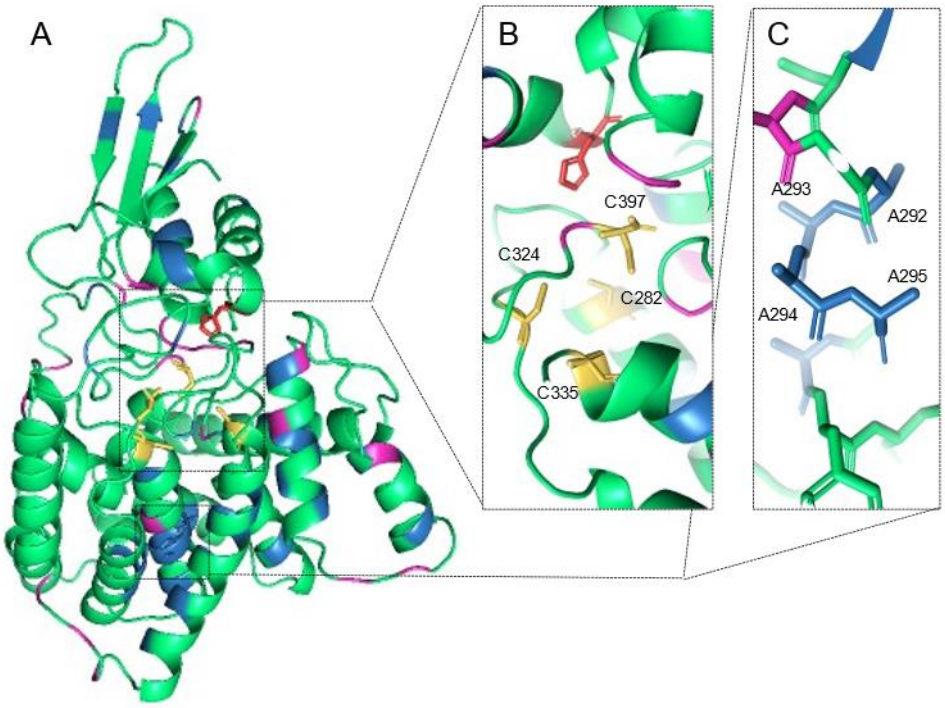

Figure 1.6: A: Homology model of the SdaB protein of *C. difficile* using the 4RQO protein of *Legionella pneumophila* as the template (www.sbg.bio.ic.ac.uk/phyre2). **B**: The cysteines involved in the coordination of the [Fe-S] cluster (not represented) are highlighted in yellow, and the catalytic histidine is shown in red. **C**: Shows the alanines in positions 292-295; deletion of Ala295 may be associated with resistance to VAN

1.3. Objectives of this study

We wanted to initiate studies aiming to understand the pathways involved in VAN resistance in *C. difficile*. Here, we focused on the *sdaB* gene because an in-frame deletion of an Ala codon (Ala295) appears in a VAN-resistant strain. Although the strain bears two other mutations (Leeds *et al.*, 2014), we reasoned that preventing the activity of SdaB, and thus impairing conversion of serine into pyruvate, could facilitate the incorporation of substrates ending in D-Ser into the PG. Our study therefore aimed at defining the contribution of *sdaB* to VAN resistance. The main goals of this dissertation were:

1) To study the expression of *sdaB* during growth and sporulation;
2) To characterize the phenotypes associated with a deletion of *sdaB* and with a mutant bearing the same mutation found in the VAN-resistant strain previously isolated;
3) Finally, to overproduce, purify and characterize the SdaB protein and its SdaB$^{\Delta Ala295}$ variant in an attempt to understand the properties of the altered protein in relation to VAN resistance.

2. Material and Methods

2.1. Strains and general growth conditions

E. coli strain DH5α was used as host for molecular cloning and plasmid propagation, while *E. coli* HB101 was used for conjugation of plasmids into *C. difficile*. *C. difficile* strains used in this study are congenic derivatives of the wild-type strain 630Δ*erm* (hereinafter referred as the wild-type, WT). Bacterial strains, plasmids and primers used in this work are described in Appendix 1, 2 and 3, respectively. *E. coli* was grown at 37ºC in Luria Bertani (LB) medium (1% tryptone, 0.5% yeast extract, 0.5% NaCl, pH 7.0). When appropriated ampicillin (100 µg mL^{-1}) and chloramphenicol (20 µg mL^{-1}) were added. Cultures of *C. difficile* 630Δ*erm* were carried out in BHI (brain heart infusion) medium, at 37ºC in an anaerobic chamber (5% H_2, 15% CO_2, 80% N_2). Liquid BHI medium was supplemented with anhydrotetracycline (aTc, 50 ng mL^{-1}) when appropriate. Bacteriological agar was normally used at a final concentration of 1.6% and, when needed, cefoxitin (25 µg mL^{-1}) and thiamphenicol (15 µg mL^{-1}) were added to the culture media. All strains were routinely stored at -80ºC in 20% glycerol.

2.2. DNA manipulation and molecular cloning

The Polymerase Chain Reaction (PCR) was used to amplify the desired DNA fragments for cloning utilizing the high fidelity Phusion DNA polymerase (Thermo Fisher Scientific). The reaction conditions were settled according to the oligonucleotides melting temperature, amplified product size and the manufacturer's indications for the DNA polymerase. PCR products were purified using the DNA Clean and ConcentratorTM - 5 Kit (Zymo research). DNA restriction and modification enzymes were acquired from Thermo Fisher Scientific and used according to the manufacturer's guidelines. All other general cloning methodologies were conducted as previously described (Sambrook and Green, 2012). Primer design for amplification of DNA from *C. difficile* 630Δ*erm* chromosome was based on the available *C. difficile* genomes from NCBI databases with accession number *CD630_RS17155*. The sequence of all newly constructed plasmids was verified by DNA sequencing.

2.3. Extraction and analysis of plasmid DNA

To identify transformants carrying the desired construct, plasmid DNA was extracted and analysed by digestion with appropriate restriction endonucleases. Isolated colonies resulting from *E. coli* DH5α transformation was incubated overnight in 10 mL of LB with chloramphenicol (20 µg mL^{-1}). Following this, 2 mL of these cultures were centrifuged 5 min at 13 000 x *g* and the sediment was suspended in 360 µL of STET buffer, 24 µL of lysozyme (10 mg mL^{-1}) and 10 µL of RNAse (10 mg mL^{-1}). Tubes were incubated at 37ºC for 1 h and after that, was boiled at 100ºC for 1 min, then, centrifuged 10 min at 13 000 x *g* and the sediment was removed with a loop. Isopropanol was added to a final concentration of 70% (v/v), and the sample centrifuged for 45 min at 13 000 x *g* at 4ºC. The sediment was collected and resuspended in 20 µL of ddH_2O. For sequencing, isolation of plasmid DNA was done using the "NZY Miniprep" (from Nzytech research) according to the protocol provided by the manufacturer.

To confirm the presence of specific DNA fragments, orange G loading buffer was added to the samples, and then they were subjected to 1% agarose gels in TAE 1X buffer. Gels run in the presence of ethidium bromide [0.001% (v/v)] at 120 V. The DNA was visualized using UV light (205 nm). The size of the fragments was measured by comparison with a commercial molecular size marker [1 Kilo base pair (kb) Plus DNA Ladder from Invitrogen].

2.4. Preparation of *E. coli* competent cells and transformation

Competent cells of *E. coli* were prepared as follows: LB medium (100 mL) was inoculated with 1:100 of an overnight *E. coli* culture and the new culture incubated at 37°C to an OD_{550} ~ 0.6. This culture was placed on ice for 15 min and centrifuged at 3500 x *g* for 20 min at 4°C. Then, the supernatant was removed, and the sediment was resuspended in ice-cold RF1 buffer, pH 5.8 (12 mg mL^{-1} RbCl, 9.9

mg mL^{-1} $MnCl_2$, 1.5 mg mL^{-1} $CaCl_2$, 11% glycerol, 3% KAc 1M pH 7.46) by pipetting gently up and down (30 mL per 100 mL of culture). After 15 min incubation on ice, the tube was centrifuged at 3 500 x *g* for 20 min at 4°C and the supernatant was removed. Then, the sediment was resuspended in ice-cold RF2 buffer, pH 6.8 (1.2 mg mL^{-1} RbCl, 8.3 mg mL^{-1} $CaCl_2$, 10% glycerol, 2% MOPS 0.5 M, pH 6.8) (8 mL per 100 mL of culture). Competent cells were stored at -80ºC, in aliquots of 200 µL and snap freeze in liquid nitrogen.

For transformation, competent *E. coli* cells were added to a ligation mix and incubated for 40 min on ice. A thermal shock was performed during 90 s at 42ºC followed by 2 min on ice. After a recovery period in 1 mL of LB medium at 37ºC, for 2 h, tubes were centrifuge 2 min at 6 000 x *g*. The supernatant (1 mL) was discarded, and the sediment was resuspended in the remaining supernatant; dilutions, if appropriate, were then plated in LA with the required antibiotic and the plates incubated overnight at 37ºC.

2.5. Conjugation into *C. difficile*

Plasmids were transformed into *E. coli* donor, HB101, and then conjugated into *C. difficile* 630Δ*erm*. *E. coli* HB101 with the plasmid of interest was inoculated in 5 mL of LB and incubated at 37ºC with agitation. At the same time, *C. difficile* 630Δ*erm* was inoculated with 10 mL of BHI and incubated at 37ºC under anaerobic conditions. At an OD_{600} of approximately 1, 1 mL of the *E. coli* culture was centrifuged at 4 000 x *g* for 2 min and the supernatant was discarded. The sediment was washed in 1 mL of LB. *E. coli* cells were resuspended in 300 µL of the *C. difficile* cell suspension and the conjugative mixture was pipetted in spots in a BHI plate. This plate was incubated under anaerobic conditions overnight. In the next day, cells were carefully scraped with a loop on the surface of the BHI plate. This content was resuspended in an eppendorf tube with 1 mL of BHI. Aliquots of 200 µL were then plated in 3 different BHI plates with cefoxitin (25 µg mL^{-1}) and thiamphenicol (15 µg mL^{-1}). Thiamphenicol was used to select for the *catP*-carrying plasmid and cefoxitin was used to counter select against *E. coli* HB101 after conjugation. Plates were incubated overnight at 37ºC, under anaerobic conditions.

2.6. Allele-Coupled Exchange (ACE) mutagenesis

After 3 days, the first conjugant colonies that had the plasmid containing the deletion of the gene, started to appear. The isolated ones were streaked into BHI supplemented with cefoxitin and thiamphenicol. This step was repeated one more time to select for the single cross-over, which means that the plasmid was integrated in the chromosome. Clones were then transferred to *C. difficile* minimal medium supplemented with FOA (100 mg mL^{-1}) and uracil (1 mg mL^{-1}). Colonies which grew in this medium were rounder and yellow than the usual and they took 3 days to show up. The ones that were able to grow meaning that the first single cross-over excised the plasmid with the *pyrE* gene and because of that, cells were resistant to the FOA. Those ones were transferred to BHI supplemented only with cefoxitin exclude the presence of the plasmid (which have the thiamphenicol resistance mark) in the mutant strain. After this, a loop was necessary to collect the isolated colony, inoculate into a new BHI plate supplemented with cefoxitin, and to resuspend in 5% Chelex resin (Sigma-Aldrich). After the genomic DNA extraction, the second single cross–over was verified by PCR. At this point, a strain with deletion for the gene under study in a background Δ*pyrE* was constructed.

To revert the *pyrE*$^-$ background, the strain was conjugated with *E. coli* HB101 (pRP4) carrying pMTL-YN1 (containing the *pyrE* gene), and the conjugant colonies were then transferred into *C. difficile* minimal medium (CDMM). The ones which grew in this medium, were analysed by PCR to confirm the *pyrE* reversion. The positive clones were finally tested in BHI supplemented with cefoxitin and thiamphenicol to exclude the presence of the plasmid in the mutant strain.

2.7. Microscopy and image analysis

C. difficile was grown in BHI overnight at 37ºC, under anaerobic conditions. In the morning, the OD_{600} was set to 0.05. For $SNAP^{Cd}$ labelling, *C. difficile* was also grown in 70:30 sporulation medium [15.75 g Bacto peptone (BD Difco), 0.875 g proteose peptone (BD Difco), 0.175 g ammonium sulphate $(NH_4)^2SO_4$, 0.265 g tris base, 2.775 g brain heart infusion extract (BD Difco), 0.375 g yeast extract (BD Difco) and 3 g agar in 200 mL dH_2O) with 10% (w/v) cysteine and thiamphenicol (15 µg mL^{-1})]; in a CDMM (Karasawa *et al.*, 1995) solidified with 1.5% agar (from BD) and sporulation medium (SM) [9% bacto tryptone, 0.5% bacto peptone, 1% $(NH4)_2SO_4$ and 0.15% tris base, pH 7.4]. At the indicated times, 200 µL of culture were added to 1 µL of TMR (50 µM) to a final concentration of 250 nM and the mixture incubated for 30 min in the dark. For vancomycin labelling, imipenem (4 µg mL^{-1}) was added at an OD_{600} ~ 0.5, and the mixture incubated for 2 h. After 2 h, BODIPY® FL vancomycin (Thermo Fisher) was added to 500 µL of the culture to a final concentration of 2 mg L^{-1} and the mixture incubated for 15 min.

Following labelling, the cells were removed from the anaerobic chamber and collected by centrifugation (6 000 x *g* for 2 min at room temperature), washed 3 times in 1 mL of 1x PBS and, finally, resuspended in 200 µL of 1x PBS. For vancomycin labelling, cells were resuspended in 1x PBS with 1 µL of FM4-64. For $SNAP^{Cd}$ labelling, cells (3 µL) were mounted on a 1.7% agarose coated glass slide. For $SNAP^{Cd}$ labelling, cells were observed on a Leica DM6000B microscope equipped with a phase contrast Uplan F1 100x objective and a CCD IxonEM camera (from Andor Technologies; (Serrano *et al.*, 2011)). The images were taken with an exposure time of 50 ms for bright field and 3 000 ms for TMR. Images were acquired using the Metamorph software suite version 5.8 (from Universal Imaging). For quantification of the SNAP signal resulting from the transcriptional fusion, 4x4 pixel regions were defined in the desired cell. For vancomycin labelling, cells were observed on a Zeiss LSM 880 Confocal Microscope with Fast Airyscan microscope using a 63x objective. Image analysis was done using the Fiji ImageJ software.

2.8. Antimicrobial susceptibility testing

Minimum inhibitory concentrations (MICs) of vancomycin were determined by diffusion gradient using Etest® strips (bioMérieux), according to the manufacturer's instructions. Etest strips ranged from 0.016 to 256 µg mL^{-1}. Strains grown in BHI supplemented with cefoxitin (25 µg mL^{-1}) plates. A pre-inoculum was done in BHI and in the next morning, an inoculum where the culture overnight must be diluted to an OD_{600} of 0.05 was done. After growth of the inoculum to an OD_{600} of 1, a 1:100 dilution was made, and the plates were seeded with 150 µL of the diluted culture. After the surface of the BHI plate was completely dry, Etest® strips were applied to each plate. The plates were incubated anaerobically at 37°C for 48 and 96 h.

MICs were also tested in liquid cultures on 24-wells plates. After growth of a pre-inoculum overnight, a culture was prepared at OD_{600} of 0.05. At each well was added 3 mL of culture and vancomycin added at the desired concentration. A sterility control (BHI only) was also prepared. After 10 and 24 h of incubation, the OD_{600} was measured.

2.9. Biofilm production assays

Biofilms assays were performed as described previously (Dubois, Yannick D N Tremblay, *et al.*, 2019; Tremblay *et al.*, 2021). In 24-well polystyrene tissue culture-treated plates (from Greiner bio-one, Austria), a BHI overnight culture was diluted 1:100 in 1 mL per well of BHI medium supplemented with L-cysteine hydrochloride (1.27 M), D-glucose (1 M) and sodium deoxycholate (DOC) (100 mM) (BHISG-DOC), and in *C. difficile* medium optimized for biofilm formation (CDMOB) [Casein hydrolysate (10 mg mL^{-1}), L-Tryptophane (0.5 mg mL^{-1}), L-Cysteine (0.01 mg mL^{-1}), L-Leucine (0.0033 mg mL^{-1}), L-Isoleucine 0.0033 mg mL^{-1}), L-Valine (0.0033 mg mL^{-1}), Na_2HPO_4 (5 mg mL^{-1}), $NaHCO_3$ (5 mg mL^{-1}), KH_2PO_4 (0.9 mg mL^{-1}) NaCl (0.9 mg mL^{-1}), $(NH_4)_2SO_4$ (0.04 mg mL^{-1}), $CaCl_2 \cdot 2H_2O$ (0,026

mg mL^{-1}), $MgCl_2 \cdot 6H_2O$ (0,02 mg mL^{-1}), $MnCl_2 \cdot 4H_2O$ (0,01 mg mL^{-1}), $CoCl_2$ $6H_2O$ (0.001 659 mg mL^{-1}) $FeSO_4 \cdot 7H_2O$ (0.004 mg mL^{-1}) D-biotin (0.001 mg mL^{-1}), calcium-D-pantothenate (0.001 mg mL^{-1}) and pyridoxine (0.0001 mg mL^{-1})]. Pyruvate (100 mM), DOC (240 µM) and D-Glucose (1 M) were added, when necessary.

The plates were incubated at 37ºC in anaerobic conditions for 24 and 48 h. After incubation, the medium was removed by inversion of the plates. The wells were carefully washed twice with phosphate-buffered saline (PBS) solution and between each wash the biofilms were air dried for 10 min. The biofilms were then stained with crystal violet (CV; 0.2% w/v) for 30 min. The CV was removed by inversion and the wells were air dried for 15 min, followed by two washes with 1x PBS. Dye bound biofilm mass was solubilized by adding 1 mL of a 50:50 ethanol-acetone solution, and the absorbance, corresponding to the biofilm biomass, was measured at λ_{600} with a spectrophotometer (Ultraspec2100 pro). When needed, the solubilized dye was diluted 1:100 in the same 50:50 ethanol-acetone solution and measured again.

2.10. Overproduction and purification of SdaB

A 10 mL overday culture of *E. coli* BL21λDE3 Suf^{++} containing plasmid with His-tagged in LB with ampicillin (100 µg mL^{-1}) was used to inoculate 100 mL of auto-induction media [for a final volume of 100 mM of LB, 1x 5052, 1x NPs (0.5 M $[NH_4]_2SO_4$, 1 M KH_2PO_4 and 1 M Na_2HPO_4, pH 6.75) and 1 mM $MgSO_4$] containing 100 µg mL^{-1} ampicillin and 50 µM $FeCl_3$. The cultures were grown at 37°C shaking for 18 h. The bacteria were harvested by centrifugation at 4ºC for 15 min at 7 000 x *g* and freezing in liquid nitrogen. The cells were thawed in 10 mL of Buffer A (50 mM HEPES, pH 7.5, 100 mM NaCl, 1 mM DTT), under anaerobic conditions, and lysed using a French pressure cell (18 000 lb/in^2). The lysate was centrifuged for 30 min at 42 000 x *g* at 4ºC.

The supernatant was loaded onto a nickel-nitrilotriacetic acid column that was equilibrated in Buffer A, and the column was washed with 50 mL of Buffer A containing 10% glycerol and 40 mM imidazole. Finally, the protein was eluted with Buffer A containing 10% glycerol and 250 mM imidazole. Fractions that displayed a brown colour were pooled and concentrated using a Vivapore concentrator 7,500 and exchanged into Buffer B (50 mM HEPES, pH 8.0, 100 mM NaCl, 10% glycerol, 1 mM DTT) by protein desalting columns. The protein was routinely frozen in small aliquots and stored in liquid N_2 until ready for use. Proteins in the extracts were resolved on 12.5% SDS-PAGE gels. The gels were first scanned in an iBright Western Blot Imaging Systems.

2.11. N-terminal sequence analysis

For the N-terminal sequence analysis, the sponges and the SDS-PAGE gel were soak in 1X electroblotting buffer for PVDF membranes (polyvinylidene difluoride) (0.192 M glycine, 0.025 M tris pH 8.3, 20% methanol, pH 8.3) for 5-10 min at room temperature. At the same time, the PVDF membrane was saturate in 100% methanol for a few s, and then, transfer to 1X electroblotting buffer in a separate container and soak for 5 min at room temperature. Proteins were electrophoretically transferred at 100 V for 90 min. The membrane was rinsed briefly with ddH_2O and then stained. For protein detection, the membrane was stained with 0.1% Coomassie; 50% methanol and 7% acetic acid, during 10 min; and destained with 90% methanol and 10% acetic acid, for 10 min. Allow the membrane to fully dry. The desired band was extracted, and the N-terminal sequence determined by Edman degradation (PO 101LA).

2.12. Immunoblotting

Proteins were electrophoretically transferred from SDS-PAGE gel to nitrocellulose membranes (Supported Nitrocellulose, 0.45 µm; from BioRad) at 100 V for 90 min using transfer buffer (14.4 g L^{-1} glycine, 3.02 g L^{-1} tris base, 10% EtOH). The membrane was incubated in 10 mL of 5% milk in PBS-T (blocking solution: 1 mL Tween 20, 100 mL PBS, 900 mL ddH_2O) for 1 h with agitation. The blocking solution was then removed, and the antibody solution was added in 10 mL of PBS-T with 0.5% milk;

anti-Histag antibodies were used at a dilution of 1:1000. The membrane was incubated overnight with the antibody solution at 4ºC without agitation. The antibody solution was then discarded, and the membrane was washed 3 times in PBS-T. A rabbit peroxidase-conjugated secondary antibody (from Sigma) was added in 10 mL of PBS-T with 0.5% milk at a dilution of 1:5000. The membrane was incubated 30 min at room temperature with agitation. Lastly, the membrane was washed 3 more times in PBS-T (10 min each) and the protein detected using an iBright Western Blot Imaging System (ThermoFisher).

3. Results

3.1. Expression of the *sdaB* gene during growth and sporulation

We started this study by analysing the expression of the *sdaB* gene during growth and sporulation. For that, we constructed a transcriptional fusion of the promoter region of the *sdaB* gene to the *SNAP* tag. Work from the laboratory has established the SNAP tag as a fluorescent reporter for studying gene transcription and protein localization in *C. difficile* (Cassona, 2018). Inspection of the *sdaB* region of the chromosome suggests that the gene is monocistronic; it is divergently oriented with respect to the upstream *dapA2* gene, coding for a putative 4-hydroxy-tetrahydrodipicolinate synthase, and in the same orientation but at a distance of about 1 kb from the downstream gene, *CD630_32210*, of unknown function (**Figure 3.1A**). A DNA fragment extending 342 bp upstream of the *sdaB* start codon was amplified by PCR and fused to the *SNAP* gene such that the reporter is produced from the translational initiation signals of the *sdaB* gene (see the Material and Methods section and **Appendices 2** and **3**). The fusion was constructed in pMTL84121, a low copy number plasmid (Heap *et al.*, 2009) to produce pIM01 (**Appendix 2**; **Figure 3.1B** and **C**). The DNA segment from the *sdaB* regulatory region inserted in pIM01, shows sequences that match the consensus for recognition by the σ^A and σ^F containing forms of RNA polymerase, suggesting that the gene may be expressed both during growth and in the forespore, during sporulation (**Figure 3.1C**). pIM01 was introduced in *C. difficile* 630Δ*erm* (WT) by conjugation to give strain AHCD1618 (**Appendix 1**).

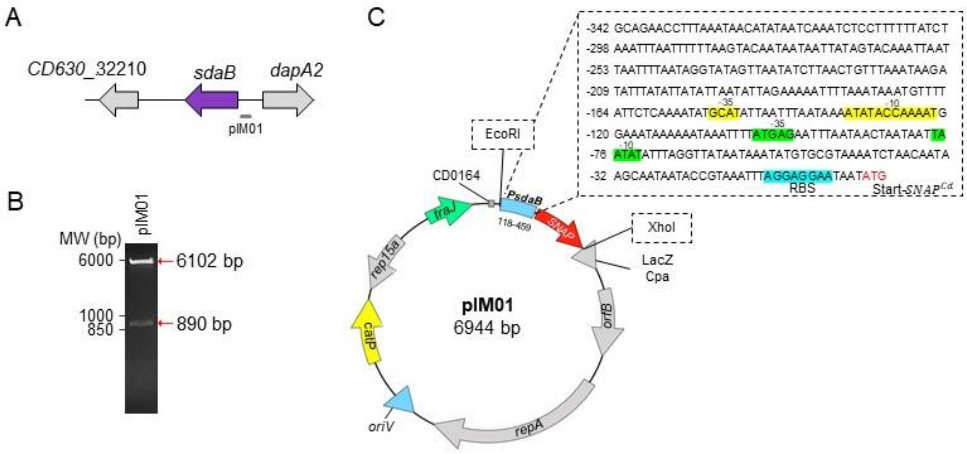

Figure 3.1: Construction of a P_{sdaB}-*SNAP* fusion. A: Schematic representation of the *sdaB* region of the *C. difficile* 630Δ*erm* chromosome. The region presents in pIM01, bearing a P_{sdaB}-*SNAP* transcriptional fusion is represented by the horizontal line below the genetic map. **B**: Analysis of the structure of plasmid pIM01 using the restriction enzymes EcoRI and XhoI. The position and sizes of the expected products are shown on the right side of the panel (red arrows). The position on molecular size markers (MW, in bp) is shown on the left side of the panel. **C**: Map of pIM01 and the *sdaB* promoter region. pIM01 is derived from pMTL84121 and contains the promoter region of the *sdaB* gene fused to the *SNAP* gene (890 pb). In sequence of the promoter region, the -10 and -35 promoter elements that match the consensus for σ^A (shaded in green) and σ^F (shaded in yellow) recognition are indicated. The ribosome binding site (RBS, shaded in blue) and the *sdaB* start codon (red) are also indicated.

We monitored production of the SNAP reporter as a proxy for the activity of the *sdaB* promoter. We examined production of the SNAP reporter during growth and stationary phase of an otherwise WT strain, in a medium, BHI, that supports sporulation. In addition, we monitored SNAP production in cultures of congenic derivatives of *C. difficile* 630Δ*erm* bearing deletion mutations of the *spo0A* and *codY* genes (strains AHCD1640 and AHCD1636, respectively; **Appendix 1**). Our rational for the analysis of these strains was that both CodY and Spo0A control adaptive changes in gene expression at the onset of stationary phase. Specifically, Spo0A is required for entry into sporulation (Pereira *et al.*, 2013), and CodY, monitors the nutritional status of the cell, sensing intracellular levels of GTP and branched-chain amino acids (Dineen *et al.*, 2010). Moreover, CodY is also a repressor of sporulation (Nawrocki

et al., 2016). The strains carrying the P_{sdaB}-*SNAP* fusion were grown in BHI medium and samples collected after 6, 8, 10 and 12 h after inoculation. All strains showed similar growth rates and, after about 10 h, they entered into the stationary phase of growth (**Figure 3.2**).

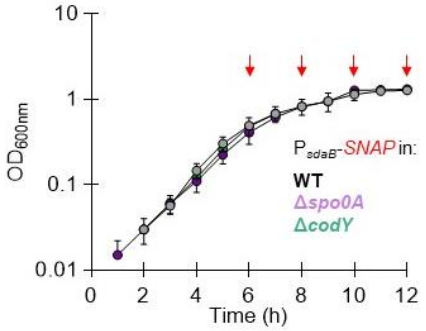

Figure 3.2*:* Growth of strains bearing a P_{sdaB}-*SNAP* transcriptional fusion. Growth of cultures of *C. difficile* 630Δ*erm* and its congenic *spo0A* and *codY* derivatives carrying the P_{sdaB}-*SNAP* transcriptional fusion (in pIM01) in BHI was followed by measuring the OD_{600} until 12 h after inoculation. The red arrows indicate the points at which samples were withdrawn for measuring *SNAP* production. The OD_{600} values are shown ± standard deviation for three independent experiments.

The cells were labelled with TMR and examined by phase contrast and fluorescence microscopy (**Figure 3.3**). In the WT (630Δ*erm*), at any time point tested, about 80% of the population displayed fluorescence above the background (**Figure 3.3A**). However, for the WT the average fluorescence signal for the cell population increased from 6 to 10 h (153.71 to 313.27 A.U., respectively) but at 12 h the mean value of the fluorescence intensity decreased (to 277.16 A.U.) (**Figure 3.3B**). Thus, expression seemed enhanced transiently upon entry into stationary phase. In the *spo0A* mutant, vegetative expression is maintained in about 80% of the cells, but at 12 h, only about 70% of the population displayed fluorescence above the background. In the Δ*spo0A* cells the average fluorescence signal for the cell population increased from 6 to 8 h (273.44 to 288.92 A.U., respectively) but after 10 h the mean of the fluorescence intensity started to decrease. Finally, in the Δ*codY* mutant at 6 and 10 h, about 70% of the population displayed fluorescence above the background, but the percentage decreased to only 50% of the population at 8 and 12 h (**Figure 3.3A**). In the Δ*codY* cells the average fluorescence signal for the cell population is higher at 6 h (179.22 A.U.), decreasing at 8 h (100.93 A.U.); however, the mean of the fluorescence intensity increases to 141.25 A.U. at 12 h (**Figure 3.3B**). The average fluorescence intensity did not differ significantly between the WT and the Δ*spo0A* or Δ*codY* mutants. Therefore, *sdaB* is expressed during exponential growth and at the onset of stationary phase, decreasing during late stationary phase, except possibly in the *codY* mutant (**Figure 3.3**). Thus, under our conditions, Spo0A not seems to control the expression of *sdaB*. This expression pattern is consistent with the presence of a possible σ^A-type promoter in the *sdaB* regulatory region (**Figure 3.1C**).

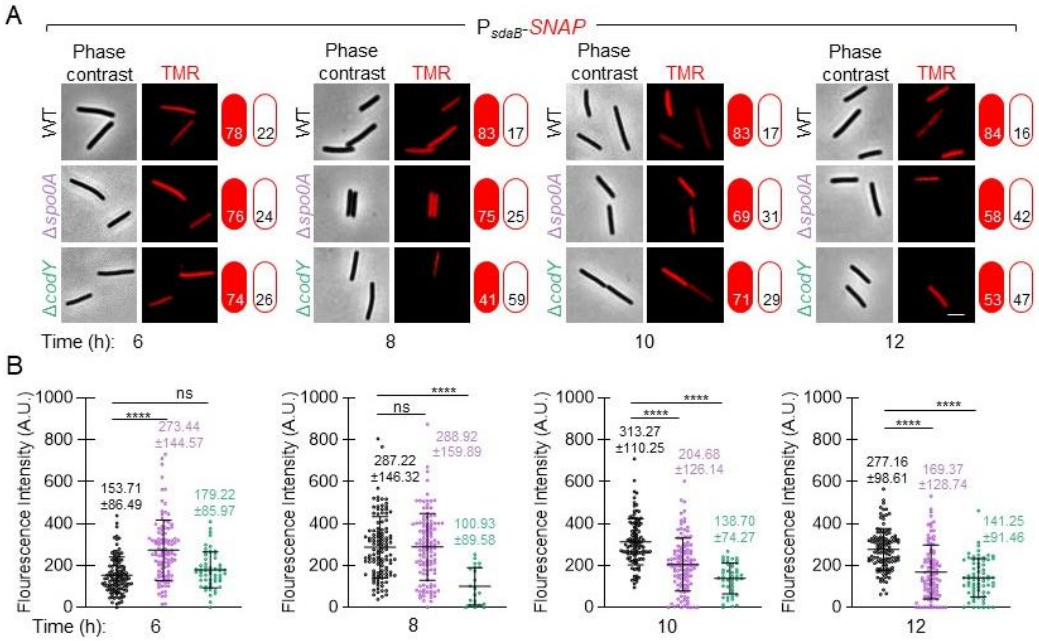

Figure 3.3: Expression of P*sdaB*-*SNAP* in BHI. **A**: Phase contrast and fluorescence microscopy analysis of *C. difficile* 630Δ*erm* (WT), and *spo0A* and *codY* congenic derivatives carrying pIM01. The cells were collected 6, 8, 10 and 12 h after inoculation in BHI, labelled with TMR-Star and examined by phase contrast and fluorescence microscopy (red signal). The panels are representative of the expression patterns observed, weak and strong expression, and the percentage of cells exhibiting each is shown on the graphical representation on the right. Scale bar, 1 μm. **B**: Quantitative analysis of the fluorescence intensity at the single cell level (n = 100 cells). The numbers in the graph represent the mean and the standard deviation of the fluorescence intensity for each strain, colour coded as in panel A, at the indicated times (in h). The asterisk (****$p \leq 0.0001$) and "ns" (non-significant) represent the statistical significance using the nonparametric Kolmogorov-Smirnov test (KS-test).

Although the results described above suggested that expression of *sdaB* is not under sporulation control, we wanted to independently test this result using conditions where sporulation, induced on a solid medium, 70:30, is more synchronized (Serrano *et al.*, 2011). We used the same transcriptional fusion to monitor SNAP production during sporulation. Soon after the initiation of sporulation, the sporulating cell undergoes an asymmetric division originating two cells of unequal sizes, a larger mother cell (MC) and a smaller forespore (PS). The PS and the MC then follow different lines of gene expression controlled by sporulation specific RNA polymerase sigma factors, σ^F and σ^G in the forespore and σ^E and σ^K in the mother cell (Pereira *et al.*, 2013). Samples of the culture containing the *sdaB* promoter fused to the *SNAP* gene were collected 14 and 24 h after inoculation onto 70:30 plates (Serrano *et al.*, 2011). Cells were labelled with TMR and examined by phase contrast and fluorescence microscopy. In this medium, *sdaB* is expressed in cells that do not present signs of sporulation, and in sporulating cells, both in the MC and in the PS (**Figure 3.4A**). Quantification of the fluorescence intensity showed that in the MC and PS the average fluorescence signal decreased from 14 to 24 h (181.94 to 118.69, and 330.02 to 193.67, respectively) (**Figure 3.4B**). Moreover, the average fluorescence signal at both time points is higher in the PS than in the MC (**Figure 3.4B**). The presence in the *sdaB* regulatory region of a possible σ^F-dependent with -35 and -10 sequences is located between bases -149 and -122, relative to the start codon (**Figure 3.1C**). No sequences that conform to those recognized by the mother cell-specific sigma factors are *seen* in the *sdaB* regulatory region, suggesting that expression in the MC may result from protracted expression by vegetative cells.

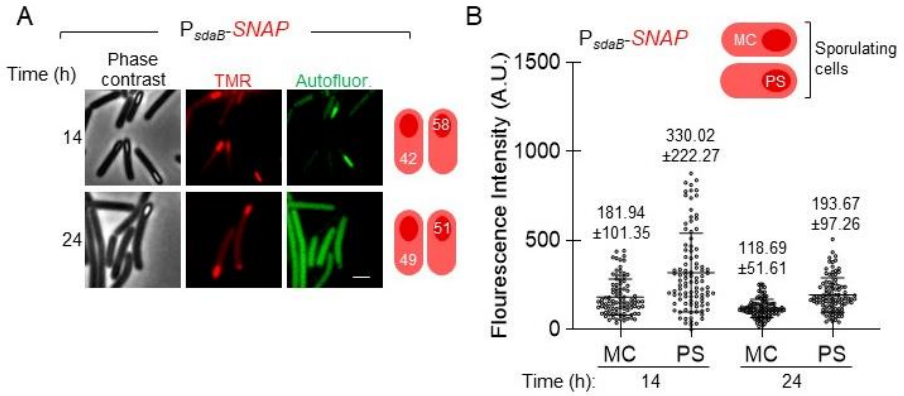

Figure 3.4*:* Expression of P$_{sdaB}$-*SNAP* in sporulating cells. **A**: *C. difficile* 630Δ*erm* carrying pIM01 were inoculated on plates of 70:30 medium and cells collected 14 and 24 h after. The cells were labelled with TMR-Star and examined by phase contrast and fluorescence microscopy. The TMR-Star signal is shown in the red channel and the auto-fluorescence of *C. difficile* cells is shown in the green channel. The panels are representative of the expression patterns observed. The cartoon represents the percentage of sporulating cells showing SNAP accumulation in the forespore or the mother cell. Scale bar, 1µm. **B**: Quantitative analysis of the fluorescence intensity from P$_{sdaB}$-*SNAP* for the mother cell or the forespore at the indicated times (in h). The numbers are average ± standard deviation from three independent experiments. MC: mother cell; PS: forespore.

We also tested the role of sporulation specific RNA polymerase sigma factors in *sdaB* expression during sporulation by examining the expression of the P$_{sdaB}$-*SNAP* fusion in mutants for *sigF*, *sigE*, *sigG* and *sigK*; consistent with the result obtained for the *spo0A* mutant, in any mutant was the expression of *sdaB* affected (data not shown). We do not presently understand why the expression of P$_{sdaB}$-*SNAP* increases in the PS at late stages in the process.

3.2. Construction of an in-frame deletion mutant of *sdaB*

The *sdaB* gene codes for a putative L-Serine deaminase. Leeds *et al.* (2014) isolated two strains with reduced susceptibility to VAN. One strain bears mutations in *murG*, *CD3659* and *sdaB;* and the other strain has a mutation in *rpoC* (Leeds *et al.*, 2014). Although the mutants were never studied in detail, the isolation of these strains suggests that VAN resistance can emerge by different mechanisms consistent with previous reports (Gardete and Tomasz, 2014). In the VAN-resistant isolate, *sdaB* has a mutation leading to a single amino acid deletion in a stretch of alanines (positions 292-295) (Leeds *et al.*, 2014). We wanted to test whether the *sdaB* mutation contributed to resistance to VAN and within mind we first constructed a strain carrying an in-frame deletion of *sdaB*.

The allele exchange cassette (ACE) methodology (Ng *et al.*, 2013) was used to inactivate the *sdaB* gene through deletion of the DNA sequence between bases 1015 and 2171 within the coding region of the gene (**Figure 3.5A**). An ACE cassette was assembled composed of a left homology arm (LHA) and a right homology arm (RHA) relative to *sdaB*. The LHA (982 bp) was amplified by PCR using primers P1: *sdaB*33-Fw and P2: *sdaB*1015-Rev (**Appendix 3**). The RHA (989 bp) was amplified by PCR using primers P3: *sdaB*2171-Fw and P4: *sdaB*3160-Rev (**Appendix 3**). The two fragments were joined by splicing by overlap extension (SOE) PCR and the resulting fragment of 1971 bp was inserted between the BamHI and XhoI sites of pMTL-YN3 (Ng *et al.*, 2013) to produce pIM02 (**Figure 3.5B**; **Appendix 2**). pIM02 was introduced in *C. difficile* 630Δ*erm*Δ*pyrE* by conjugation (**Appendix 1**). The transconjugants obtained were restreaked two times in BHI with thiamphenicol and cefoxitin to select for the single cross-over. Clones were then transferred to *C. difficile* minimal medium supplemented with FOA and uracil. The ones that were able to grow are resistant to the FOA, which means that the first single cross-over excised the plasmid with the *pyrE* gene. Those were transferred to BHI supplemented only with cefoxitin exclude the presence of the plasmid in the mutant strain. Large colonies were tested for the second single cross–over verified by PCR using two pairs of primers (**Figure 3.5C**): P5: *sdaB*4_Fw + P6: *sdaB*3185_Rev and P7: *pyrE*-vef-Fw + P8: *pyrE*-vef-Rev (**Appendix 3**). The coding

region of the WT allele is 3281 bp-long, while in the deletion allele the coding region is 1971 bp-long (**Figure 3.5B and C**). A strain with an in-frame deletion of the *sdaB* gene in a Δ*pyrE* background was in this manner obtained.

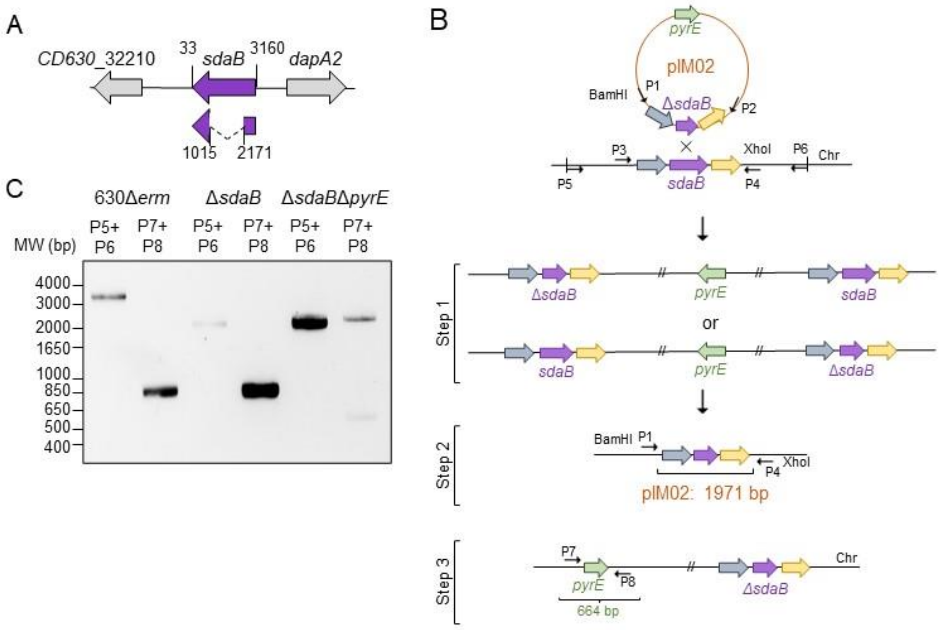

Figure 3.5: Disruption of the *sdaB* gene in the 630Δ*erm*Δ*pyrE* strain. A: Schematic representation of the *sdaB* region of the *C. difficile* 630Δ*erm* chromosome showing the segment of DNA deleted to produce and in-frame deletion of *sdaB*. **B**: pIM02 carries a left homology arm (LHA), a right homology arm (RHA) and the *pyrE* gene. The LHA was amplified by PCR using primers P1 and P2, and RHA was amplified by PCR using P3 and P4 (see **Appendix 3**). The two fragments were joined by SOE PCR and inserted between the BamHI and XhoI sites of pMTL-YN3 (Ng et al., 2013) to produce pIM02. The fusion of the LHA with the RHA creates an in-frame deletion removing codons 1015 to 2171 of *sdaB* gene. The plasmid integrates into the *sdaB* locus by a single, reciprocal cross-over event (Campbel-type mechanism). **C**: Chromosomal DNA from a prospective mutant was prepared and subject to PCR with the indicated primers (represented in panel B; sequences given in **Appendix 3**). The wild type *sdaB* gene has 3281 bp while the deletion allele has 1971 bp. The reverted *pyrE* allele in the Δ*sdaB* shows the same size as in 630Δ*erm* (WT). Since our original strain 630Δ*erm*Δ*pyrE*Δ*sdaB* also has a specific in-frame deletion of the *pyrE* locus, ACE can be used to introduce a wild-type copy of the *sdaB* gene into the chromosome at the *pyrE* locus concomitant with the correction of this allele back to the WT (PyrE+ phenotype). MW: 1 kb Plus DNA ladder.

On the isolated *sdaB* mutant, the *pyrE*$^{-}$ gene was converted back to *pyrE*$^{+}$ using plasmid pMTL-YN1 (Ng *et al.*, 2013) as described in the material and methods chapter. The presence of the WT *pyrE* gene was confirmed by PCR using primers P7 and P8 that anneal to regions upstream and downstream of *pyrE*, respectively. The colony tested was positive since the reverted *pyrE* allele in the Δ*sdaB* mutant shows the same size as in 630Δ*erm* (WT) (**Figure 3.5C**). Since our original strain 630Δ*erm*Δ*pyrE*Δ*sdaB* also has a specific in-frame deletion of the *pyrE* locus, ACE can be used to introduce a wild-type copy of the *sdaB* gene into the chromosome at the *pyrE* locus concomitant with the correction of this allele back to the WT (*PyrE*$^{+}$ phenotype) (**Figure 3.5**; **Appendix 1**).

3.3. Deletion of the *sdaB* gene decreases susceptibility to VAN

To analyse the impact of the *sdaB* mutation on susceptibility to VAN, the WT strain and the *sdaB pyrE*$^{+}$ mutant were grown in BHI supplemented with cefoxitin plates. An inoculum was done and allowed to grow until an OD_{600} of about 1, after which the BHI plates were seeded with 150 µL of the diluted culture and an Etest was applied to each plate (**Figure 3.6**; WT, **A** and **C**; *sdaB pyrE*$^{+}$, **B** and **D**). The minimum inhibitory concentration (MIC) of each strain is determined by the intersection of the organism growth with the strip as measured using the scale inscribed on the strip (**Figure 3.6A-D**). Both at 48 (**Figure 3.6A**) and 96 h of incubation (**Figure 3.6C**), the MIC for the WT strain was between 1.5-2 µg mL^{-1}, consistent with the literature (Ammam *et al.*, 2013). On the other hand, the *sdaB* mutant

showed a higher MIC, between 2-6 µg mL^{-1}, at both times (**Figure 3.6B and D**). The blue arrows in **figure 3.6** (panels **B** and **D**) indicate colonies of the mutant which appear within the area of inhibition and may have higher resistance to VAN.

MICs were also tested in liquid cultures grown on 24-wells plates. After 10 and 24 h of inoculation on BHI supplemented with the respective VAN concentration, the OD_{600} was measured. As before, the WT (**Figure 3.6E** and **F**, orange bars) and the *sdaB* mutant (blue bars) show different results. The WT showed growth until a VAN concentration of 2 µg mL^{-1} after 10 and 24 h incubation, whereas the *sdaB* mutant showed growth until 4 µg mL^{-1} of VAN (**Figure 3.6E** and **F**). These results suggest that the *sdaB* gene affects the resistance of *C. difficile* to VAN.

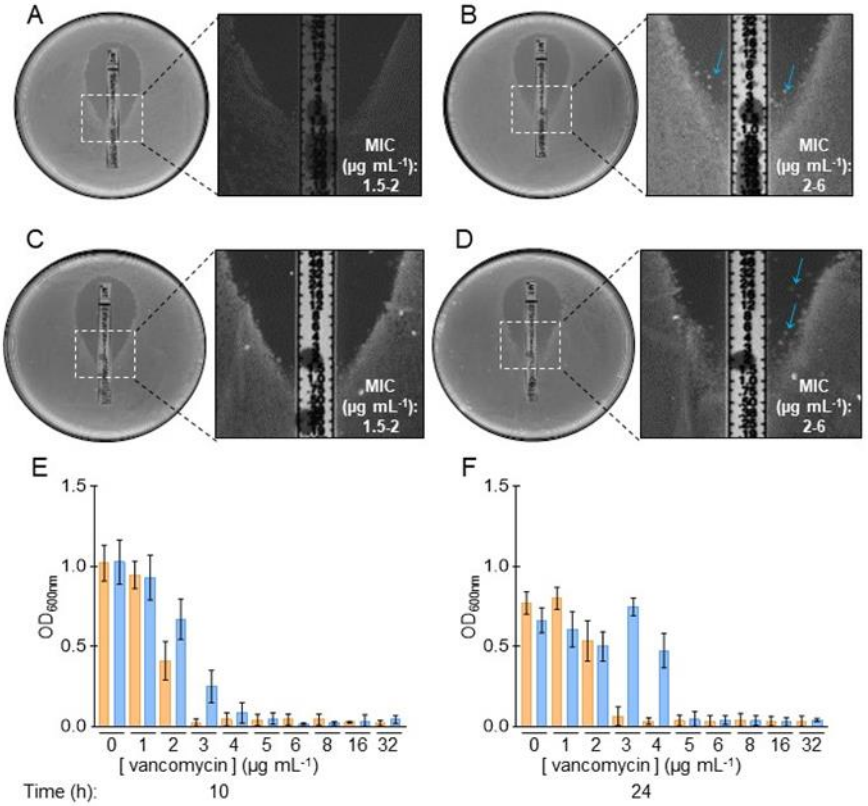

Figure 3.6*:* Susceptibility of *C. difficile* 630Δ*erm* and *sdaB pyrE*$^+$ to VAN. *C. difficile* 630Δ*erm* (**A**, **C**) and a *sdaB pyrE*$^+$ mutant (**B**, **D**) were tested using the Etest gradient diffusion method with VAN, on BHI agar 48 (**A**, **B**) and 96 h (**C**, **D**) after inoculation. The MIC is determined by the intersection of the organism growth with the strip as measured using the scale inscribed on the strip. The blue arrows indicate colonies of the mutant which appear to have higher resistance to VAN. The liquid MIC for VAN was tested 10 (**E**) and 24 h (**F**) after inoculation in BHI. Orange bars, 630Δ*erm* (WT); blue bars, *sdaB pyrE*$^+$ mutant. According to the European Committee on Antimicrobial Susceptibility Testing (EUCAST), reduced susceptibly to VAN is defined as a MIC of > 2 µg mL^{-1} (Banawas, 2018).

3.4. *sdaB* mutant affect biofilm formation

We assessed the biofilm production ability of each strain on 24-well plates with BHI medium supplemented with L-cysteine hydrochloride, D-glucose, and DOC (BHISG-DOC; see the Material and Methods section), 24 and 48 h after inoculation and with minimal medium optimized for *C. difficile* biofilm (CDMOB; see the Material and Methods section) supplemented with 100 mM Glucose and, when necessary, with 240 µM DOC and 100 mM pyruvate, at 48 h (**Figure 3.7A**). At 24 h, no biofilm was produced in CDMOB (data not shown). In BHISG-DOC, while there were no significant differences at 24 h between the strains, the *sdaB* mutant produced significantly more biofilm at 48 h in comparison with the WT (**Figure 3.7A**). In CDMOB supplemented with 100 mM Glucose and DOC or pyruvate, the WT produced slightly more biofilm than the *sdaB* mutant (**Figure 3.7B**). On the other hand, in CDMOB supplemented with only glucose, the *sdaB* mutant produced significantly more biofilm than the WT. Unlike the *sdaB* mutant, which produced more biofilm in the presence of glucose, the WT

produced more biofilm in the presence of glucose and DOC. Moreover, the *sdaB* produced almost five times more biofilm in BHISG-DOC as compared to CDMOB at 48 h (**Figure 3.7A** and **B**).

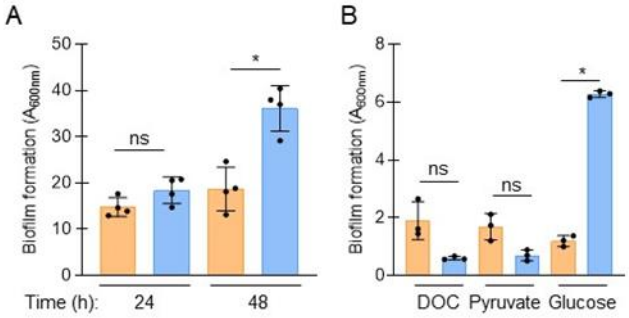

Figure 3.7: Biofilm formation by *C. difficile* 630Δ*erm* and the *sdaB pyrE*$^+$ mutant. A: Biofilm formation in BHISG supplemented with 240 µM DOC, as assessed by the OD_{600}, measured 24 and 48 h after inoculation. **B**: Biofilm formation in CDMOB supplemented with 100 mM Glucose and with 240 µM DOC, 100 mM pyruvate, or none, respectively, 48 h after inoculation. Orange bars, 630Δ*erm* (WT); blue bars, *sdaB pyrE*$^+$ mutant. The asterisk (* $p \leq 0.05$) and "ns" (non-significant), represent the statistical significance determined using the nonparametric Mann-Whitney test.

3.5. *sdaB* mutant affected by presence of imipenem

VAN inhibits cell wall synthesis by binding to the dipeptide D-Alanyl-D-Ala of PG precursors (Isidro *et al.*, 2017). One of the motivations of this work was the possibility that deletion of the *sdaB* gene could result in increased incorporation of D-Alanyl-D-Ser into the PG and hence higher resistance to VAN (see the Introduction section). One way to test this possibility was to label cells of the WT and the mutant with a fluorescent derivative of VAN (BODIPY® FL) which binds to D-Alanyl-D-Ala motifs. The WT strain and the *sdaB* mutant were grown in BHI and at an OD_{600} of about 0.5 imipenem was added to inhibit utilization of substrates ending in D-Alanyl-D-Ala and to inhibit carboxypeptidases that could remove the terminal D-Ala (Peltier *et al.*, 2011). As a control for background fluorescence, imipenem was not added to the cultures which were otherwise processed in the same manner. After 2 h of the addition of imipenem, BODIPY® FL was added and after 15 min of incubation, the cells were collected, labelled with FM4-64, and examined by fluorescence microscopy (**Figure 3.8A**). The membrane dye FM4-64 allowed to stain the asymmetric septum and the membrane whereas BODIPY® FL was used to test whether less D-Alanyl-D-Ala accumulated in the PG.

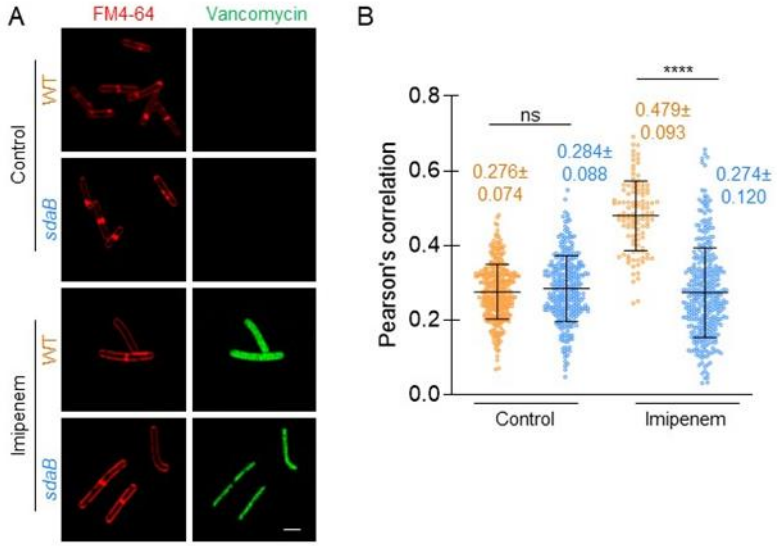

Figure 3.8: Vancomycin labelling of *C. difficile* 630Δ*erm* and *sdaB pyrE*$^+$ cells. A: Cultures were grown in BHI until an OD_{600} of about 0.5 at which time imipenem was added. As a control for background fluorescence, imipenem was not added to the cultures which were otherwise processed in the same manner. After 2 h, BODIPY® FL VAN was added and after 15 min of incubation, cells were collected, labelled with FM4-64, and examined by fluorescence microscopy. Scale bar, 1µm. **B**: Pearson's correlation coefficient between the red (membrane dye, FM4-64) and green (BODIPY® FL) signals. The numbers in

the graph represent the mean and the standard deviation of the fluorescence intensity. The asterisk (**** $p \leq 0.0001$) and "ns" (non-significant) represent the statistical significance using the nonparametric Kolmogorov-Smirnov test (KS-test).

The results of preliminary experiments are shown in **Figure 3.8**. In the presence of imipenem, the *sdaB* mutant exhibits lower levels of VAN fluorescence than the WT (**Figure 3.8A**). We determined a Pearson's correlation coefficient between the red and green signals. In the presence of imipenem, WT shows higher levels of BODIPY® FL fluorescence than the *sdaB* mutant, since both the septum and membrane are labelled (**Figure 3.8B**). This indicates reduced accumulation of D-Alanyl-D-Ala motifs in the PG, in agreement with the idea that in the *sdaB* mutant this motif may be underrepresented, in favour of D-Ala-D-Ser.

3.6. Overproduction and purification of SdaB

An overall goal of this project was to correlate the phenotype of a *sdaB* mutant with the *in vitro* activity of the protein; note that while it is likely that SdaB is a L-Serine deaminase, this need to be demonstrated. At the same time, and after establishing the properties of the WT enzyme, we wanted to know what the consequences of deletion of the Ala (as found in the epidemic strain) would be. We first constructed a plasmid designed for the overproduction and purification of the WT protein. First, primers *sdaB*1004-Fw and *sdaB*2194-Rev were used to PCR amplify the coding region of *sdaB* (**Appendix 3**). The resulting PCR product was digested with NdeI and BamHI and cloned between the same sites of pET-16b (Novagen), to create pIM03 (**Figure 3.9A** and **B**; **Appendix 2**), which has an His_6-tag encoding sequence at the 5´-end of *sdaB* (data not shown). We then used pIM03 as a template to delete the codon for Ala295 through QuickChange site-directed mutagenesis. QuickChange mutagenesis employs PCR using oligonucleotide primer pairs that carry the desired mutation, deletion, or insertion. It uses complementary primer pairs in the same PCR reaction. The parental methylated DNA can be eliminated from the newly synthesized unmethylated mutant DNA by digesting with DpnI restriction enzyme (Munteanu *et al.*, 2012). The SdaB mutation was created by SOE PCR using primers *sdaB*1889-ΔA295-Fw and *sdaB*1885-Rev (**Appendix 1**), to create pIM04 (**Figure 3.9A** and **C**; **Appendix 2**). These two plasmids were then transformed into *E. coli* strain BL21λDE3 Suf^{++} (Corless *et al.*, 2020). During initial tests for the overproduction of His_6-SdaB, we noticed that two closely migrating bands appeared in the 43 kDa region of the gel (the expected size of His_6-SdaB); moreover, no band was found when production of the His_6-$SdaB^{\Delta A295}$ form was induced from pIM04. The results persisted when overproducing host such as BL21(DE3) and C43 were used, and under different growth conditions, including the use of terrific broth medium, and M9 minimal medium at different temperatures, and induction regimes (auto-induction versus induction with IPTG).

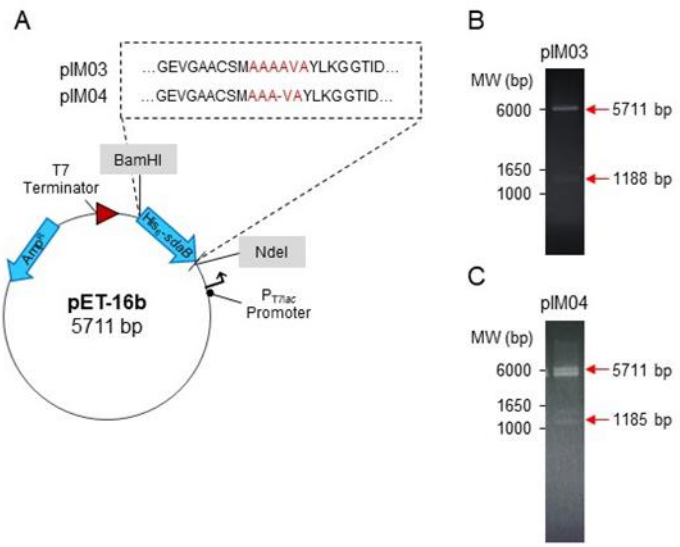

Figure 3.9: Constructs for SdaB overproduction. A: Map of pIM03 and pIM04 for the overproduction of SdaB. Plasmids are derived from pET-16b and carry the *sdaB* gene (1188 bp; pIM03) and the *sdaB* gene with a single amino acid deletion, Ala295 (1185 bp; pIM04) both fused to an N-terminal His_6-Tag. The ampicillin resistance gene, a T7 Terminator and the T7lac promoter are indicated. **B**: Restriction analysis of plasmid pIM03 (1188 bp; B) and pIM04 (1185 bp, C) using the restriction enzymes BamHI and NdeI. The position and sizes of the expected products are shown on the right side of the panel (red arrows). The position on molecular size markers (MW, in bp) is shown on the left side of the panel.

Because all the attempts were dined under aerobic conditions, we decided to induce production and carry out purification first of the WT protein under anaerobic conditions by means of an autoinduction regime (see Materials and Methods section) containing ampicillin and $FeCl_3$, at 37ºC and with shaking (120 rpm) for 18 h. The cells were harvested by centrifugation at 4ºC for 15 min at 7 000 x *g* and freezing in liquid nitrogen. The cells were thawed in 10 mL of Buffer A (50 mM HEPES, pH 7.5, 100 mM NaCl, 1 mM DTT), under anaerobic conditions, and lysed using a French pressure cell. The lysate was centrifuged for 30 min at 42 000 x *g* at 4ºC. Since this protein is rapidly inactivated by exposure to air, it has be purified and assayed under strictly anaerobic conditions (Hofmeister *et al.*, 1993), except the centrifugation steps. His_6-SdaB was overproduced and found in the supernatant fraction of a whole cell extract (**Figure 3.10A**, red arrow). The supernatant was then applied to a Ni^{2+}-affinity column, for the purification of the protein. The protein, was then purified anaerobically and had a brown colour, consistent with the presence of an iron–sulfur cluster (Burman *et al.*, 2004). Most of His_6-SdaB eluted as a single band at a concentration of imidazole of 250 mM (**Figure 3.10A**). As a control, an *E. coli* strain BL21λDE3 Suf^{++} bearing the empty pET-16b vector was used in parallel (**Figure 3.10**). In contrast, His_6-$SdaB^{\Delta A295}$ was found in the cell sediment, indicating that the protein was produced in an insoluble form (**Figure 3.10B**, red arrow). Most likely, the folding of the protein was significantly changed as the result of deleting Ala295.

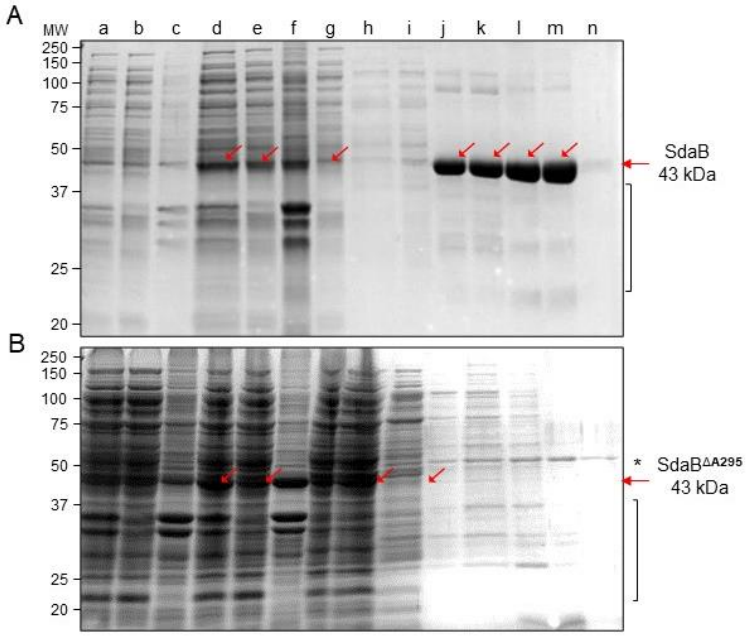

Figure 3.10*:* Anaerobic purification of His$_6$-SdaB (A) and His$_6$-tagged SdaB$^{\Delta A295}$ (B). SDS–polyacrylamide gels [12.5% (w/v) polyacrylamide] documenting different stages of protein purification are shown. Total cell extract (lane a), supernatant (lane b) and sediment (lane c) from BL21λDE3 Suf++ pET16b; Total cell extract (lane d), supernatant (lane e) and sediment (lane f) from BL21λDE3 Suf++ carrying pIM03 or pIM04; lane g, an aliquot of the flow-through from the column; lane h and i, of purified protein with 10% glycerol and 40 mM imidazole; lane j and k of purified protein with 10% glycerol and 100 mM imidazole; lane l and m of purified protein with 10% glycerol and 250 mM imidazole; lane n of purified protein with 10% glycerol and 500 mM imidazole. The asterisks and the lane on the right side of the panels mark nonspecific species that bind to the column. MW, molecular mass markers. Gels were stained with Coomassie Brilliant Blue and imaged using the Bright software (www.thermofisher.com).

3.7. SdaB is an oxygen-labile iron-sulfur enzyme

As a test for the presence of an iron-sulfur cluster in SdaB, we determined ultraviolet-visible (UV-visible) absorption spectrum of the protein. In addition to the protein peak at 280 nm, the spectrum revealed, two broad shoulders at 300 to 350 nm and at around 420 nm (solid line), which are characteristic of iron–sulfur proteins (Burman *et al.*, 2004) (**Figure 3.11**). When SdaB was purified in the presence of oxygen (broken line), the broad shoulder at 395–420 nm was not observed (**Figure 3.11**), suggesting that the iron–sulfur cluster is oxygen-labile.

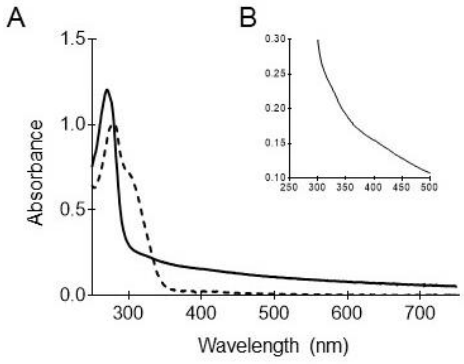

Figure 3.11: SdaB is an oxygen-labile iron-sulfur enzyme. UV–visible spectra of aerobically purified His-tagged SdaB (**broken line**) and anaerobically purified His-tagged SdaB (**solid line**), showing loss of absorbance at 420 nm upon exposure to air (**A**). The enzyme was dissolved in Buffer A. In addition to the protein peak at 280 nm, two broad shoulders at 300 to 350 nm and at 420 nm should appears (**B**). These spectral features are characteristic of enzymes containing iron-sulfur clusters (Burman et al., 2004).

4. Discussion and Conclusion

4.1. *sdaB* and resistance to VAN

The two main antibiotics currently used to treat *C. difficile*, are MTZ and the glycopeptide VAN (Kouhsari *et al.*, 2019). MTZ, normally used for the treatment of mild-to-moderate CDI, is no longer recommended as a first-line drug for CDI in adults and its use is in decline. Moreover, resistance to MTZ correlates with the presence of a plasmid acquired by horizontal gene transfer and resistance to the antibiotic is increasing. VAN, reserved in the past for severe infections and recurrent CDI, is increasingly used as a first-line antibiotic but resistant strains have been reported and their prevalence is increasing (Louie *et al.*, 2011; Srikhanta *et al.*, 2019). The widespread dissemination of VAN resistance, adding to the multiple drug-resistant phenotype of *C. difficile* would create a very serious problem and stresses the importance of both surveillance and the design of therapies based on an understanding of the molecular basis of resistance (Kouhsari *et al.*, 2019). The pathways leading to VAN resistance in *C. difficile*, however, are poorly understood.

VAN inhibits cell wall synthesis by binding the C-terminal dipeptide D-Alanyl-D-Alanine of the muramyl-pentapeptide part of PG precursors (Gardete and Tomasz, 2014; Liu and Breukink, 2016) (**Figure 1.4**). VAN resistance, first found over three decades ago in *Enterococci*, has since disseminated worldwide, was acquired by other organisms and is now a serious public health issue (Ammam *et al.*, 2013; Stogios and Savchenko, 2020). VAN resistance in the *Enterococci* relies on the expression of *van* gene clusters which allow replacement of the dipeptide termini of PG precursors from D-Ala-D-Ala to D-Ala-D-Lac or D-Ala-D-Ser, both of which have reduced affinity for VAN (Stogios and Savchenko, 2020). *van* clusters include a regulatory and an enzymatic module (Shen *et al.*, 2020; Stogios and Savchenko, 2020). The first is a regulatory module that codes for a membrane embedded VAN-sensor kinase, VanS, and a response regulator, VanR, which is phosphorylated and thereby activated by VanS. The second module, whose transcription is activated by the phosphorylated form of VanR, VanR~P, codes for enzymes responsible for the synthesis of D-Ala-D-Lac or D-Ala-D-Ser precursors and for the elimination of cytoplasmic precursors ending in D-Ala-D-Ala, or the D-Ala-D-Ala peptide (Ammam *et al.*, 2013; Shen *et al.*, 2020; Stogios and Savchenko, 2020).

Susceptibility to VAN in *C. difficile* is intriguing because the vast majority of strains carry a *vanG* type cluster, which is sufficient to confer resistance against the glycopeptide in other pathogens. In *vanG*-type clusters, *vanG* codes for a D-Ala:D-Ser ligase, VanXY for a carboxypeptidase/D,D-dipeptidase, and VanT for a D-Ser racemase (Ammam *et al.*, 2013). However, disruption of the $vanG^{Cd}$ cluster in *C. difficile*, lowers only slightly the MIC^{VAN}, from 1.5 mg L^{-1} to 0.75 mg L^{-1} (Shen *et al.*, 2020). The cluster is functional: i) the $vanG^{Cd}$ cluster is inducible by VAN and results in the accumulation of UDP-NAM-pentapeptide[D-Ser] in the cell wall (Ammam *et al.*, 2013; Tsutsumi *et al.*, 2014; Stogios and Savchenko, 2020); ii) its introduction in *E. coli* allows survival in the presence of VAN; iii) enzymatic assays shows that the VanT, VanS and VanXY enzymes are active, although VanT slightly prefers L-Ala to L-Ser (Ammam *et al.*, 2013; Shen *et al.*, 2020).

Importantly, clinical isolates of ribotype 027 and VAN-resistant laboratory mutants also of ribotype 027 with MIC^{VAN} between 4 and 16 mg L^{-1}, *i.e.*, up to 8 times higher than that of the parental strain, bear single amino acid substitutions in VanR that renders it constitutively active or in VanS, impairing its phosphatase activity and resulting in a constitutively active VanR~P. Following chemical mutagenesis of a susceptible strain, my colleague Mariana Valente selected mutants with increased resistance to VAN (Valente, 2021). Some, but not all of the mutations map to *vanS*. These mutations, which result in a modest increase in the MIC^{VAN} (from 2 to 4 or 8 mg L^{-1}), are also thought to impair the phosphatase activity of VanS. Together, these observations indicate that the *vanG* cluster contributes to resistance, but the evidence from our laboratory suggests that the mutations in *vanS* do not result *per s*e in a dramatic

increase in resistance, and that additional mutations may be needed for high level resistance. Therefore, there might be one or more bottlenecks limiting the emergence of VAN resistance in *C. difficile*.

One bottleneck preventing expression of resistance may occur at the level of the MurF ligase, which adds the dipeptide to the NAM-tripeptide precursor and shows a preference for D-Ala-D-Ala over D-Ala-D-Ser (Barreteau *et al.*, 2008; Liu and Breukink, 2016). Other bottlenecks, however, are likely to exist. For instance, two strains selected for reduced susceptibility to VAN *in vitro* (MIC^{VAN} of 16 mg L^{-1}) had multiple and/or pleotropic mutations (Leeds *et al.*, 2014). One strain bears three mutations, in *murG*, *sdaB* and *CD3659*. MurG converts lipid I to lipid II, the lethal target of VAN (**Figure 4.1**; see more on *murG* below). The second mutation is an in-frame deletion in the L-Serine deaminase, *sdaB*. The third mutation inactivates a putative RNA/single-stranded DNA exonuclease, *CD3659*, suggesting the increase in the levels of one or more relevant RNA's. Another strain had a mutation in *rpoC* (Leeds *et al.*, 2014). Both the *rpoC* and *CD3659* mutations are likely to be pleiotropic, affecting the expression of several genes (**Figure 4.2**). Importantly, the absence of mutations in the $vanG^{Cd}$ cluster in some of the mutants selected for increased resistance to VAN by my colleague Mariana Valente, also suggests that there are multiple mechanisms by which VAN resistance can arise (Valente, 2021).

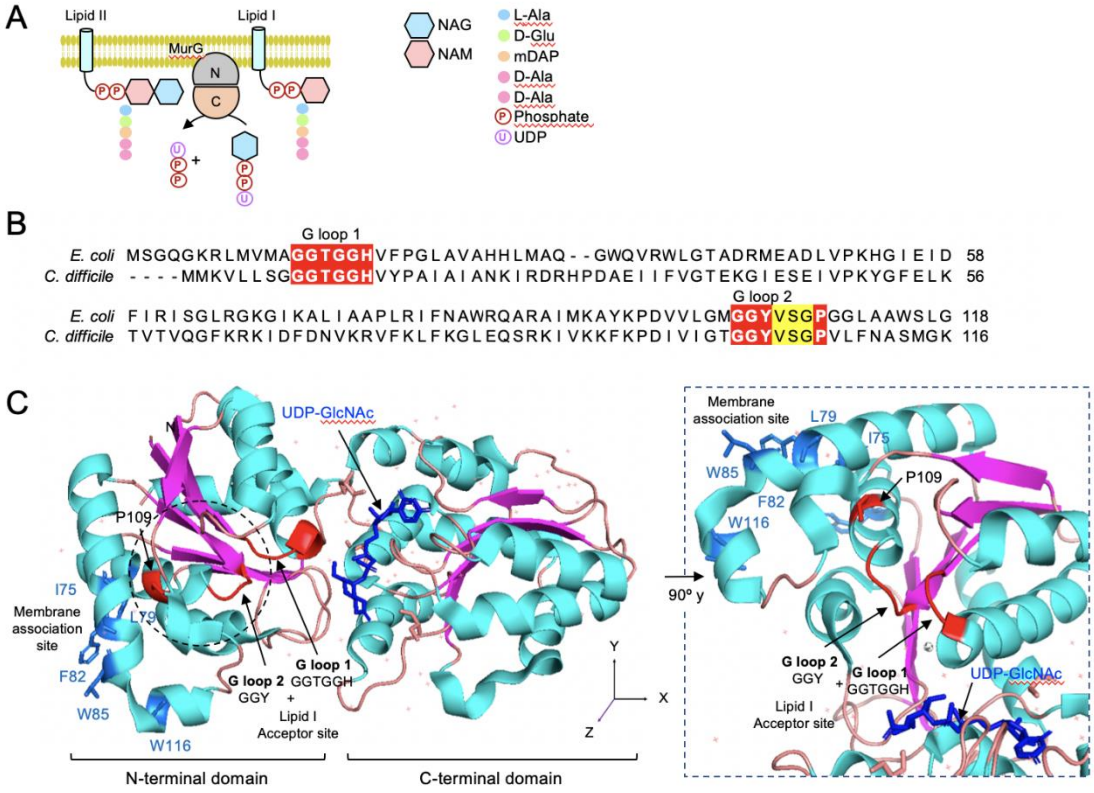

Figure 4.1: The MurG structure. A: The panel illustrates the reaction catalysed by MurG which converts lipid I into lipid II, by adding UDP-NAG to undecaprenyl-pyrophosphoryl-NAM-pentapeptide (lipid I). MurG has two domains, N and C, with the N-domain interacting with the membrane. **B**: Clustal Ω amino acid sequence alignment between the MurG proteins of *E. coli* and *C. difficile*. Only the first 118/116 residues of the proteins are aligned, to show the G loop 1 and G loop 2 motifs and the conserved proline (boxed in red) that is the site of the P108 substitution in an epidemic strain of *C. difficile*. The residues in yellow are part of the helix where the proline residue is located. **C**: Structure of the *E. coli* MurG protein (pdb code 1NLM) in complex with UDP-NAG (blue). The figure shows the N- and C-terminal domains. UDP-NAG binds to the C-terminal domain, whereas the lipid I acceptor site is located in the N-terminal domain. The G loops 1 and 2 are highlighted in red, as is the conserved proline residue. The G loops 3 and 4, in the C-terminal domain, are not indicated for simplicity. Hydrophobic residues in a membrane association site located in the N-terminal domain are shown in stick mode and in blue. These residues alternate with positively charged residues (not represented) suggesting that the interaction involves both hydrophobic contacts and contacts with the phospholipid head groups. Note the proximity of the lipid I acceptor site with the membrane interaction site. The panel on the right is a magnified rotation view of the G loop 1 and G loop 2 regions, showing the relative position of P108 in close proximity to the G loops 1 and 2 region.

That VAN resistance can arise through multiple pathways is also supported by studies in *S. aureus*. Strains with intermediate MIC^{VAN} values (3-8 mg L^{-1}) known as VISA, carry several mutations, often in two-component sensory regulatory systems controlling the transcription of genes involved in cell wall synthesis and autolysis, but mutations in *rpoC*, coding for the β' subunit of RNA polymerase have also been found (Gardete and Tomasz, 2014). Phenotypes common to VISA strains include a thicker cell wall, deficient cell separation following division and decreased rates of autolysis. One way VISA strains protect lipid II from VAN is by increasing the representation of D-Ala-D-Ala in the mature cell wall (Gardete and Tomasz, 2014). This creates false targets that maintain VAN away from lipid II and the site of new cell wall synthesis close to the cell membrane. Impaired activity of D,D-carboxypeptidases may also increase D-Ala-D-Ala at the cell wall, contributing to the VISA phenotype (Gardete and Tomasz, 2014). All these considerations potentially apply to *C. difficile*, motivating our proposal to characterize the pathways leading to VAN resistance in this important human pathogen (**Figure 4.2**).

The presence of the mutations in *murG*, *sdaB* and *CD3659* in one of the VAN-resistant isolates selected *in vitro* (Leeds *et al.*, 2014) also offers the opportunity to study the individual contributions of the mutations to resistance and hence the contributions of the corresponding pathways. The triple mutant genotype suggests that the MurG-dependent step in the pathway of PG synthesis might normally be a bottleneck for resistance. MurG catalyses formation of lipid II from lipid I and UDP-NAG (**Figures 4.1A**). MurG consists of two domains separated by a deep cleft: the C-terminal domain contains the UDP-NAG binding site while the N-terminal domain contains the acceptor binding site for lipid I and a membrane association site. The association of MurG with the cytoplasmic surface of the cell membrane allows the coupling between the soluble UDP-NAG substrate, which binds to the C-domain, and the membrane bound acceptor sugar, lipid I. Residue Pro108 in $MurG^{Cd}$ (homologous to P109 in the *E. coli* protein) is conserved among MurG orthologues (**Figure 4.1B** only shows the alignment between the *E. coli* and the *C. difficile* proteins, for simplicity). To gain insight into the position of P108 relative to other important motifs in the protein, we used the structure of *E. coli* MurG in complex with UDP-NAG (pdb code 1NLM) (Hu *et al.*, 2003), to generate a homology model of $MurG^{Cd}$ using the Phyre2 server (http://www.sbg.bio.ic.ac.uk/phyre2) (**Figure 4.1C**). $MurG^{Ec}$ is the closest structural homologue of $MurG^{Cd}$ (Ha *et al.*, 2000; Hu *et al.*, 2003). We found that P108 is close to the N-terminal end of a short helix located close to glycine rich G loop 1 (GGTGGH), which is itself close to G loop 2 (GGY); the glycine-rich G loop motif is involved in binding the negatively charged phosphates in nucleotide binding proteins and are presumed to be involved in binding the phosphates in lipid I (Baker *et al.*, 1992; Carugo and Argos, 1997) (**Figure 4.1C**; note that G loop motifs in the C-terminal domain, involved in biding the phosphates in UDP-NAG are not represented). Also importantly, both Pro108 and the G1 and G2 loops are not far from the binding site for the lipid I acceptor substrate. Hence, we presume that the P108L substitution affects the configuration of the G loop 1 and 2 region, possibly facilitating the interaction of substrates ending in D-Alanyl-D-Ser.

However, additional evidence for a limiting step in the PG biosynthetic pathway, comes from the presence of the mutation in the *sdaB* gene. Deletion of three redundant L-Ser deaminases in *E.coli* causes the accumulation of L-Ser and gross alterations in cell shape, size, and division (Shao *et al.*, 1994). These phenotypes are rescued by overproduction of MurC, which adds L-Ala to NAM, or by the overproduction of FtsW, a transglycosylase required for cell division (Real *et al.*, 2008; Fay *et al.*, 2010a; Higgins and Dworkin, 2012; Meeske *et al.*, 2016; Sjodt *et al.*, 2020) (**Figure 1.4**). This suggests that FtsW may not efficiently accept D-Ala-D-Ser precursors and thus an essential requirement for D-Ala-D-Ala for cell division. Division in *C. difficile* may also require D-Ala-D-Ala precursors as work in the laboratory showed that a fluorescent derivative of VAN only stains the division septum, and that induction of the cluster interferes with the normal pattern of division site selection (**Figure 4.3**).

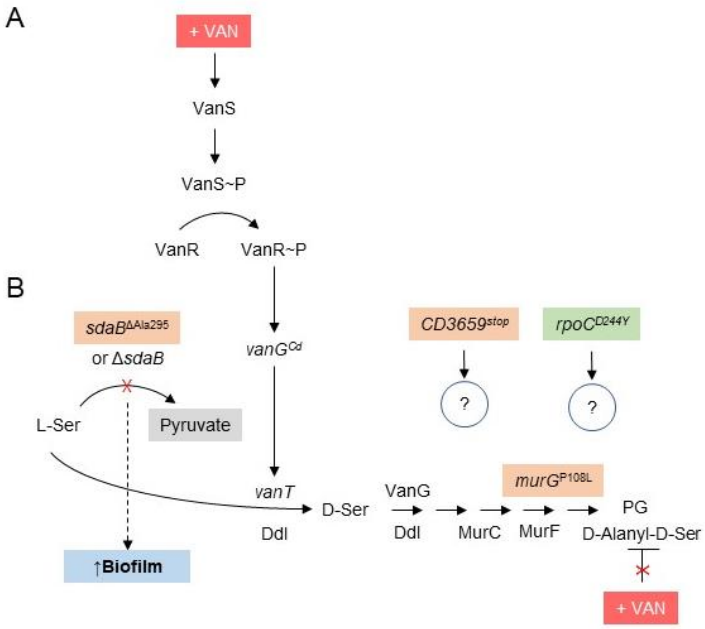

Figure 4.2: Model for the role of the mutations found in the VAN-resistant epidemic strains. A: In the presence of VAN, the VanS sensor kinase auto-phosphorylates and transfers the phosphoryl group to the VanR response regulator. Phosphorylated VanR then activates transcription of the *vanG*^{Cd} operon, which includes the *vanG* gene coding for a D-Ser ligase. **B**: A VAN resistance strain has mutations in *sdaB* (an in-frame deletion of an Ala within the protein core, ΔAla295), *murG* (a P108L substitution close to the binding site for lipid I) and a stop codon in *CD3659* (light orange boxes). Deletion of the *sdaB* gene, as presumably the in-frame deletion mutation, may prevent formation of pyruvate from L-Ser leading to accumulation of the later. This results in increased biofilm formation by the mutant. VanG, together with the Ddl racemase, converts L-Ser into D-Ser, which then can enter the PG biosynthetic pathway resulting in increased incorporation of muropeptides ending in D-Alanyl-D-Ser, which are inefficiently bound by VAN. This confers a certain degree of resistance to VAN. The *sdaB* mutation is thought to synergize with the P108L form of MurG, which may interact better with lipid I ending in D-Alanyl-D-Ser to afford VAN resistance. Another strain has a missense mutation in the *rpoC* gene (green box) causing the D244Y substitution. It seems possible that both the *CD3659* and *rpoC* mutations are pleiotropic, but it is not presently known how they contribute to VAN resistance.

Importantly, if the *sdaB* mutation impairs the activity of the enzyme, this may indicate that the VAN resistance strictly dependent on induction of the *vanG*^{Cd} cluster may be limited by the intracellular level of Ser. To establish whether the *sdaB* gene directly contributes to VAN resistance was a key motivation for this work.

4.2. Expression of *sdaB* during growth and stationary phase

We started our study by examining the expression of the *sdaB* gene during growth and sporulation using a transcriptional fusion of the *sdaB* promoter to the *SNAP*^{Cd} reporter (Pereira *et al.*, 2013; Saujet *et al.*, 2013; Serrano, Kint, *et al.*, 2016; Cassona, 2018). We found expression of the P$_{sdaB}$-*SNAP*^{Cd} fusion to occur during growth and during transition to the stationary phase, consistent with the presence of a possible σ^A-type promoter in the *sdaB* regulatory region (**Figure 3.1**). Neither CodY nor Spo0A affected expression of the fusion and thus *sdaB* is not under sporulation control and does not respond to the amino acids, leucine, isoleucine and valine (branched chain) that are sensed by CodY (Dineen *et al.*, 2010; Pereira *et al.*, 2013; Nawrocki *et al.*, 2016). *E. coli*, for example, does not use any L-SD in any known metabolic pathway. It cannot use the enzyme to bypass a block in triose isomerization in the Embden Meyerhof pathway, although conversion of serine to pyruvate would constitute such a sidestep. It cannot use L-Serine as sole carbon source, while it is a good carbon and energy source when other compounds are presented with it, but it use serine as carbon source as a result of mutations (Zhang and Newman, 2008). To use serine, particularly as energy source, the cell also requires an efficient transport system to bring it into the cell. Main uptake systems are (i) energized by a sodium gradient and carries both serine and threonine, and (ii) use the proton gradient as a driving force, much more specific for L-

Serine (Shao *et al.*, 1994). The conversion of L-Serine to pyruvate might be limited quantitatively, either because cells exposed only to L-Serine do not have high enough levels of L-SD or because they maintain what they have in an inactive form. Since glycine and leucine are inducers of L-SD, their effect be due the fact that the activity of L-SD to may in uninduced cells is insufficient (Newman and Walker, 1982; Su *et al.*, 1989). In future work, we will test the influence of glycine and leucine as possible inducers of *sdaB* in *C. difficile*, and whether the WT but not a *sdaB* mutant, use L-Serine as the sole carbon source.

Accumulation of the reporter in sporulating cells most likely reflects protracted expression that initiated in cells prior to the onset of sporulation. At late sampling points, the signal from the $SNAP^{Cd}$ reporter accumulated in the forespore. Although a possible σ^F-dependent promoter is present in the *sdaB* regulatory region, none of the mutants for the sporulation sigma factors (neither a *spo0A* mutation which is epistatic over the sigma factor mutations) affected the expression of the fusion and we do not presently understand the origin of the late forespore-specific signal. In any case, the finding that at least during intermediate times in sporulation expression of P_{sdaB}-$SNAP^{Cd}$ is detected in the two cells (mother cell and forespore) does not exclude a potential role for the *sdaB* gene during sporulation. If deletion of *sdaB* gene creates conditions for increased incorporation of D-Ala-D-Ser into the PG then, in the presence of VAN, it could in principle alter the composition of the spore cortex and germ cell wall layers. This is important because an alteration in the structure of the spore cortex, in particular, could impair degradation of this layer during spore germination and comprise the infection. These possibilities have not yet been tested.

4.3. Deletion of *sdaB* increases the MIC^{VAN} and reduces incorporation of D-Ala-D-Ala in the PG

Using the ACE methodology (Ng *et al.*, 2013), we constructed a mutant bearing an in-frame deletion mutation of the coding region of the *sdaB* gene (**Figure 3.5**). The *sdaB* null mutant was first used to test whether the susceptibility to VAN increased. We used Etests and MIC determination in liquid medium and found that the mutant showed a higher MIC, between 2-6 μg mL^{-1}, than the WT in both tests (**Figure 3.6**). These observations are in line with the prediction that deletion of *sdaB* could increase the MIC^{VAN} and suggest that the mutation could favour the flow of L-Ser in the direction of the PG biosynthetic pathway (see model on **Figure 4.2**). Unfortunately, until the conclusion of this work, it was not possible to obtain an in-frame deletion mutant of the same alanine found in the screen of Leeds and co-authors (Leeds *et al.*, 2014). Results discussed below, suggest however that the original mutation may significantly impair enzyme activity.

If the increase in the MIC^{VAN} was due to increased representation of D-Ala-D-Ser in the PG, then labelling of living cells with a fluorescent derivative of VAN (VAN-FL) should be reduced. Consistent with this prediction, VAN-FL labelling of *sdaB* cells was markedly reduced. The experiments were carried out in the presence of imipenem, which inhibits both the LDTs and the DDTs (**Figure 3.8**). This was important because the LDTs use muro-tetrapeptides as substrates while the DDTs use muro-pentapeptides as substrates, to catalyse formation of 3-3 and 4-3 crosslinks, respectively (Barreteau *et al.*, 2008). In other words, in the absence of imipenem, VAN-FL labelling would be low. In fact, in a WT strain in the absence of imipenem, labelling is restricted to the division septum (**Figure 4.3**, experiment performed by Mónica Serrano). This is consistent with the idea that there might be a requirement for D-Ala-D-Ala and DDTs activity for cell division whereas the activity of the LDTs may be confined to the lateral walls of the cell (**Figure 4.3D**). In the presence of VAN, WT cells showed string labelling by VAN-FL along the entire surface of the cell but strikingly, this binding was much weaker in the *sdaB* mutant (**Figure 3.8**). This suggests that increased representation of D-Ala-D-Ser in the PG and that SdaB works as a gatekeeper, regulating the availability of L-Ser for pyruvate production or to the PG biosynthetic pathway (**Figure 4.2**).

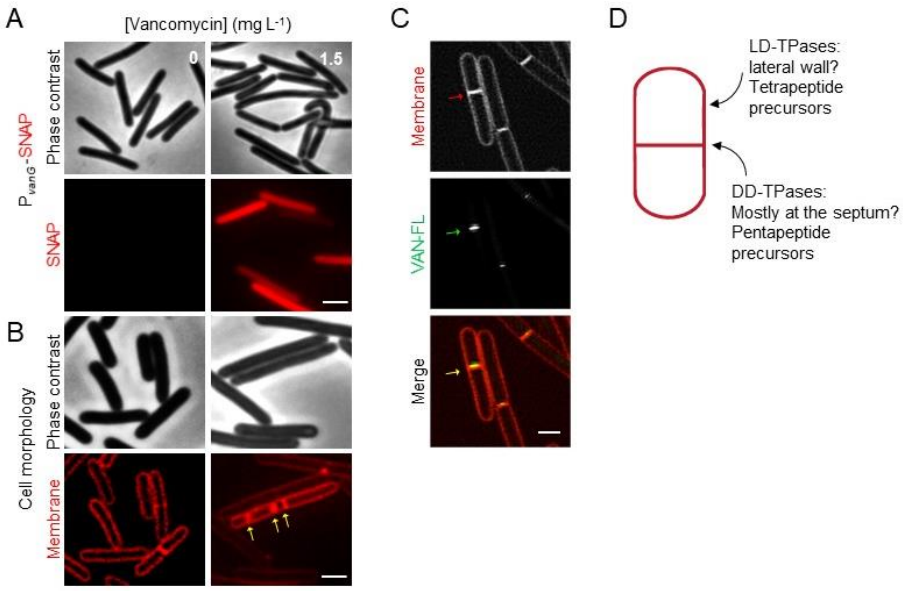

Figure 4.3: VAN affect cell division. A: Phase contrast and fluorescence microscopy analysis of a transcriptional fusion of the promoter region of the *vanG* gene to the *SNAP* tag, in the absence (0 mg L^{-1}) and in the presence (1.5 mg L^{-1}) of VAN. Scale bar, 1 µm. **B**: WT cells imaged by phase contrast and fluorescence microscopy stained with the membrane dye FM4-64, in the absence (0 mg L^{-1}) and in the presence (1.5 mg L^{-1}) of VAN. The yellow arrows indicate the position of multiple division septum. **C**: WT cells were labelled with FM4-64 and examined by fluorescence microscopy. The arrows indicate the position of the division septum: red arrow with FM4-64, green arrow with fluorescent vancomycin (VAN-FL), and yellow arrow the merge of the 2 images. Scale bar, 1 µm. **D**: Model of one *C. difficile* cell, with the division septum and the supposed site of action of the LDTs (which use tetrapeptide precursors as donor substrates) and the DDTs (which use pentapeptides precursors).

In future work we will analyse the structure of the purified PG, to determine whether or not D-Ser incorporation increases in the *sdaB* mutant.

4.4. Deletion of *sdaB* increases biofilm formation

Since pyruvate was shown to induce biofilm formation in *C. difficile* we also evaluated biofilm production of the *sdaB* null mutant in rich (BHISG) and minimal media (CDMOB) in response to different metabolites (DOC, pyruvate and glucose) (Dubois *et al.*, 2019, Tremblay *et al.*, 2021). We found that the *sdaB* mutation increases biofilm formation in rich medium with DOC and in minimal medium in the presence of glucose (**Figure 3.7**). Interestingly in both conditions glucose is added to the medium (see Material and Methods section). In *C. difficile*, CcpA is the major regulator of carbon catabolite repression (CCR) and controls the use of alternate carbon sources. In 2012, Antunes *et al.*, described that in *C. difficile* the expression of *sdaB* is positively controlled by CcpA in the presence of glucose (Antunes *et al.*, 2012). This indicates that when glucose is present in the medium *sdaB* is involved in serine degradation to form pyruvate increasing its intracellular levels. It is obviously important, in future work, to test the effect of CcpA in the expression of *sdaB* under our culturing conditions.

Recently Tremblay *et al.* propose a model in which during exponential phase pyruvate is secreted and glucose is preferentially used until the bacteria enter stationary phase. In stationary phase, there is a metabolic shift and cells use alternative sources of energy. As growth progress it will start to import extracellular pyruvate to maintain viability and trigger biofilm formation (Tremblay *et al.*, 2021). We hypothesized that in the presence of glucose, deletion of *sdaB* reduces the intracellular level of pyruvate, which results in the import of extracellular pyruvate early in stationary phase and at the onset of biofilm formation (**Figure 4.4**). Reduced intracellular levels of pyruvate may activate a pyruvate-import system (CstA) via a two-component system (TCS) formed by the response regulator (*CD630*_26010) and the membrane-associated kinase (*CD630*_26020) which senses extracellular pyruvate (Dubois *et al.*, 2016). Uptake of extracellular pyruvate through the CstA transporter has been suggested to promote biofilm

formation (Tremblay *et al.*, 2021) and in contrast to *sdaB*, *cstA* is repressed by CcpA in the presence of glucose (Antunes *et al.*, 2012). According to our model, the early onset of biofilm formation with the consequent increased biofilm biomass at 48 h would still be dependent on CstA. Thus a double mutant *cstA sdaB* should decrease the levels of biofilm formation to the single mutant *cstA* level (Tremblay *et al.*, 2021). This will be tested in future work; also, to be tested is whether the exogeneous addition of purified pyruvate dehydrogenase to the cultures will revert the enhanced biofilm phenotype of the *sdaB* mutant (Tremblay *et al.*, 2021).

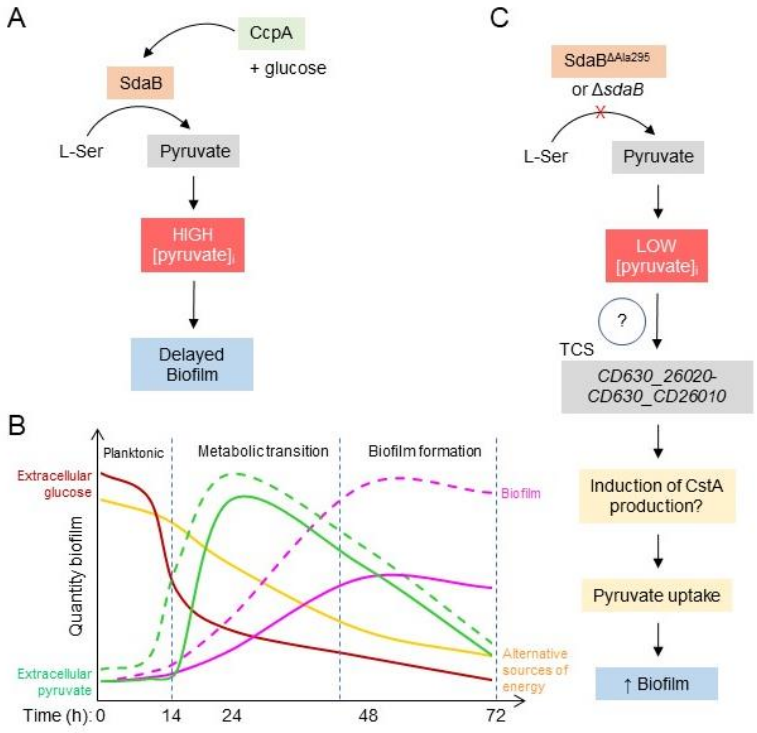

Figure 4.4: Role of *sdaB* on biofilm formation. A: In *C. difficile* the expression of *sdaB* is positively controlled by CcpA in the presence of glucose. This indicates that when glucose is present in the medium *sdaB* is involved in serine degradation to form pyruvate increasing its intracellular levels, delaying biofilm. **B**: Hypothetical model of the changes in the quantity biofilm over time. During exponential phase, pyruvate is secreted, and glucose is preferentially used until the bacteria enter stationary phase, after approximately 14 h of growth. After entry into stationary phase, there is a metabolic shift driven by CcpA, and cells start using alternative sources of energy. In the presence of glucose, deletion of *sdaB* (**broken line**) reduces the intracellular level of pyruvate in comparison with the WT (**solid line**), which results in the import of extracellular pyruvate early in stationary phase and at the onset of biofilm formation. Reduced intracellular levels of pyruvate will sense extracellular pyruvate via TCS (*CD630*_26010-26020) and will start actively importing extracellular pyruvate via CstA. **C**: The figure expands the biofilm-related part of **Figure 4.2**. It suggests that deletion of *sdaB* may reduce the intracellular level of pyruvate, and results in increased biofilm production (**broken line**). We hypothesize that reduced intracellular levels of pyruvate may activate a pyruvate-import system (CstA) via a two-component system (TCS). Uptake of extracellular pyruvate through the CstA transporter has been suggested to promote biofilm formation. It is not presently known whether deletion of *sdaB* induces expression of the genes required for pyruvate sensing and transport (question mark). The gene *CD630*_26010 codes for a response regulator transcription factor and *CD630*_26020 codes for a sensor histidine kinase (HK).

4.5. Properties of SdaB

The homology model presented in **Figure 1.6**, suggested that the in-frame deletion mutation of alanine codon 295 found in a VAN-resistant isolate (Leeds *et al.*, 2014), resulted in the deletion of the N-terminal alanine in a helix located just below the iron-sulfur cluster. The shortening of this helix is expected to affect proper position of the cluster and also the structure of a core region of the protein. In other words, it could act as a complete or at least partial loss-of-function alteration. To test this idea, we perform a biochemical characterization of the SdaB protein. SdaB is an [Fe-S] cluster serine deaminase, that have been reported to be unstable, losing activity quickly during its purification (Cicchillo *et al.*, 2004). To maximize purification of an active enzyme, SdaB and SdaB$^{\Delta A295}$ were expressed as a fusion

to an N-terminal His_6-tag in *E. coli* strain BL21λDE3 Suf^{++} and purified under anaerobic conditions in an anaerobic chamber (**Figure 3.10**). We used this strain because the *E. coli* BL21 (DE3) has a mutation that inactive the function of one of the two native Suf pathways responsible for the biogenesis of [Fe-S] clusters. Correction of the mutation, combined with additional changes elevate Suf protein levels in BL21λDE3 Suf^{++}, and increased the yield and cluster occupancy of [Fe-S] cluster-containing enzymes, facilitating biochemical analysis (Corless *et al.*, 2020). We purified the WT His_6-SdaB protein to nearly homogeneity. However, we were unable to overproduce the His_6-$SdaB^{\Delta A295}$ protein in soluble form, in spite of several attempts, suggesting that the fold of the protein was significantly altered. Although we do not presently understand why the folding of the protein could have been significantly changed as the result of deleting Ala295 it seems possible that the mutation created a loss-of-function (or null) mutant in *C. difficile* (Leeds *et al.*, 2014).

One way to bypass this problem would be to replace Alanine 295 by the smaller amino acid glycine, or by the slightly larger valine. Assuming that at least one of these mutations would not result in protein instability, we could then finalize our biochemical analysis of the WT in parallel with the altered protein(s). In addition to basic enzymology to verify L-Ser deaminase activity, kinetic constants and factors that may control enzyme activity and that might be relevant *in vivo*, we plan to characterize the [Fe-S] cluster using electron paramagnetic resonance (EPR), nuclear magnetic resonance (NMR), and Raman spectroscopy.

4.6. Final considerations

This study implicates SdaB in VAN resistance in *C. difficile*. The results in this dissertation suggest that the availability of L-Ser may be a bottleneck in the expression of VAN resistance even when VAN induces the $vanG^{Cd}$ operon. Moreover, the evidence presented here point to increased incorporation of D-Ala-D-Ser into the cell wall PG (or at least to reduced representation of D-Ala-D-Ala motifs) and therefore that the *sdaB* mutation may synergize with other mutations, such as $murG^{P108L}$, to confer VAN resistance. High-level VAN resistance may require multiple mutations. In a future work, it would be interesting to combine the *sdaB* deletion with the $murG^{P108L}$ allele and perhaps with other mutations, including those isolated in our group in the *vanS* gene.

Finally, unravelling the pathways leading to VAN resistance may allow the identification of targets for novel therapeutics aiming specifically at mitigating the threat posed by the emergence and dissemination of VAN-resistant strains.

5. References

Abdrabou, A. M. M., Ul Habib Bajwa, Z., Halfmann, A., Mellmann, A., Nimmesgern, A., Margardt, L., Bischoff, M., von Müller, L., Gärtner, B. and Berger, F. K. (2021) 'Molecular epidemiology and antimicrobial resistance of *Clostridioides difficile* in Germany, 2014–2019', *International Journal of Medical Microbiology*, 311(4). doi: 10.1016/j.ijmm.2021.151507.

Van Acker, H., Van Dijck, P. and Coenye, T. (2014) 'Molecular mechanisms of antimicrobial tolerance and resistance in bacterial and fungal biofilms', *Trends in Microbiology*, 22(6), pp. 326–333. doi: 10.1016/j.tim.2014.02.001.

Al-Tawfiq, J. A., Rabaan, A. A., Bazzi, A. M., Raza, S. and Noureen, M. (2020) '*Clostridioides* (*Clostridium*) *difficile*-associated disease: Epidemiology among patients in a general hospital in Saudi Arabia', *American Journal of Infection Control*, 48(10), pp. 1152–1157. doi: 10.1016/j.ajic.2020.01.011.

Alabdali, Y. A. J., Oatley, P., Kirk, J. A. and Fagan, R. P. (2019) 'A cortex-specific PBP contributes to cephalosporin resistance in *Clostridium difficile*', *BioRxiv*. doi: https://doi.org/10.1101/715458.

Álvarez, R., Ortega-Fuentes, C., Queraltó, C., Inostroza, O., Díaz-Yáñez, F., González, R., Calderón, I. L., Fuentes, J. A., Paredes-Sabja, D. and Gil, F. (2020) 'Evaluation of functionality of type II toxin-antitoxin systems of *Clostridioides difficile* R20291', *Microbiological Research*, 239(March), pp. 1–4. doi: 10.1016/j.micres.2020.126539.

Ammam, F., Meziane-cherif, D., Mengin-Lecreulx, D., Blanot, D., Patin, D., Boneca, I. G., Courvalin, P., Lambert, T. and Candela, T. (2013) 'The functional *vanG*^{Cd} cluster of *Clostridium difficile* does not confer vancomycin resistance', *Molecular Microbiology*, 89(4), pp. 612–625. doi: 10.1111/mmi.12299.

Antunes, A., Camiade, E., Monot, M., Courtois, E., Barbut, F., Sernova, N. V., Rodionov, D. A., Martin-Verstraete, I. and Dupuy, B. (2012) 'Global transcriptional control by glucose and carbon regulator CcpA in *Clostridium difficile*', *Nucleic Acids Research*, 40(21), pp. 10701–10718. doi: 10.1093/nar/gks864.

Awad, M. M., Johanesen, P. A., Carter, G. P., Rose, E. and Lyras, D. (2015) '*Clostridium difficile* virulence factors: Insights into an anaerobic spore-forming pathogen', *Gut Microbes*, 5(5), pp. 579–593. doi: 10.4161/19490976.2014.969632.

Babakhani, F., Bouillaut, L., Gomez, A., Sears, P., Nguyen, L. and Sonenshein, A. L. (2012) 'Fidaxomicin inhibits spore production in *Clostridium difficile*', *Clinical Infectious Diseases*, 55(SUPPL.2), pp. 162–169. doi: 10.1093/cid/cis453.

Baker, P. J., Britton, K. L., Rice, D. W., Rob, A. and Stillman, T. J. (1992) 'Structural consequences of sequence patterns in the fingerprint region of the nucleotide binding fold. Implications for nucleotide specificity.', *Journal of molecular biology*, 228(2), pp. 662–671. doi: 10.1016/0022-2836(92)90848-e.

Banawas, S. S. (2018) '*Clostridium difficile* Infections: A Global Overview of Drug Sensitivity and Resistance Mechanisms', *BioMed Research International*, 2018, p. 9. doi: 10.1155/2018/8414257.

Barreteau, H., Kovač, A., Boniface, A., Sova, M., Gobec, S. and Blanot, D. (2008) 'Cytoplasmic steps of peptidoglycan biosynthesis', *FEMS Microbiology Reviews*, 32(2), pp. 168–207. doi: 10.1111/j.1574-6976.2008.00104.x.

Bartlett, J. G. (1994) '*Clostridium difficile*: history of its role as an enteric pathogen and the current state of knowledge about the organism', *Clinical Infectious Diseases*, 18(Suppl 4), pp. S265–S272. doi: 10.1093/clinids/18.Supplement_4.S265.

Boudry, P., Semenov, E., Monot, M., Datsenko, K. A., Lopatina, A., Sekulovic, O., Ospina-Bedoya, M., Fortier, L. C., Severinov, K., Dupuy, B. and Soutourina, O. (2015) 'Function of the CRISPR-cas system of the human pathogen: *Clostridium difficile*', *mBio*, 6(5), pp. 1–16. doi: 10.1128/mBio.01112-15.

Brouwer, M. S. M., Roberts, A. P., Hussain, H., Williams, R. J., Allan, E. and Mullany, P. (2013) 'Horizontal gene transfer converts non-toxigenic *Clostridium difficile* strains into toxin producers',

Nature Communications, 4, pp. 1–6. doi: 10.1038/ncomms3601.
Burke, K. E. and Lamont, J. T. (2014) '*Clostridium difficile* infection: A worldwide disease', *Gut and Liver*, 8(1), pp. 1–6. doi: 10.5009/gnl.2014.8.1.1.
Burman, J. D., Harris, R. L., Hauton, K. A., Lawson, D. M. and Sawers, R. G. (2004) 'The iron-sulfur cluster in the L-Serine dehydratase TdcG from *Escherichia coli* is required for enzyme activity', *FEBS Letters*, 576(3), pp. 442–444. doi: 10.1016/j.febslet.2004.09.058.
Cartman, S. T., Kelly, M. L., Heeg, D., Heap, J. T. and Minton, N. P. (2012) 'Precise manipulation of the *Clostridium difficile* chromosome reveals a lack of association between the *tcdC* genotype and toxin production', *Applied and Environmental Microbiology*, 78(13), pp. 4683–4690. doi: 10.1128/AEM.00249-12.
Carugo, O. and Argos, P. (1997) 'NADP-dependent enzymes. I: Conserved stereochemistry of cofactor binding', *Proteins*, 28(1), pp. 10–28. doi: 10.1002/(sici)1097-0134(199705)28:1<10::aid-prot2>3.0.co;2-n.
Cassona, C. P. (2018) *Single cell analysis of toxinogenesis by vegatative and sporulating cells in the enteric pathogen Clostridioides difficile*. Universidade Nova de Lisboa.
Cicchillo, R. M., Baker, M. A., Schnitzer, E. J., Newman, E. B., Krebs, C. and Booker, S. J. (2004) '*Escherichia coli* L-serine deaminase requires a [4Fe-4S] cluster in catalysis', *Journal of Biological Chemistry*, 279(31), pp. 32418–32425. doi: 10.1074/jbc.M404381200.
Corless, E. I., Mettert, E. L., Kiley, P. J. and Antony, E. (2020) 'Elevated Expression of a Functional Suf Pathway in *Escherichia* Sulfur Cluster-Containing Protein', *Journal of Bacteriology*, 202(3), pp. 1–11. Available at: https://jb.asm.org/content/202/3/e00496-19.
Cuenot, E., Garcia-Garcia, T., Douche, T., Gorgette, O., Courtin, P., Denis-Quanquin, S., Hoys, S., Tremblay, Y. D. N., Matondo, M., Chapot-Chartier, M.-P., Janoir, C., Dupuy, B., Candela, T. and Martin-Verstraete, I. (2019) 'The Ser/Thr Kinase PrkC Participates in Cell Wall Homeostasis and Antimicrobial Resistance in *Clostridium difficile*.', *Infection and immunity*, 87(8). doi: 10.1128/IAI.00005-19.
Czepiel, J., Dróżdż, M., Pituch, H., Kuijper, E. J., Perucki, W., Mielimonka, A., Goldman, S., Wultańska, D., Garlicki, A. and Biesiada, G. (2019) '*Clostridium difficile* infection: review', *European journal of clinical microbiology & infectious diseases : official publication of the European Society of Clinical Microbiology*, 38(7), pp. 1211–1221. doi: 10.1007/s10096-019-03539-6.
Dembek, M., Kelly, A., Barwinska-Sendra, A., Tarrant, E., Stanley, W. A., Vollmer, D., Biboy, J., Gray, J., Vollmer, W. and Salgado, P. S. (2018) 'Peptidoglycan degradation machinery in *Clostridium difficile* forespore engulfment', *Molecular Microbiology*, 110(3), pp. 390–410. doi: 10.1111/mmi.14091.
Depestel, D. D. and Aronoff, D. M. (2013) 'Epidemiology of *Clostridium difficile* infection', *Journal of pharmacy practice*, 26(5), pp. 464–475. doi: 10.1177/0897190013499521.
Derouaux, A., Turk, S., Olrichs, N. K., Gobec, S., Breukink, E., Amoroso, A., Offant, J., Bostock, J., Mariner, K., Chopra, I., Vernet, T., Zervosen, A., Joris, B., Frère, J. M., Nguyen-Distèche, M. and Terrak, M. (2011) 'Small molecule inhibitors of peptidoglycan synthesis targeting the lipid II precursor', *Biochemical Pharmacology*, 81(9), pp. 1098–1105. doi: 10.1016/j.bcp.2011.02.008.
Dineen, S. S., McBride, S. M. and Sonenshein, A. L. (2010) 'Integration of metabolism and virulence by *Clostridium difficile* CodY', *Journal of Bacteriology*, 192(20), pp. 5350–5362. doi: 10.1128/JB.00341-10.
Dineen, S. S., Villapakkam, A. C., Nordman, J. T. and Sonenshein, A. L. (2007) 'Repression of *Clostridium difficile* toxin gene expression by CodY', *Molecular Microbiology*, 66(1), pp. 206–219. doi: 10.1111/j.1365-2958.2007.05906.x.
Donnelly, M. L., Forster, E. R., Rohlfing, A. E. and Shen, A. (2020) 'Differential effects of "resurrecting" Csp pseudoproteases during *Clostridioides difficile* spore germination', *Biochemical Journal*, 477(8), pp. 1459–1478. doi: 10.1042/BCJ20190875.

Du, H., Bing, J., Hu, T., Ennis, C. L., Nobile, C. J. and Huang, G. (2020) '*Candida auris*: Epidemiology, biology, antifungal resistance, and virulence', *PLoS pathogens*, 16(10), p. e1008921. doi: 10.1371/journal.ppat.1008921.

Dubois, T., Dancer-Thibonnier, M., Monot, M., Hamiot, A., Bouillaut, L., Soutourina, O., Martin-Verstraete, I. and Dupuy, B. (2016) 'Control of *Clostridium difficile* physiopathology in response to cysteine availability', *Infection and Immunity*, 84(8), pp. 2389–2405. doi: 10.1128/IAI.00121-16.

Dubois, T., Tremblay, Yannick D N, Briandet, R. and Dupuy, B. (2019) 'A microbiota-generated bile salt induces biofilm formation in *Clostridium difficile*', *Biofilms and Microbiomes*, pp. 1–12. doi: 10.1038/s41522-019-0087-4.

Dubois, T., Tremblay, Yannick D.N., Hamiot, A., Martin-Verstraete, I., Deschamps, J., Monot, M., Briandet, R. and Dupuy, B. (2019) 'A microbiota-generated bile salt induces biofilm formation in *Clostridium difficile*', *Biofilms and Microbiomes*, (April), pp. 1–12. doi: 10.1038/s41522-019-0087-4.

Elliott, B., Androga, G. O., Knight, D. R. and Riley, T. V. (2017) '*Clostridium difficile* infection: Evolution, phylogeny and molecular epidemiology', *Infection, Genetics and Evolution*, 49, pp. 1–11. doi: 10.1016/j.meegid.2016.12.018.

Enoch, D. A., Murray-Thomas, T., Adomakoh, N., Dedman, D., Georgopali, A., Francis, N. and Karas, A. (2020) 'Risk of complications and mortality following recurrent and non-recurrent *Clostridioides difficile* infection: a retrospective, observational, database study in England', *Journal of Hospital Infection*. doi: 10.1016/j.jhin.2020.09.025.

Fay, A., Meyer, P. and Dworkin, J. (2010a) 'Interactions between late-acting proteins required for peptidoglycan synthesis during sporulation', *Journal of Molecular Biology*, 399(4), pp. 547–561. doi: 10.1016/j.jmb.2010.04.036.

Fay, A., Meyer, P. and Dworkin, J. (2010b) 'Interactions between late acting proteins required for peptidoglycan synthesis during sporulation', *Journal of Molecular Biology*, 399(4), pp. 547–561. doi: doi:10.1016/j.jmb.2010.04.036.

Fimlaid, K. A., Bond, J. P., Schutz, K. C., Putnam, E. E., Leung, J. M., Lawley, T. D. and Shen, A. (2013) 'Global Analysis of the Sporulation Pathway of *Clostridium difficile*', *PLoS Genetics*, 9(8). doi: 10.1371/journal.pgen.1003660.

Freeman, J., Vernon, J., Morris, K., Nicholson, S., Todhunter, S., Longshaw, C. and Wilcox, M. H. (2015) 'Pan-European longitudinal surveillance of antibiotic resistance among prevalent *Clostridium difficile* ribotypes', *Clinical microbiology and infection : the official publication of the European Society of Clinical Microbiology and Infectious Diseases*, 21(3), pp. 248.e9-248.e16. doi: 10.1016/j.cmi.2014.09.017.

Frieden, T. (2019) 'Antibiotic resistance threats in the United States', *Centers for Disease Control and Prevention*, p. 114.

Gardete, S. and Tomasz, A. (2014) 'Mechanisms of vancomycin resistance in *Staphylococcus aureus*', *Journal of Clinical Investigation*, 124(7), pp. 2836–2840. doi: 10.1172/JCI68834.

Geiger, T. and Wolz, C. (2014) 'Intersection of the stringent response and the CodY regulon in low GC Gram-positive bacteria', *International Journal of Medical Microbiology*, 304(2), pp. 150–155. doi: 10.1016/j.ijmm.2013.11.013.

Gencic, S. and Grahame, D. A. (2020) 'Diverse energy-conserving pathways in *Clostridium difficile*: Growth in the absence of amino acid stickland acceptors and the role of the Wood-Ljungdahl pathway', *Journal of Bacteriology*, 202(20). doi: 10.1128/JB.00233-20.

Ghose, C., Eugenis, I., Edwards, A. N., Sun, X., McBride, S. M. and Ho, D. D. (2016) 'Immunogenicity and protective efficacy of *Clostridium difficile* spore proteins', *Anaerobe*, 37, pp. 85–95. doi: 10.1016/j.anaerobe.2015.12.001.

Ghosh, A. S., Chowdhury, C. and Nelson, D. E. (2008) 'Physiological functions of D-alanine carboxypeptidases in *Escherichia coli*', *Trends in microbiology*, 16(7), pp. 309–317. doi:

10.1016/j.tim.2008.04.006.
Goodwine, J., Gil, J., Doiron, A., Valdes, J., Solis, M., Higa, A., Davis, S. and Sauer, K. (2019) 'Pyruvate-depleting conditions induce biofilm dispersion and enhance the efficacy of antibiotics in killing biofilms in vitro and in vivo', *Scientific Reports*, 9(1), pp. 1–16. doi: 10.1038/s41598-019-40378-z.
Goudarzi, M., Seyedjavadi, S. S., Goudarzi, H., Aghdam, E. M. and Nazeri, S. (2014) '*Clostridium difficile* Infection: Epidemiology, Pathogenesis, Risk Factors, and Therapeutic Options', *Hindawi Publishing Corporation*, p. 9. doi: 10.1155/2014/916826.
Grabowski, R. and Buckel, W. (1991) 'Purification and properties of an iron-sulfur-containing and pyridoxal-phosphate-independent L-Serine dehydratase from *Peptostreptococcus asaccharolyticus*', *European Journal of Biochemistry*, 199(1), pp. 89–94. doi: 10.1111/j.1432-1033.1991.tb16095.x.
Greenwich, J., Reverdy, A., Gozzi, K., Di Cecco, G., Tashjian, T., Godoy-Carter, V. and Chai, Y. (2019) 'A decrease in serine levels during growth transition triggers biofilm formation in *Bacillus subtilis'*, *Journal of Bacteriology*, 201(15). doi: 10.1128/JB.00155-19.
Gu, H., Yang, Y., Wang, M., Chen, S., Wang, H., Li, S., Ma, Y. and Wang, J. (2018) 'Novel Cysteine Desulfidase CdsB Involved in Releasing Cysteine Repression of Toxin Synthesis in *Clostridium difficile*', *Frontiers in Cellular and Infection Microbiology*, 7(JAN), pp. 1–14. doi: 10.3389/fcimb.2017.00531.
Ha, S., Walker, D., Shi, Y. and Walker, S. (2000) 'The 1.9 Å crystal structure of *Escherichia coli* MurG, a membrane-associated glycosyltransferase involved in peptidoglycan biosynthesis', *Protein Science*, 9(6), pp. 1045–1052. doi: 10.1110/ps.9.6.1045.
Harnvoravongchai, P., Pipatthana, M., Chankhamhaengdecha, S. and Janvilisri, T. (2017) 'Insights into drug resistance mechanisms in *Clostridium difficile*', *Essays in biochemistry*, 61(1), pp. 81–88. doi: 10.1042/EBC20160062.
Heap, J. T., Pennington, O. J., Cartman, S. T. and Minton, N. P. (2009) 'A modular system for Clostridium shuttle plasmids', *Journal of Microbiological Methods*, 78(1), pp. 79–85. doi: 10.1016/j.mimet.2009.05.004.
Henriques, A. O., Beall, B. W., Roland, K. and Moran, C. P. J. (1995) 'Characterization of *cotJ*, a sigma E-controlled operon affecting the polypeptide composition of the coat of *Bacillus subtilis* spores', *Journal of bacteriology*, 177(12), pp. 3394–3406. doi: 10.1128/jb.177.12.3394-3406.1995.
Henriques, A. O., de Lencastre, H. and Piggot, P. J. (1992) 'A *Bacillus subtilis* morphogene cluster that includes *spoVE* is homologous to the mra region of *Escherichia coli*', *Biochimie*, 74(7–8), pp. 735–748. doi: 10.1016/0300-9084(92)90146-6.
Henriques, A. O. and Moran, C. P. (2007) 'Structure, assembly, and function of the spore surface layers', *Annual Review of Microbiology*, 61, pp. 555–588. doi: 10.1146/annurev.micro.61.080706.093224.
Higgins, D. and Dworkin, J. (2012) 'Recent progress in *Bacillus subtilis* sporulation', *FEMS microbiology reviews*, 36(1), pp. 131–148. doi: 10.1111/j.1574-6976.2011.00310.x.
Hofmeister, A. E. M., Grabowski, R., Linder, D. and Buckler, W. (1993) 'L-Serine and L-Threonine dehydratase from *Clostridium propionicum*: Two enzymes with different prosthetic groups', *European Journal of Biochemistry*, 215(2), pp. 341–349. doi: 10.1111/j.1432-1033.1993.tb18040.x.
Høiby, N., Bjarnsholt, T., Givskov, M., Molin, S. and Ciofu, O. (2010) 'Antibiotic resistance of bacterial biofilms', *International Journal of Antimicrobial Agents*, 35, pp. 322–332. doi: 10.1016/j.ijantimicag.2009.12.011.
Hong, H. A., Hitri, K., Hosseini, S., Kotowicz, N., Bryan, D., Mawas, F., Wilkinson, A. J., van Broekhoven, A., Kearsey, J. and Cutting, S. M. (2017) 'Mucosal antibodies to the C terminus of toxin A prevent colonization of *Clostridium difficile*', *Infection and Immunity*, 85(4), pp. 1–13. doi: 10.1128/IAI.01060-16.
Hu, Y., Chen, L., Ha, S., Gross, B., Falcone, B., Walker, D., Mokhtarzadeh, M. and Walker, S. (2003)

'Crystal structure of the MurG:UDP-GlcNAc complex reveals common structural principles of a superfamily of glycosyltransferases.', *Proceedings of the National Academy of Sciences of the United States of America*, 100(3), pp. 845–849. doi: 10.1073/pnas.0235749100.

Isidro, J., Mendes, A. L., Serrano, M., Henriques, A. O. and Oleastro, M. (2017) 'Overview of *Clostridium difficile* Infection: Life Cycle, Epidemiology, Antimicrobial Resistance and Treatment', in *Clostridium difficile - A Comprehensive Overview*. Shymaa Ena. IntechOpen, pp. 5–35. doi: http://dx.doi.org/10.5772/intechopen.69053.

Isidro, J., Menezes, J., Serrano, M., Borges, V., Paixão, P., Mimoso, M., Martins, F., Toscano, C., Santos, A., Henriques, A. O. and Oleastro, M. (2018) 'Genomic study of a *Clostridium difficile* multidrug resistant outbreak-related clone reveals novel determinants of resistance', *Frontiers in Microbiology*, 9(DEC), pp. 1–9. doi: 10.3389/fmicb.2018.02994.

Isidro, J., Santos, A., Nunes, A., Borges, V., Silva, C., Vieira, L., Mendes, A. L., Serrano, M., Henriques, A. O., Gomes, J. P. and Oleastro, M. (2018) 'Imipenem Resistance in *Clostridium difficile* Ribotype 017, Portugal', *Emerging infectious diseases*, 24(4), pp. 741–745. doi: 10.3201/eid2404.170095.

Janoir, C., Denève, C., Bouttier, S., Barbut, F., Hoys, S., Caleechum, L., Chapetón-Montes, D., Pereira, F. C., Henriques, A. O., Collignon, A., Monot, M. and Dupuy, B. (2013) 'Adaptive strategies and pathogenesis of *Clostridium difficile* from in vivo transcriptomics', *Infection and Immunity*, 81(10), pp. 3757–3769. doi: 10.1128/IAI.00515-13.

Jim O'Neill (2016) 'Tackling Drug-Resistant Infections Globally: Final Report and Recommendations', *The Review on Antimicrobial Resistance*, (May), pp. 1–80.

Karasawa, T., Ikoma, S., Yamakawa, K. and Nakamura, S. (1995) 'A defined growth medium for *Clostridium difficile*', *Microbiology*, 141(2), pp. 371–375. doi: 10.1099/13500872-141-2-371.

Knippel, R. J., Wexler, A. G., Miller, J. M., Beavers, W. N., Weiss, A., de Crécy-Lagard, V., Edmonds, K. A., Giedroc, D. P. and Skaar, E. P. (2020) '*Clostridioides difficile* Senses and Hijacks Host Heme for Incorporation into an Oxidative Stress Defense System', *Cell Host and Microbe*, 28(3), pp. 411-421.e6. doi: 10.1016/j.chom.2020.05.015.

Kodori, M., Ghalavand, Z., Yadegar, A., Eslami, G., Azimirad, M., Krutova, M., Abadi, A. and Zali, M. R. (2020) 'Molecular characterization of pathogenicity locus (PaLoc) and *tcdC* genetic diversity among tcdA+B+ *Clostridioides difficile* clinical isolates in Tehran, Iran', *Anaerobe*, 66, p. 102294. doi: 10.1016/j.anaerobe.2020.102294.

Kouhsari, E., Douraghi, M., Krutova, M., Fakhre Yaseri, H., Talebi, M., Baseri, Z., Moqarabzadeh, V., Sholeh, M. and Amirmozafari, N. (2019) 'The emergence of metronidazole and vancomycin reduced susceptibility in *Clostridium difficile* isolates in Iran', *Journal of Global Antimicrobial Resistance*, 18, pp. 28–33. doi: 10.1016/j.jgar.2019.01.027.

Lawler, A. J., Lambert, P. A. and Worthington, T. (2020) 'A Revised Understanding of *Clostridioides difficile* Spore Germination', *Trends in Microbiology*, 28(9), pp. 744–752. doi: 10.1016/j.tim.2020.03.004.

Lawson, P. A., Citron, D. M., Tyrrell, K. L. and Finegold, S. M. (2016) 'Reclassification of *Clostridium difficile* as *Clostridioides difficile* (Hall and O'Toole 1935) Prévot 1938', *Anaerobe*, 40, pp. 95–99. doi: 10.1016/j.anaerobe.2016.06.008.

Leeds, J. A., Sachdeva, M., Mullin, S., Whitney Barnes, S. and Ruzin, A. (2014) '*In vitro* selection, via serial passage, of *Clostridium difficile* mutants with reduced susceptibility to fidaxomicin or vancomycin', *Journal of Antimicrobial Chemotherapy*, 69(1), pp. 41–44. doi: 10.1093/jac/dkt302.

Lin, R., D'Ari, R. and Newman, E. B. (1992) 'λ placMu insertions in genes of the leucine regulon: Extension of the regulon to genes not regulated by leucine', *Journal of Bacteriology*, 174(6), pp. 1948–1955. doi: 10.1128/jb.174.6.1948-1955.1992.

Liu, Y. and Breukink, E. (2016) 'The membrane steps of bacterial cell wall synthesis as antibiotic targets', *Antibiotics*, 5(3). doi: 10.3390/antibiotics5030028.

Louie, T. J., Miller, M. A., Mullane, K. M., Weiss, K., Lentnek, A., Golan, Y., Gorbach, S., Sears, P. and Shue, Y.-K. (2011) 'Fidaxomicin versus Vancomycin for *Clostridium difficile* Infection', *New England Journal of Medicine*, 364(5), pp. 422–431. doi: 10.1056/nejmoa0910812.

Mainardi, J.-L., Villet, R., Bugg, T. D., Mayer, C. and Arthur, M. (2008) 'Evolution of peptidoglycan biosynthesis under the selective pressure of antibiotics in Gram-positive bacteria', *FEMS microbiology reviews*, 32(2), pp. 386–408. doi: 10.1111/j.1574-6976.2007.00097.x.

McBride, S. M. and Sonenshein, A. L. (2011) 'The *dlt* operon confers resistance to cationic antimicrobial peptides in *Clostridium difficile*', *Microbiology (Reading, England)*, 157(Pt 5), pp. 1457–1465. doi: 10.1099/mic.0.045997-0.

McKee, R. W., Mangalea, M. R., Purcell, E. B., Borchardt, E. K. and Tamayo, R. (2013) 'The second messenger cyclic Di-GMP regulates *Clostridium difficile* toxin production by controlling expression of *sigD'*, *Journal of Bacteriology*, 195(22), pp. 5174–5185. doi: 10.1128/JB.00501-13.

Meeske, A. J., Riley, E. P., Robins, W. P., Uehara, T., Mekalanos, J. J., Kahne, D., Walker, S., Kruse, A. C., Bernhardt, T. G. and Rudner, D. Z. (2016) 'SEDS proteins are a widespread family of bacterial cell wall polymerases', *Nature*, 537(7622), pp. 634–638. doi: 10.1038/nature19331.

El Meouche, I., Peltier, J., Monot, M., Soutourina, O., Pestel-Caron, M., Dupuy, B. and Pons, J. L. (2013) 'Characterization of the SigD regulon of *C. difficile* and its positive control of toxin production through the regulation of *tcdR'*, *PLoS ONE*, 8(12), pp. 1–17. doi: 10.1371/journal.pone.0083748.

Mitrofanova, O., Mardanova, A., Evtugyn, V., Bogomolnaya, L. and Sharipova, M. (2017) 'Effects of *Bacillus* Serine Proteases on the Bacterial Biofilms', *BioMed Research International*, 2017. doi: 10.1155/2017/8525912.

Mondal, S. I., Akter, A., Draper, L. A., Ross, R. P. and Hill, C. (2021) 'Characterization of an endolysin targeting *Clostridioides difficile* that affects spore outgrowth', *International Journal of Molecular Sciences*, 22(11). doi: 10.3390/ijms22115690.

Munteanu, B., Braun, M. and Boonrod, K. (2012) 'Improvement of PCR reaction conditions for site-directed mutagenesis of big plasmids', *Journal of Zhejiang University: Science B*, 13(4), pp. 244–247. doi: 10.1631/jzus.B1100180.

Nagy, E. (2018) 'What do we know about the diagnostics, treatment and epidemiology of *Clostridioides* (*Clostridium*) *difficile* infection in Europe?', *Journal of Infection and Chemotherapy*, 24(3), pp. 164–170. doi: 10.1016/j.jiac.2017.12.003.

Nawrocki, K. L., Edwards, A. N., Daou, N., Bouillaut, L. and McBride, S. M. (2016) 'CodY-dependent regulation of sporulation in *Clostridium difficile*', *Journal of Bacteriology*, 198(15), pp. 2113–2130. doi: 10.1128/JB.00220-16.

Newman, E. B. and Walker, C. (1982) 'L-Serine degradation in *Escherichia coli* K-12: a combination of L-Serine, glycine, and leucine used as a source of carbon', *Journal of Bacteriology*, 151(2), pp. 777–782. doi: 10.1128/jb.151.2.777-782.1982.

Ng, Y. K., Ehsaan, M., Philip, S., Collery, M. M., Janoir, C., Collignon, A., Cartman, S. T. and Minton, N. P. (2013) 'Expanding the Repertoire of Gene Tools for Precise Manipulation of the *Clostridium difficile* Genome: Allelic Exchange Using pyrE Alleles', *PLoS ONE*, 8(2). doi: 10.1371/journal.pone.0056051.

Nobile, C. J. and Johnson, A. D. (2015) '*Candida albicans* Biofilms and Human Disease', *Annual review of microbiology*, 69, pp. 71–92. doi: 10.1146/annurev-micro-091014-104330.

O'Grady, K., Knight, D. R. and Riley, T. V. (2021) 'Antimicrobial resistance in *Clostridioides difficile*', *European Journal of Clinical Microbiology and Infectious Diseases*, (0123456789). doi: 10.1007/s10096-021-04311-5.

O'Toole, I. C. H. and E. (1935) 'Intestinal flora in new-born infants', *American Journal of Diseases of Children*, 49(2), pp. 390–402.

Ogawa, H., Gomi, T., Nishizawa, M., Hayakawa, Y., Endo, S., Hayashi, K., Ochiai, H., Takusagawa,

F., Pitot, H. C., Mori, H., Sakurai, H., Koizumi, K., Saiki, I., Oda, H., Fujishita, T., Miwa, T., Maruyama, M. and Kobayashi, M. (2006) 'Enzymatic and biochemical properties of a novel human serine dehydratase isoform', *Biochimica et Biophysica Acta - Proteins and Proteomics*, 1764(5), pp. 961–971. doi: 10.1016/j.bbapap.2006.02.010.

Onainor, E. (2012) 'Crystal structure of L-Serine Dehydratase from *Legionella pneumophila*', *Protein Data Bank*, pp. 105–112.

Peltier, J., Courtin, P., El Meouche, I., Lemée, L., Chapot-Chartier, M. P. and Pons, J. L. (2011) '*Clostridium difficile* has an original peptidoglycan structure with a high level of N-acetylglucosamine deacetylation and mainly 3-3 cross-links', *Journal of Biological Chemistry*, 286(33), pp. 29053–29062. doi: 10.1074/jbc.M111.259150.

Peng, Z., Jin, D., Kim, H. B., Stratton, C. W., Wu, B., Tang, Y.-W. and Sun, X. (2017) 'Update on Antimicrobial Resistance in *Clostridium difficile*: Resistance Mechanisms and Antimicrobial Susceptibility Testing.', *Journal of clinical microbiology*, 55(7), pp. 1998–2008. doi: 10.1128/JCM.02250-16.

Pereira, F. C., Saujet, L., Tomé, A. R., Serrano, M., Monot, M., Couture-Tosi, E., Martin-Verstraete, I., Dupuy, B. and Henriques, A. O. (2013) 'The Spore Differentiation Pathway in the Enteric Pathogen *Clostridium difficile*', *PLoS Genetics*, 9(10). doi: 10.1371/journal.pgen.1003782.

Permpoonpattana, P., Phetcharaburanin, J., Mikelsone, A., Dembek, M., Tan, S., Brisson, M. C., La Ragione, R., Brisson, A. R., Fairweather, N., Hong, H. A. and Cutting, S. M. (2013) 'Functional characterization of *Clostridium difficile* spore coat proteins', *Journal of Bacteriology*, 195(7), pp. 1492–1503. doi: 10.1128/JB.02104-12.

Pizarro-Guajardo, M., Chamorro-Veloso, N., Vidal, R. M. and Paredes-Sabja, D. (2019) 'New insights for vaccine development against *Clostridium difficile* infections', *Anaerobe*, 58, pp. 73–79. doi: 10.1016/j.anaerobe.2019.04.009.

Polivkova, S., Krutova, M., Capek, V., Sykorova, B. and Benes, J. (2021) 'Fidaxomicin versus metronidazole, vancomycin and their combination for initial episode, first recurrence and severe *Clostridioides difficile* infection — An observational cohort study', *International Journal of Infectious Diseases*, 103, pp. 226–233. doi: 10.1016/j.ijid.2020.11.004.

Rabin, N., Zheng, Y., Opoku-Temeng, C., Du, Y., Bonsu, E. and Sintim, H. O. (2015) 'Biofilm formation mechanisms and targets for developing antibiofilm agents', *Future Medicinal Chemistry*, 7(4), pp. 493–512. doi: 10.4155/fmc.15.6.

Real, G., Fay, A., Eldar, A., Pinto, S. M., Henriques, A. O. and Dworkin, J. (2008) 'Determinants for the subcellular localization and function of a nonessential SEDS protein', *Journal of bacteriology*, 190(1), pp. 363–376. doi: 10.1128/JB.01482-07.

Ribis, J. W., Fimlaid, K. A. and Shen, A. (2018) 'Differential requirements for conserved peptidoglycan remodeling enzymes during *Clostridioides difficile* spore formation', *Molecular Microbiology*, 110(3), pp. 370–389. doi: 10.1111/mmi.14090.

Rohani, A., Moore, J. H., Su, Y. H., Stagnaro, V., Warren, C. and Swami, N. S. (2018) 'Single-cell electro-phenotyping for rapid assessment of *Clostridium difficile* heterogeneity under vancomycin treatment at sub-MIC (minimum inhibitory concentration) levels', *Sensors and Actuators, B: Chemical*, 276(April), pp. 472–480. doi: 10.1016/j.snb.2018.08.137.

Sambrook, J. and Green, M. R. (2012) *Molecular Cloning: A Laboratory Manual*. 4th edn, *Cold Spring Harbor Laboratory Press*. 4th edn. Edited by J. Inglis, A. Boyle, and G. Alexander. Cold Spring Harbor Laboratories, New York: Inglis J. doi: 10.3724/SP.J.1141.2012.01075.

Sapkota, M., Marreddy, R. K. R., Wu, X., Kumar, M. and Hurdle, J. G. (2020) 'The early stage peptidoglycan biosynthesis Mur enzymes are antibacterial and antisporulation drug targets for recurrent *Clostridioides difficile* infection', *Anaerobe*, 61, p. 102129. doi: 10.1016/j.anaerobe.2019.102129.

Saujet, L., Monot, M., Dupuy, B., Soutourina, O. and Martin-Verstraete, I. (2011) 'The key sigma factor

of transition phase, sigh, controls sporulation, metabolism, and virulence factor expression in *Clostridium difficile*', *Journal of Bacteriology*, 193(13), pp. 3186–3196. doi: 10.1128/JB.00272-11.
Saujet, L., Pereira, F. C., Henriques, A. O. and Martin-Verstraete, I. (2015) 'The regulatory network controlling spore formation in *Clostridium difficile*', *FEMS Microbiology Reviews*. doi: 10.1111/jace.14264.
Saujet, L., Pereira, F. C., Serrano, M., Soutourina, O., Monot, M., Shelyakin, P. V., Gelfand, M. S., Dupuy, B., Henriques, A. O. and Martin-Verstraete, I. (2013) 'Genome-Wide Analysis of Cell Type-Specific Gene Transcription during Spore Formation in *Clostridium difficile*', *PLoS Genetics*, 9(10). doi: 10.1371/journal.pgen.1003756.
Sauvage, E. and Terrak, M. (2016) 'Glycosyltransferases and Transpeptidases/Penicillin-Binding Proteins: Valuable Targets for New Antibacterials', *Antibiotics (Basel, Switzerland)*, 5(1). doi: 10.3390/antibiotics5010012.
Scheffers, D.-J. and Pinho, M. G. (2005) 'Bacterial Cell Wall Synthesis: New Insights from Localization Studies', *Microbiology and Molecular Biology Reviews*, 69(4), pp. 585–607. doi: 10.1128/mmbr.69.4.585-607.2005.
Serrano, M., Crawshaw, A. D., Dembek, M., Monteiro, J. M., Pereira, F. C., Pinho, M. G., Fairweather, N. F., Salgado, P. S. and Henriques, A. O. (2016) 'The SpoIIQ-SpoIIIAH complex of *Clostridium difficile* controls forespore engulfment and late stages of gene expression and spore morphogenesis', *Molecular Microbiology*, 100(1), pp. 204–228. doi: 10.1111/mmi.13311.
Serrano, M., Kint, N., Pereira, F. C., Saujet, L., Boudry, P., Dupuy, B., Henriques, A. O. and Martin-Verstraete, I. (2016) 'A Recombination Directionality Factor Controls the Cell Type-Specific Activation of σ^K and the Fidelity of Spore Development in *Clostridium difficile*', *PLoS Genetics*, 12(9), pp. 1–34. doi: 10.1371/journal.pgen.1006312.
Serrano, M., Real, G., Santos, J., Carneiro, J., Moran, C. P. and Henriques, A. O. (2011) 'A negative feedback loop that limits the ectopic activation of a cell type-specific sporulation sigma factor of Bacillus subtilis', *PLoS Genetics*, 7(9). doi: 10.1371/journal.pgen.1002220.
Shao, Z. Q., LIN, R. T. and Newman, E. B. (1994) 'Sequencing and characterization of the *sdaC* gene and identification of the *sdaCB* operon in *Escherichia coli* K12', *European Journal of Biochemistry*, 222(3), pp. 901–907. doi: 10.1111/j.1432-1033.1994.tb18938.x.
Shao, Z. Q. and Newman, E. B. (1993) 'Sequencing and characterization of the *sdaB* gene from *Escherichia coli* K-12', *European Journal of Biochemistry*, 212(3), pp. 777–784. doi: 10.1111/j.1432-1033.1993.tb17718.x.
Shen, A. (2020) '*Clostridioides difficile* Spore Formation and Germination: New Insights and Opportunities for Intervention', *Annual Review of Microbiology*, 74, pp. 545–566. doi: 10.1146/annurev-micro-011320.
Shen, A., Edwards, A. N., Sarker, M. R. and Paredes-Sabja, D. (2019) 'Sporulation and germination in Clostridial pathogens', *Gram-Positive Pathogens*, 7(6), pp. 903–926. doi: 10.1128/9781683670131.ch56.
Shen, W. J., Deshpande, A., Hevener, K. E., Endres, B. T., Garey, K. W., Palmer, K. L. and Hurdle, J. G. (2020) 'Constitutive expression of the cryptic *vanG*^{Cd} operon promotes vancomycin resistance in *Clostridioides difficile* clinical isolates', *Journal of Antimicrobial Chemotherapy*, 75(4), pp. 859–867. doi: 10.1093/jac/dkz513.
Sjodt, M., Rohs, P. D. A., Gilman, M. S. A., Erlandson, S. C., Zheng, S., Green, A. G., Brock, K. P., Taguchi, A., Kahne, D., Walker, S., Marks, D. S., Rudner, D. Z., Bernhardt, T. G. and Kruse, A. C. (2020) 'Structural coordination of polymerization and crosslinking by a SEDS–bPBP peptidoglycan synthase complex', *Nature Microbiology*, 5(6), pp. 813–820. doi: 10.1038/s41564-020-0687-z.
Smits, W. K., Lyras, D., Lacy, D. B., Wilcox, M. H. and Kuijper, E. J. (2016) '*Clostridium difficile* infection', *Nature reviews. Disease primers*, 2, p. 16020. doi: 10.1038/nrdp.2016.20.

Sobhanifar, S., King, D. T. and Strynadka, N. C. J. (2013) 'Fortifying the wall: Synthesis, regulation and degradation of bacterial peptidoglycan', *Current Opinion in Structural Biology*, 23(5), pp. 695–703. doi: 10.1016/j.sbi.2013.07.008.

Sorg, J. A. (2014) 'Microbial bile acid metabolic clusters: The bouncers at the bar', *Cell Host and Microbe*, 16(5), pp. 551–552. doi: 10.1016/j.chom.2014.10.015.

Soto, S. M. (2013) 'Role of efflux pumps in the antibiotic resistance of bacteria embedded in a biofilm', *Virulence*, 4(3), pp. 223–229. doi: 10.4161/viru.23724.

Spigaglia, P., Mastrantonio, P. and Barbanti, F. (2018) 'Antibiotic Resistances of *Clostridium difficile*', *Advances in experimental medicine and biology*, 1050, pp. 137–159. doi: 10.1007/978-3-319-72799-8_9.

Srikhanta, Y. N., Hutton, M. L., Awad, M. M., Drinkwater, N., Singleton, J., Day, S. L., Cunningham, B. A., McGowan, S. and Lyras, D. (2019) 'Cephamycins inhibit pathogen sporulation and effectively treat recurrent *Clostridioides difficile* infection', *Nature microbiology*, 4(12), pp. 2237–2245. doi: 10.1038/s41564-019-0519-1.

Stewart, P. S. and Costerton, J. W. (2001) 'Antibiotic resistance of bacteria in biofilms', *Lancet (London, England)*, 358(9276), pp. 135–138. doi: 10.1016/s0140-6736(01)05321-1.

Stogios, P. J. and Savchenko, A. (2020) 'Molecular mechanisms of vancomycin resistance', *Protein Science*, 29(3), pp. 654–669. doi: 10.1002/pro.3819.

Su, H. S., Lang, B. F. and Newman, E. B. (1989) 'L-Serine degradation in *Escherichia coli* K-12: cloning and sequencing of the *sdaA* gene', *Journal of bacteriology*, 171(9), pp. 5095–5102. doi: 10.1128/jb.171.9.5095-5102.1989.

Sutterlin, L. (2018) 'Peptidoglycan Cross-Linking Activity of L,D-Transpeptidases from *Clostridium difficile* and Inactivation of These Enzymes by _B-Lactams', *Antimicrob Agents Chemother*, 62(1), pp. 1–10.

Taggart, M. G., Snelling, W. J., Naughton, P. J., La Ragione, R. M., Dooley, J. S. G. and Ternan, N. G. (2021) 'Biofilm regulation in *Clostridioides difficile*: Novel systems linked to hypervirulence', *PLOS Pathogens*, 17(9), p. e1009817. doi: 10.1371/journal.ppat.1009817.

Taguchi, A., Welsh, M. A., Marmont, L. S., Lee, W., Sjodt, M., Kruse, A. C., Kahne, D., Bernhardt, T. G. and Walker, S. (2019) 'FtsW is a peptidoglycan polymerase that is functional only in complex with its cognate penicillin-binding protein', *Nature microbiology*, 4(4), pp. 587–594. doi: doi:10.1038/s41564-018-0345-x.

Tickler, I. A., Goering, R. V, Whitmore, J. D., Lynn, A. N. W., Persing, D. H. and Tenover, F. C. (2014) 'Strain types and antimicrobial resistance patterns of *Clostridium difficile* isolates from the United States, 2011 to 2013.', *Antimicrobial agents and chemotherapy*, 58(7), pp. 4214–4218. doi: 10.1128/AAC.02775-13.

Tremblay, Y. D. N., Durand, B. A. R., Hamiot, A., Martin-Verstraete, I., Oberkampf, M., Monot, M. and Dupuy, B. (2021) 'Metabolic adaption to extracellular pyruvate triggers biofilm formation in *Clostridioides difficile*', *ISME Journal*, (June). doi: 10.1038/s41396-021-01042-5.

Tsutsumi, L., Owusu, Y., Hurdle, J. and Sun, D. (2014) 'Progress in the Discovery of Treatments for C. difficile Infection: A Clinical and Medicinal Chemistry Review', *Current Topics in Medicinal Chemistry*, 14(1), pp. 152–175. doi: 10.2174/1568026613666131113154753.

Valente, M. C. (2021) *Mechanisms of resistance to vancomycin in Clostridioides difficile*. Universidade Nova da Lisboa.

Vasudevan, P., Weaver, A., Reichert, E. D., Linnstaedt, S. D. and Popham, D. L. (2007) 'Spore cortex formation in *Bacillus subtilis* is regulated by accumulation of peptidoglycan precursors under the control of sigma K.', *Molecular microbiology*, 65(6), pp. 1582–1594. doi: 10.1111/j.1365-2958.2007.05896.x.

Venugopal, A. A. and Johnson, S. (2012) 'Fidaxomicin: A novel macrocyclic antibiotic approved for

treatment of *Clostridium difficile* infection', *Clinical Infectious Diseases*, 54(4), pp. 568–574. doi: 10.1093/cid/cir830.
Webb, B. J., Subramanian, A., Lopansri, B., Goodman, B., Jone, P. B., Ferraro, J., Stenehjem, E. and Brown, S. M. (2020) 'Antibiotic Exposure and Risk for Hospital-Associated *Clostridioides difficile* Infection', *Antimicrobial Agents and Chemotherapy*, 64(4). doi: 10.1055/s-0040-1701228.
Wolfe, C., Pagano, P., Pillar, C. M., Shinabarger, D. L. and Boulos, R. A. (2018) 'Comparison of the in vitro antibacterial activity of ramizol, fidaxomicin, vancomycin, and metronidazole against 100 clinical isolates of *Clostridium difficile* by broth microdilution', *Diagnostic Microbiology and Infectious Disease*, 92(3), pp. 250–252. doi: 10.1016/j.diagmicrobio.2018.06.002.
Wu, X., Alam, M. Z., Feng, L., Tsutsumi, L. S., Sun, D. and Hurdle, J. G. (2014) 'Prospects for flavonoid and related phytochemicals as nature-inspired treatments for *Clostridium difficile* infection.', *Journal of applied microbiology*, 116(1), pp. 23–31. doi: 10.1111/jam.12344.
Yamaguchi, T., Konishi, H., Aoki, K., Ishii, Y., Chono, K. and Tateda, K. (2020) 'The gut microbiome diversity of *Clostridioides difficile*-inoculated mice treated with vancomycin and fidaxomicin', *Journal of Infection and Chemotherapy*, 26(5), pp. 483–491. doi: 10.1016/j.jiac.2019.12.020.
Yan, Y., Grant, G. A. and Gross, M. L. (2015) 'Hydrogen-Deuterium Exchange Mass Spectrometry Reveals Unique Conformational and Chemical Transformations Occurring upon [4Fe-4S] Cluster Binding in the Type 2 L-Serine Dehydratase from *Legionella pneumophila*', *Biochemistry*, 54(34), pp. 5322–5328. doi: 10.1021/acs.biochem.5b00761.
Yarlagadda, V., Akkapeddi, P., Manjunath, G. B. and Haldar, J. (2014) 'Membrane active vancomycin analogues: A strategy to combat bacterial resistance', *Journal of Medicinal Chemistry*, 57(11), pp. 4558–4568. doi: 10.1021/jm500270w.
Zhang, L. J., Yang, L., Gu, X. X., Chen, P. X., Fu, J. L. and Jiang, H. X. (2019) 'The first isolation of *Clostridium difficile* RT078/ ST11 from pigs in China', *PLoS ONE*, 14(2), pp. 1–11. doi: 10.1371/journal.pone.0212965.
Zhang, X. and Newman, E. (2008) 'Deficiency in L-Serine deaminase results in abnormal growth and cell division of *Escherichia coli* K-12', *Molecular Microbiology*, 69(4), pp. 870–881. doi: 10.1111/j.1365-2958.2008.06315.x.
Zhu, D., Sorg, J. A. and Sun, X. (2018) '*Clostridioides difficile* biology: Sporulation, germination, and corresponding therapies for *C. difficile* infection', *Frontiers in Cellular and Infection Microbiology*, 8(FEB), pp. 1–10. doi: 10.3389/fcimb.2018.00029.

6. Appendix

Appendix 1: List of strains used in this study.

Strains	Relevant features/Sequences (5' to 3')	Source
E. coli strains		
DH5α	F-φ80*lacZ*ΔM15 Δ(*lacZY* A*argF*) U169 *recA1 end*A1 *hsd*R17 (rK-,mK+) phoA *sup*E44 λ- *thi*-1 *gyr*A96 *rel*A1	Bethesda Research laboratories
HB101	supE44 *aa*14 *gal*K2 *lac*Y1 D(*gpt-proA*) 62 *rps*L20 (*Str*^{R}) *xyl*-5 *mtl*-1 *rec*A13 D(*mcrC-mrr*) *hsd*S$_B$(r$_B$-m$_B$-) RP4	(El Meouche *et al.*, 2013)
PK11466[BL21(DE3) Suf^{++}]	BL21(DE3) but *zdh-3632::cat*, $^{-26}$ATA^{-24} bp relative to *sufA* TSS changed to $^{-26}$TAT^{-24} , Cm^R	(Corless *et al.*, 2020)
AHCD203	HB101 (pRP4) (pMTL-YN1)	(Ng *et al.*, 2013)
AHCD226	DH5α (pSR3) (pMTL-YN3)	(Ng *et al.*, 2013)
AHEC1268	Derived from HB101 containing pIM01	This study
AHEC1361	Derived from HB101 containing pIM02	"
AHEC1364	Derived from PK11466 [BL21(DE3) Suf^{++}] containing pIM03	"
AHEC1365	Derived from PK11466 [BL21(DE3) Suf^{++}] containing pIM04	"
AHEC1363	Derived from PK11466 [BL21(DE3) Suf^{++}] containing pET-16b	"
C. difficile strains		
AHCD532	630Δ*erm sigE*::intron *ermB*	(Serrano, Kint, *et al.*, 2016)
AHCD533	*630*Δ*erm sigF*::intron *ermB*	(Saujet *et al.*, 2013)
AHCD534	630Δ*erm sigG*::intron *ermB*	(Saujet *et al.*, 2013)
AHCD535	630Δ*erm sigK*::intron *ermB*	(Serrano, Kint, *et al.*, 2016)
AHCD536	630Δ*erm spo0A*::intron *ermB*	(Cassona, 2018)
AHCD772	630Δ*erm* Δ*pyrE*	(Cartman *et al.*, 2012)
AHCD1190	630Δ*erm*	(Ng *et al.*, 2013)
AHCD1243	630Δ*erm codY*::*ermB*	(Nawrocki *et al.*, 2016)
AHCD1618	Derived from 630Δ*erm* containing pIM01	This study
AHCD1636	Derived from *codY* containing pIM01	"
AHCD1637	Derived from *sigF* containing pIM01	"
AHCD1638	Derived from *sigG* containing pIM01	"
AHCD1639	Derived from *sigK* containing pIM01	"
AHCD1640	Derived from *spo0A* containing pIM01	"
AHCD1641	Derived from *sigE* containing pIM01	"
AHCD1722	Derived from 630Δ*erm* Δ*pyrE* containing pIM02	"
AHCD1723	630Δ*erm*Δ*sdaB*	"

Appendix 2: List of plasmids used in this study.

Plasmids	Relevant features/Sequences (5' to 3')	Source
pMTL84121	*Clostridium* modular plasmid carrying *catP* (Cm^R/Tm^R)	(Pereira *et al.*, 2013)
pIM01	Derived from pMTL84121 carrying a P$_{sdaB}$-*SNAP* fusion. Cm^R	This study
pIM02	Derived from pMTL-YN3 carrying a *sdaB* null mutant allele. Tm^R.	"
pMTL-YN3	Plasmid for mutation through ACE in 630Δ*erm.* Tm^R.	(Ng *et al.*, 2013)
pMTL-YN1	Plasmid to revert the *pyrE* gene through ACE in *C. difficile* 630Δ*erm*Δ*pyrE*. Tm^R.	(Ng *et al.*, 2013)
pET-16b	His-tag fusion protein expression vector. Amp^R.	Novagen
pIM03	Derived from pET-16b carrying a SdaB protein. Amp^R.	This study
pIM04	Derived from pET-16b carrying a SdaB protein ΔA295. Amp^R.	"

Appendix 3: List of primers used in this study.

Primers*	Relevant features/Sequences (5' to 3')	Source
SNAP-SOE-Fw	ATGGATAAAGATTGTGAAATGAAGAGAACC	Laboratory stock
XhoI-SNAP-Rev	CCGCTCGAGTTACCCAAGTCCTGGTTTCCCCAAACG	This study
pyrE-vef-Fw	CAATAATTTTATAACATTAACATGG	(Cassona, 2018)
pyrE-vef-Rev	GTGTTACTTAAAAAATGTAAAT	(Cassona, 2018)
*sdaB*4-Fw	CCTTCAAAGAATTTAGTTAC	This study
*sdaB*33-Fw	CGGGATCCTGTTTCTTTAGGACATATGTTAGC	"
*sdaB*659-EcoRI-Fw	GGAATTCGCAGAACCTTTAAATAAC	"
*sdaB*930-Fw	GCGGATCCTTTAGGTTATAATAAATATGTGC	"
*sdaB*1000-Rev	CACAATCTTTATCCATATTATTCCTCCTAAATTTACG	"
*sdaB*1004_Fw	GGGTTTCATATGGATACTTTAAAGGAAC	"
*sdaB*1015-Rev	GAAATGTTTAGCCTTTAAAGTATCCATATTATTCC	"
*sdaB*1885_Rev	CCTTTTAAGTATGCTACTGCTGCTGCCATAGAACAAGC	"
*sdaB*1889_Fw	GTTCTATGCGACGACGAGTAGCATACTTAAAAGGTGG	"
*sdaB*2171-Fw	GGATACTTTAAAGGCTAAACATTTCTTCTCTTG	"
*sdaB*2194_Rev	CGCGGATCCTTAGCAAGAGAAGAAATGTTTAGC	"
*sdaB*2920-Rev	GGCCTCGAGTGTCAATATCTCCTATTTGAGC	"
*sdaB*3160-Rev	GGCCTCGAGTTTTCTCATACACTTCTGGGC	"
*sdaB*3185-Rev	GCAAGTTCTCTAACTCTAAGC	"

*Introduced restriction sites are underlined